FINITE STRAIN ELASTIC-PLASTIC DEFORMATION OF GLASSY POLYMERS

by

BHARATH SAMPATHKUMARAN BAGEPALLI

B.E. Mechanical Engineering Bangalore University (1972)
M.E. Mechanical Engineering Indian Institute of Science (1974)
M.S. Applied mechanics, Yale University (1979)

SUBMITTED TO THE DEPARTMENT OF
MECHANICAL ENGINEERING
IN PARTIAL FULLFILMENT OF THE REQUIREMENTS
FOR THE DEGREE OF
DOCTOR OF SCIENCE
AT THE
MASSACHUSETTS INSTITUTE OF TECHNOLOGY
FEBRURARY 1984

Signature of Author _____
Bharath S. Bagepalli, Department of Mechanical Engineering, December 1983.

Certified by _____
Professor Ali S. Argon, Thesis Supervisor

Accepted by _____
Professor Warren M. Rohsenow, Chairman
Departmental Committee on Graduate Studies
Department of Mechanical Engineering

FINITE STRAIN ELASTIC-PLASTIC DEFORMATION OF GLASSY POLYMERS

by

BHARATH S. BAGEPALLI

Submitted to the Department of Mechanical Engineering on December 9 1983 , in partial fulfillment of the requirements for the degree of Doctor of Science in Mechanical Engineering .

ABSTRACT

A deforming glassy polymer is seen as overcoming two basic resistances: 1) a short-range elastic resistance due to the flexing of van der Waals interactions ; and , on overcoming these interactions at the onset of plastic flow , 2) a rubbery resistance due to configurational entropy change in the unwinding macromolecules . " Locking " behaviour is seen as the molecules orient themselves sufficiently .

An incremental constitutive law , via a finite-strain formulation using an updated-Lagrangian approach has been developed . The total deformation gradient is decomposed into the elastic and plastic components . The applied Cauchy stresses are determined in terms of the elastic deformation gradient , and , the rubbery resistances or back stresses are determined in terms of the plastic deformation gradient . A kinematically hardening yield function employing a Mises type of yield criteria is assumed . A pressure and rate independent formulation is developed . Incremental plastic deformation is assumed to follow normality . Since elastic strains for glassy polymers could be large , all quantities have been evaluated to include effects to the order of elastic strains .

After incorporating the constitutive model in the finite element method programme , ABAQUS , two boundary value problems were tried , for two different polymers , polycarbonate and polystyrene: 1) the formation and propagation of a neck in a round bar in tension; and 2) the drawing of a polymer out of a half-space , to model the drawing of a craze-tuft. Some experiments were done on polystyrene above Tg to examine its rubbery behaviour ; and on a round polycarbonate rod to determine its necking characteristics , to be compared with the computed results , and favourable agreement was found .

Thesis Supervisor: Professor Ali S. Argon
Title: Quentin Berg Professor of Mechanical Engineering

To

My Parents

ACKNOWLEDGEMENT

I am indebted to Professor Ali S. Argon for offering me this very interesting project to work on, and for his guidance , support and encouragement all along. He has been mainly responsible for steering the project in the direction it has taken ; this has been a very valuable and satisfying learning process for me . He has been a continuous source of ideas and constructive criticism , and I have benifited immensely from our collaboration. I have been able to freely consult him on various matters, both technical and otherwise; the advice I received was invaluable, and it always left me feeling comfortable. I express my deep appreciation and thanks for all this.

My association with Professor David Parks began when I was a student at Yale ; I have benifitted greatly from interacting with him all along. He has spent many valuable hours of his time in discussions with Professor Argon and me. This project may not have developed into its current form without his guidance, especially in developing the kinematics part of this thesis. By helping us in accessing the finite element method programme, ABAQUS professor Parks has made it possible for us to get very interesting results. For all this , and more , I am very thankful to him.

Throughout my stay at MIT , Professor Stanley Backer has provided immense practical and moral support. His advice and assistance on educational, financial and professional matters has been invaluable. Above all , Professor Backer's genuine personal concern has

been an unfailing source of strength. Mere words cannot express my gratitude for him.

I would like to acknowledge my appreciation to Professor Backer , Professor Erwin and Professor Parks who have kindly served on my thesis committee.

I would like to thank Professor Onat of Yale University , for his help and advice; his private communication with Professor Parks (1981) formed the backbone for the kinematics developed in this thesis.

I thank David Moavenzadeh of Material Science department who was very helpful with my experimental work.

My interest in mechanics was re-kindled when I took the course, The Theory and Practice of Continuum Mechanics , by Professors Bathe and Cleary; I thank them for the benifit I received from my interaction with them. The help and advice given to me by Professor Anand , both in theoritical and experimental matters is much appreciated.

I have had many helpful and enjoyable discussions on various topics with my colleagues ; in particular I express my thanks to Dr. Alan C W Lau , Burhan Ozmat , Gregory Rodin , Jim Papadapaulos and Bill Moffatt.

The support provided for this research from the National Science Foundation is much appreciated.

Finally , I give special thanks to my parents, brother and sister who have provided moral support and encouragement all along. Their concern for my well-being is heart-warming.

This thesis has been typed , and the symbols hand-filled by me; because of the complexity of the mathematical symbols used, it was not possible to have it typed professionally at a reasonable cost. The whole process has been time-consuming and laborious. I sincerely hope there are no typographical errors.

Bharath S Bagepalli
December 9 1983
Cambridge, massachusetts

FINITE STRAIN ELASTIC-PLASTIC DEFORMATION OF GLASSY POLYMERS

by

BHARATH S. BAGEPALLI

Submitted to the Department of Mechanical Engineering on December 9 1983 , in partial fulfillment of the requirements for the degree of Doctor of Science in Mechanical Engineering .

ABSTRACT

A deforming glassy polymer is seen as overcoming two basic resistances: 1) a short-range elastic resistance due to the flexing of van der Waals interactions ; and , on overcoming these interactions at the onset of plastic flow , 2) a rubbery resistance due to configurational entropy change in the unwinding macromolecules . " Locking " behaviour is seen as the molecules orient themselves sufficiently .

An incremental constitutive law , via a finite-strain formulation using an updated-Lagrangian approach has been developed . The total deformation gradient is decomposed into the elastic and plastic components . The applied Cauchy stresses are determined in terms of the elastic deformation gradient , and , the rubbery resistances or back stresses are determined in terms of the plastic deformation gradient . A kinematically hardening yield function employing a Mises type of yield criteria is assumed . A pressure and rate independent formulation is developed . Incremental plastic deformation is assumed to follow normality . Since elastic strains for glassy polymers could be large , all quantities have been evaluated to include effects to the order of elastic strains .

After incorporating the constitutive model in the finite element method programme , ABAQUS , two boundary value problems were tried , for two different polymers , polycarbonate and polystyrene: 1) the formation and propagation of a neck in a round bar in tension; and 2) the drawing of a polymer out of a half-space , to model the drawing of a craze-tuft. Some experiments were done on polystyrene above Tg to examine its rubbery behaviour ; and on a round polycarbonate rod to determine its necking characteristics , to be compared with the computed results , and favourable agreement was found .

Thesis Supervisor: Professor Ali S. Argon
Title: Quentin Berg Professor of Mechanical Engineering

TABLE OF CONTENTS

INTRODUCTION . FINITE STRAIN ELASTIC-PLASTIC DEFORMATION OF GLASSY POLYMERS

A typical amorphous polymer is made up of a random network of macromolecules ie., polymer chains , consisting of entanglements and , perhaps in some cases , crosslinks as well (Fig. 1.1) . An amorphous polymer is considered as glassy at a temperature below its glass-transition temperature , Tg , where it has much higher stiffness , than at temperatures above Tg (see Fig. 1.2).

In the initially unloaded or annealed state, a glassy polymer can be considered homogeneous and isotropic . On loading , recoverable (elastic) flexing occurs , governed by the van der Waals interaction between chains . Chain configurations are mostly unchanged when a glassy polymer is elastically flexed (Argon, 1976). With larger strains molecular segment rotations can occur , causing the polymer to yield . A polymer could suffer large strains (- over 400 percent) , with the chains thus undergoing gross changes in configuration without rupturing. This constitutes plastic deformation . The uniqueness of glassy polymers is that the memory of the initially unstrained state is retained . A return to the initial undeformed state from the highly strained state is possible by heating the polymer above Tg , provided that no gross chain slippage or rupture has occured in the network of macromolecules .

Physically , a deforming glassy polymer is seen as overcoming two basic resistances: one due to the intermolecular van der Waals interaction , and the other

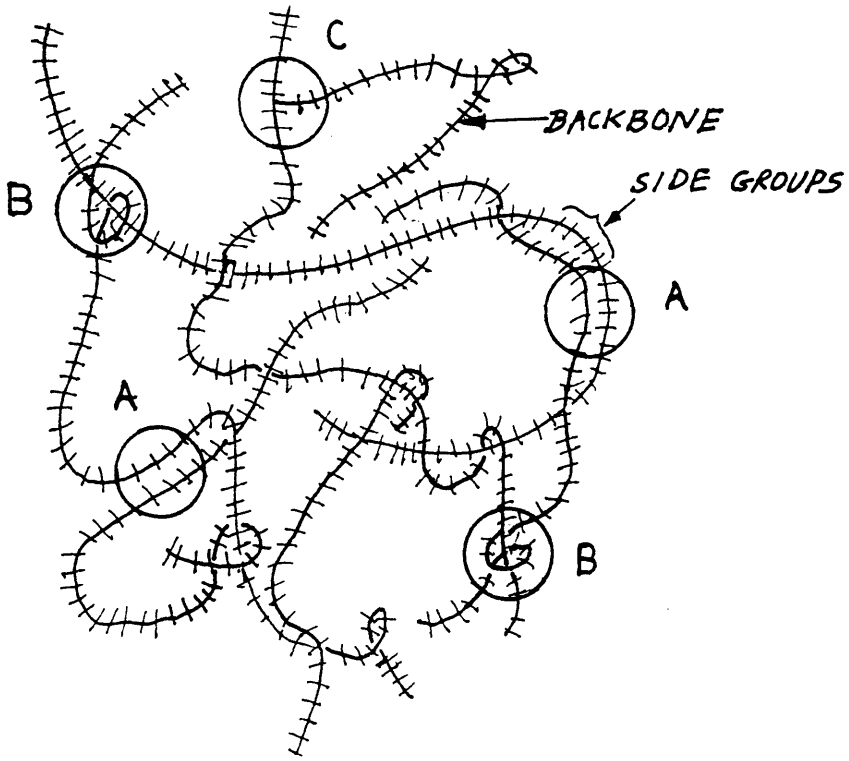

A = weak bonds (Van der Waal)

B = entanglements

C = cross links (rare)

Figure I.1 : Microscopic view of a glassy polymer

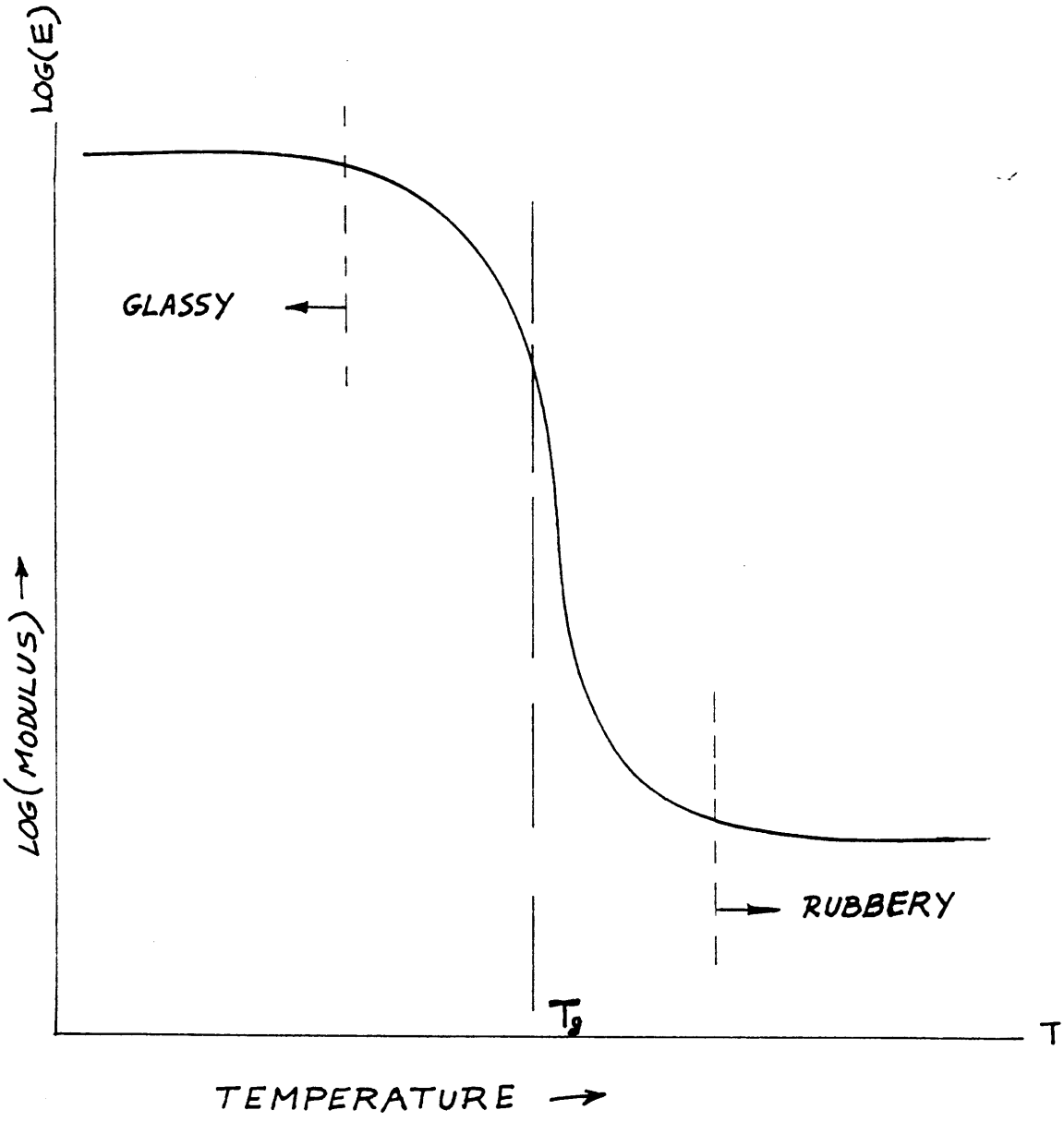

Figure I.2 : The glass transition temperature (Tg) .

due to the configurational entropy of the unfolding chains; the latter resistance is similar to that in a deforming rubber . When elastic-plastic deformation occurs ,initially the van der Waals interactions which offer the usual small scale elastic response are overcome , and finally we have the plastic response wherein small segments of the macromolecules undergo large rotations thus changing the configurational entropies of the chai .s . The accumulating orientational order constitutes an additional entropic or rubbery resistance .

In the following chapters , we see how these basic phenomena are interpreted to develop a constitutive model for the elastic-plastic deformation of glassy polymers .

In Chapter 1 , the physics of the deformation of glassy polymers is covered . For illustration , a simple case of triaxial stretching is viewed in principal coordinates .

Chapter 2 deals with " total quantities " associated with finite strain elastic-plastic analysis, including kinematics and associated stresses and state variables .

Chapter 3 deals with " incremental quantities " associated with finite strain elastic-plastic analysis . Here we see the development of evolution laws relating incremental deformations with incremental streses and state variables .

In Chapter 4 a method has been developed for dealing with rigid-body rotations between states of

deformation , wherein ,we update stresses and state variables without any integration by means of orthogonal transformations .

In Chapter 5 we demonstrate how we update stresses, state variables etc. via the evolution laws developed in in Chapter 3 , yet satisfying all the kinematic and constitutive constraints described in Chapters 3 and 4 . A method of forward integration with " constrained perturbations " during a gradient return is developed .

In the early part of Chapter 6 we see how the above development , after being coded up as a computer programme , was tested for its validity before being incorporated in the " Finite Element Method " programme , ABAQUS . Finally , we use ABAQUS to the solution of two basic boundary value problems: a) The steady growth of a neck in an axi-symmetric " uniaxial-tension " specimen , and , b) the drawing of a polymer tuft out of a half-space, which is the central problem in the thickening of crazes in glassy polymers . Comparisons are made with some experimental results on polycarbonate . We end Chapter 6 with some concluding remarks .

CHAPTER 1: THE PHYSICS OF THE DEFORMATION OF GLASSY POLYMERS

1.1 The Growth of Necks and Crazes

Consider a polymer in a " Uniaxial Tension " test as in Fig. 1.1 in which a typical load vs. elongation curve is shown. There is a region of initial elastic response followed, at "a" , by a lowering of slope, when localized plastic flow begins to occur. At or near the load-max point "b", a neck begins to form on the specimen and continues to reach stable proportions at "c", at which point the localized neck section ceases to grow smaller in diameter. Deformation beyond "c" causes the neck to extend its length at a nearly constant load. This phenomenon known as the " stable growth of a neck ", is unique to many polymers, and such isothermal behaviour is not exhibited by metals.

One of the reasons for this stable growth of a neck in polymers resides in their macromolecular nature. As the neck extends, the macromolecules in the neck begin to orient themselves parallel to the load axis and thus offer greater resistance as deformation progresses. At the point "c" in Fig.1.1 , the load to cause further deformation in the neck becomes equal to that to plastically propogate the shoulder. We thus achieve a steady drawing process .

Hence we see that the increased resistance to flow with deformation in the necked region is responsible for the stable growth of a neck. In such stable

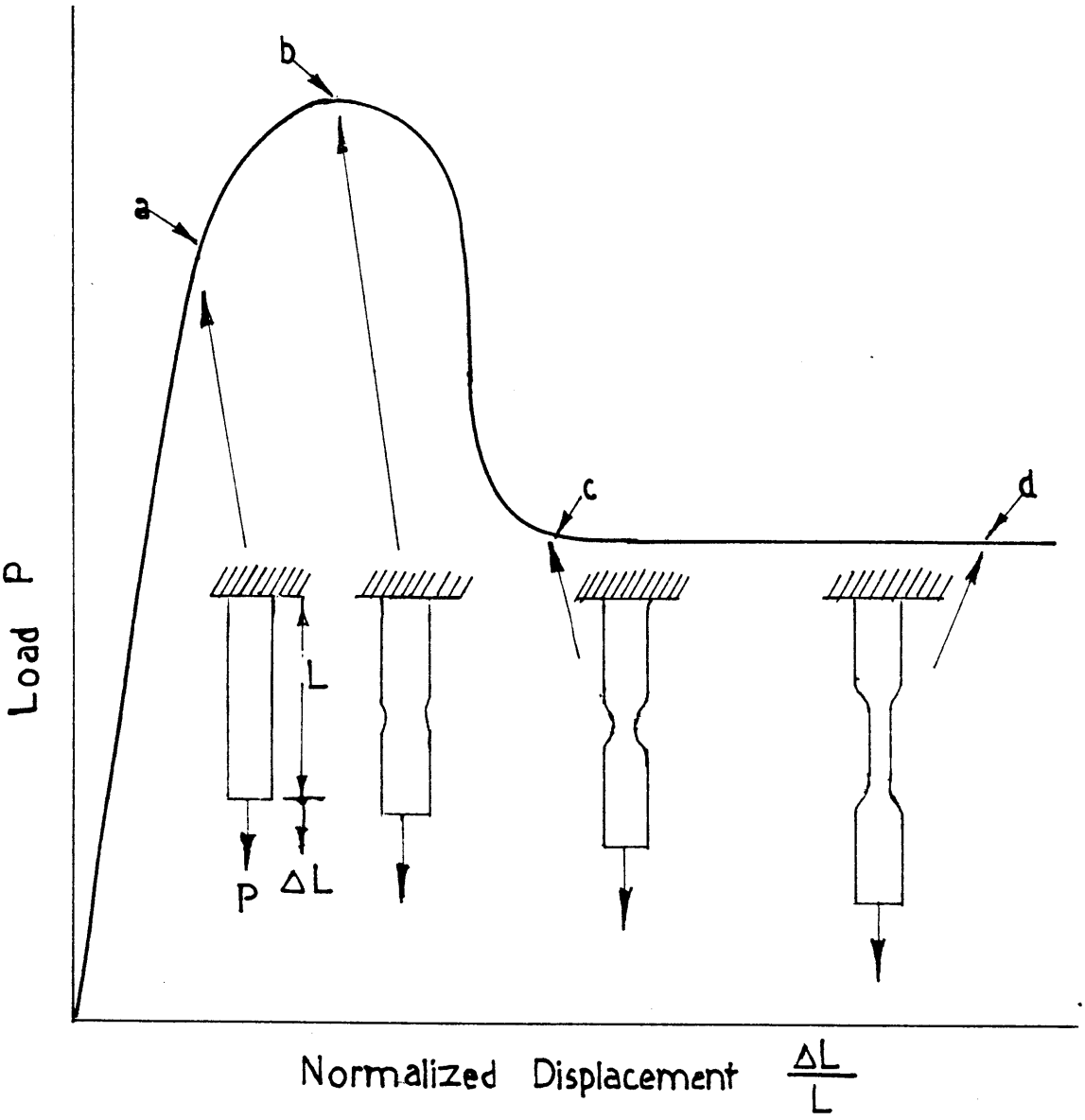

Figure 1.1 : Glassy polymer in a uniaxial tension test.

growth, it is the shoulder that suffers continuing deformation, thus adding to the length of the neck. The neck in effect consumes material from the shoulder region as it grows with increasing imposed displacement (point "d" in Fig.1.1).

A parallel phenomenon to the one described above, is observed in the stable thickening of crazes (see Fig.1.2). Crazes are crack-like entities in glassy-polymers, but unlike cracks in metals, they contain highly drawn tufts or fibrils of polymer bridging the two craze surfaces. These craze-tufts are akin to the neck described above. As a craze grows at a constant far-field stress, the fibrils are thought to extend in length and consume material from the craze flanks. One of the objectives of this study is to model one such craze tuft and to observe its growth pattern.

One approach to the study of above mentioned two phenomena is to model the constitutive behaviour of glassy polymers taking into account their macromolecular nature. Others such as Hutchinson and Neale (1983) have used phenomenologicl models .

1.2 Simple Case of Stretching

Consider the state of deformation of a glassy polymer as shown in Fig.1.3 . The initially undeformed state with stretches (1,1,1) is deformed to stretches

$$(\lambda_1, \lambda_2, \lambda_3)$$

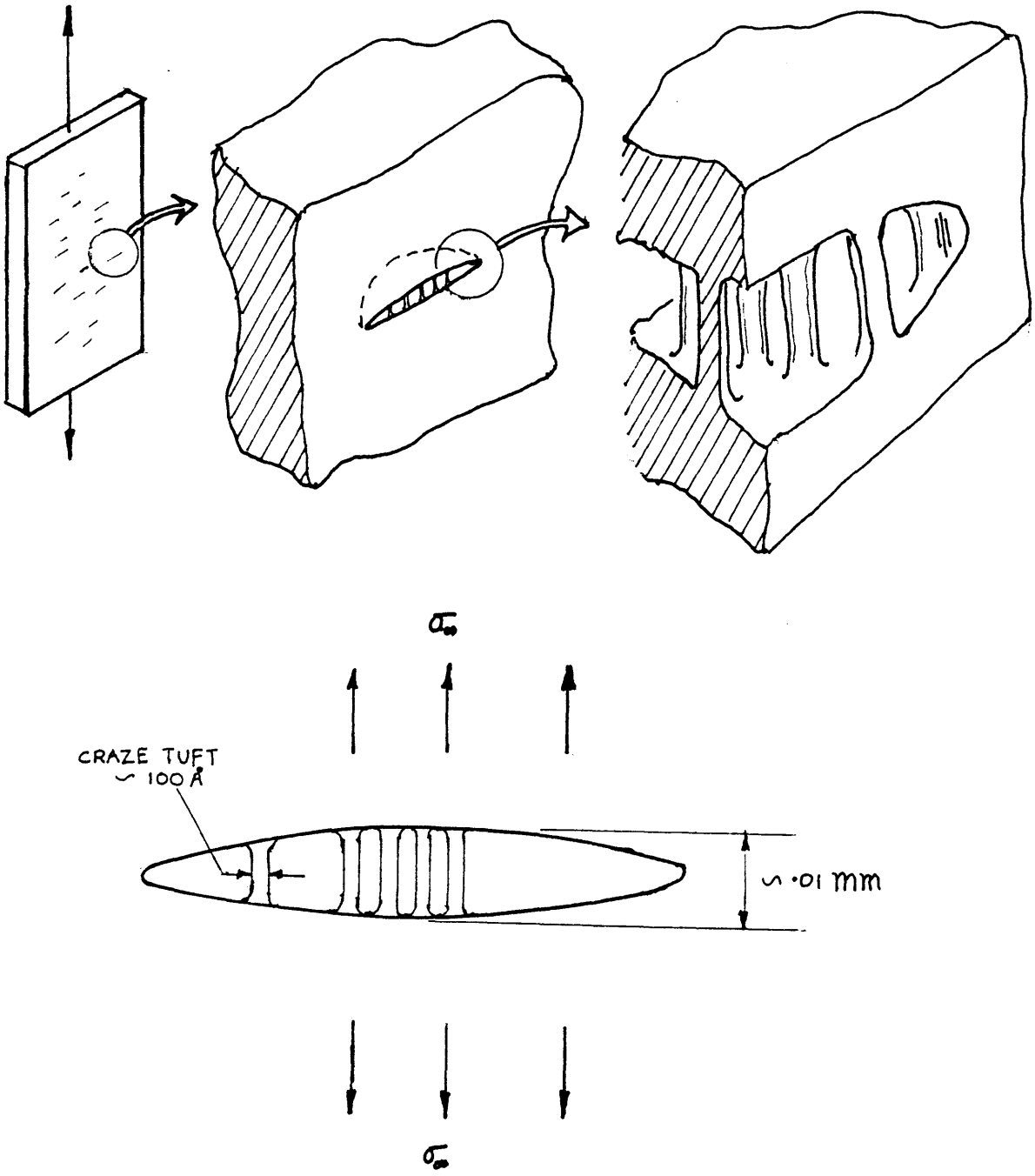

Figure 1.2 : Craze growth in glassy polymers.

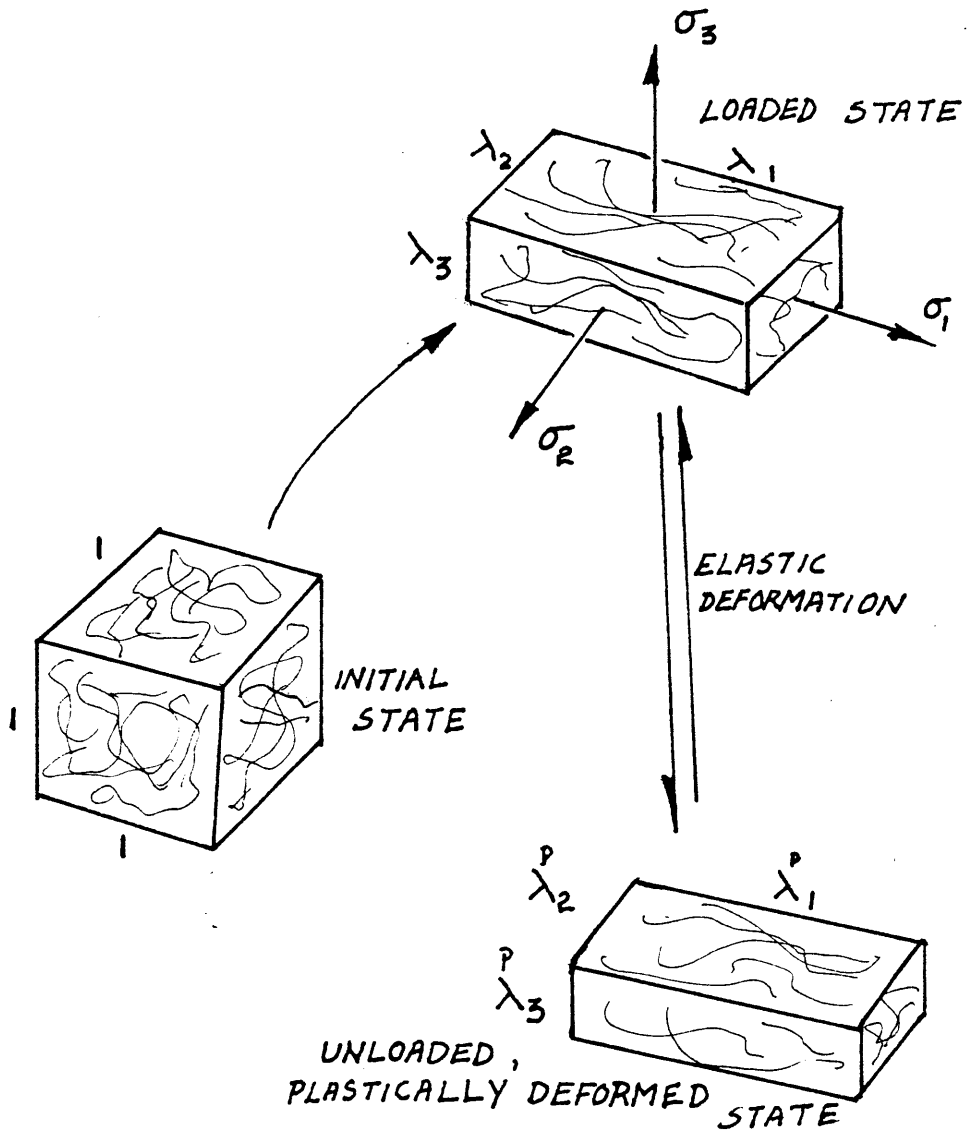

Figure 1.3 Simple case of triaxial stretching.

with applied principal Cauchy stresses

$$(\sigma_1, \sigma_2, \sigma_3)$$

Consider now, an elastically unloaded configuration with stretches

$$(\lambda_1^p, \lambda_2^p, \lambda_3^p)$$

which is the plastically deformed, load-free state. If plastic deformation occurs nondilationally as we have assumed in our case, then the product

$$(\lambda_1^p \lambda_2^p \lambda_3^p) = 1 \qquad (1.2.1)$$

In general we also have

$$\lambda_i = \lambda_i^e \lambda_i^p \qquad (\text{no sum}) \quad (1.2.2)$$

where

λ_i^e = the elastic stretch

λ_i^p = the plastic stretch

λ_i = the total stretch

1.3 The Plastic State

Let us now examine the elastically unloaded plastically deformed state ie., the " Plastic State " at a temperature below the glass-transition temperature,

Tg. If this unloaded piece were heated to above Tg as a " thought experiment " , it would begin to regain its initial plastically undeformed configuration shown in Fig.1.3 . If however, the piece is constrained to retain its dimensions at

$$(\lambda_1^p, \lambda_2^p, \lambda_3^p)$$

while heated above Tg, (neglecting thermal stress and viscous effects) we would then have to apply the tractions

$$(\sigma_1^B, \sigma_2^B, \sigma_3^B)$$

as illustrated in Fig. 1.4 . The tractions,

$$\underset{\sim}{\sigma}^B \ ,$$

are termed, the " Back Stresses " , or " Rubbery Resistances ", the latter term being used since at a temperature above Tg, a high molecular weight polymer is observed to behave like a rubber.

The Back Stress can in fact be determined by viewing the polymer (above Tg) as a rubber trying to regain its initial configuration where the polymer chains are random with no preferred orientation.

In the following sections we will obtain expressions for the back stresses using the following procedure : Initially we will use the statistical thermodynamics of rubber elasticity on the plastic state above Tg. Finally we assume that the rubbery resistances thus obtained would prevail below Tg as well .

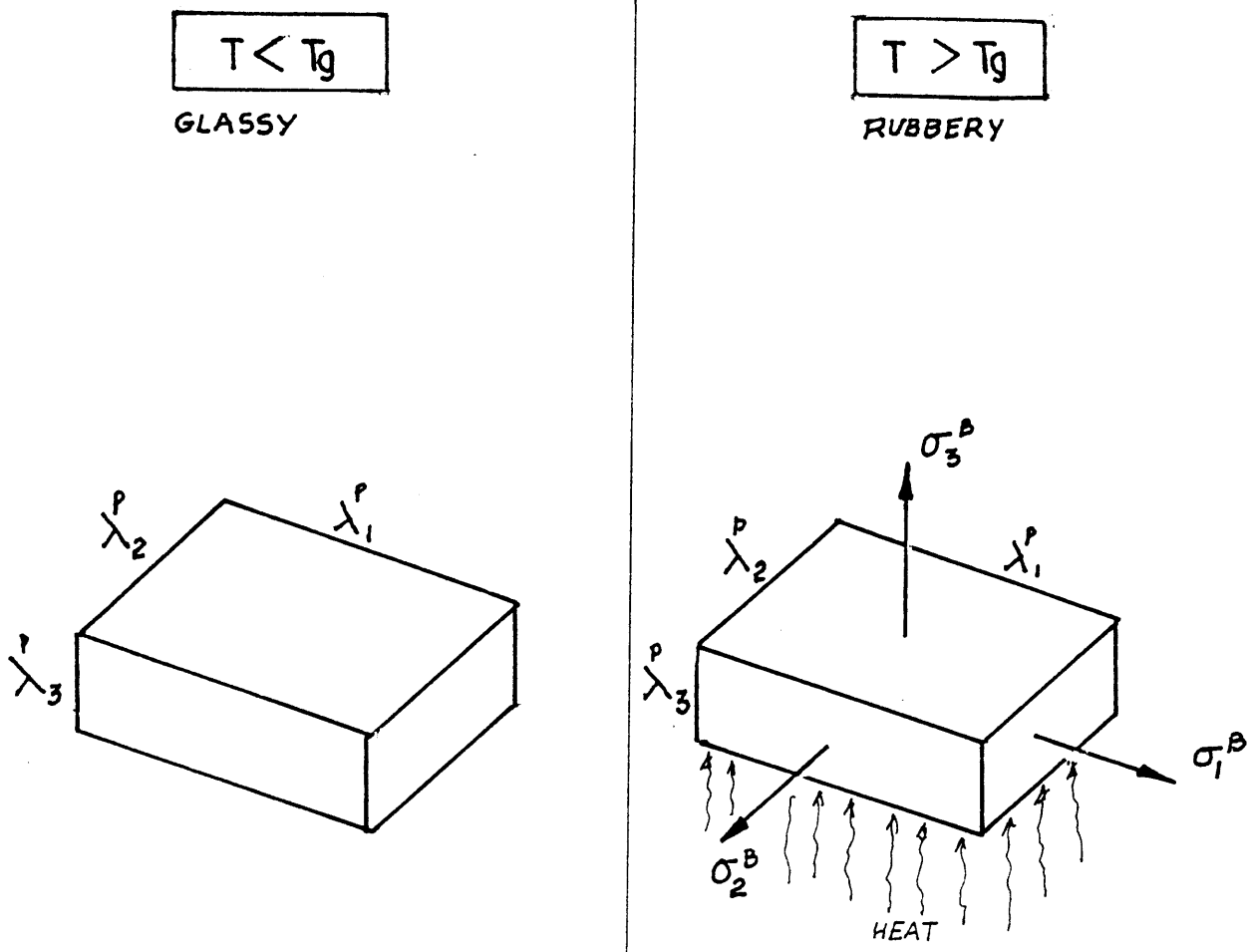

Figure 1.4 : The plastically deformed state.

1.4 Rubbery Resistances in Terms of the Plastic Stretches

The Three-Chain Model

Consider the plastic state with stretches

$$(\lambda_1^p, \lambda_2^p, \lambda_3^p)$$

We assume that the macro deformations are affine and relate to local processes directly . Initially, the network of chains is random, and there exists a typical entanglement distance , r_0 , in space obtained interms of the link length, L, and the number of links, N , between entanglements as in Fig.1.5 , (Treloar , 1975). We have

$$r = N^{\frac{1}{2}} L \ . \qquad (1.4.1)$$

This is based on the probability of finding two entanglements of a chain, a distance r_0 apart; the distribution is Gaussian at small strains. As the chain is stretched, the distance between entanglements changes. Affine deformation implies that along a direction with a stretch ratio

$$\lambda_i^p$$

the new entanglement distance is

$$r_i = \lambda_i^p r_0 \qquad (1.4.2)$$

At moderate stretches, however, we no longer have a Gaussian chain , but a non-Gaussian chain ; the

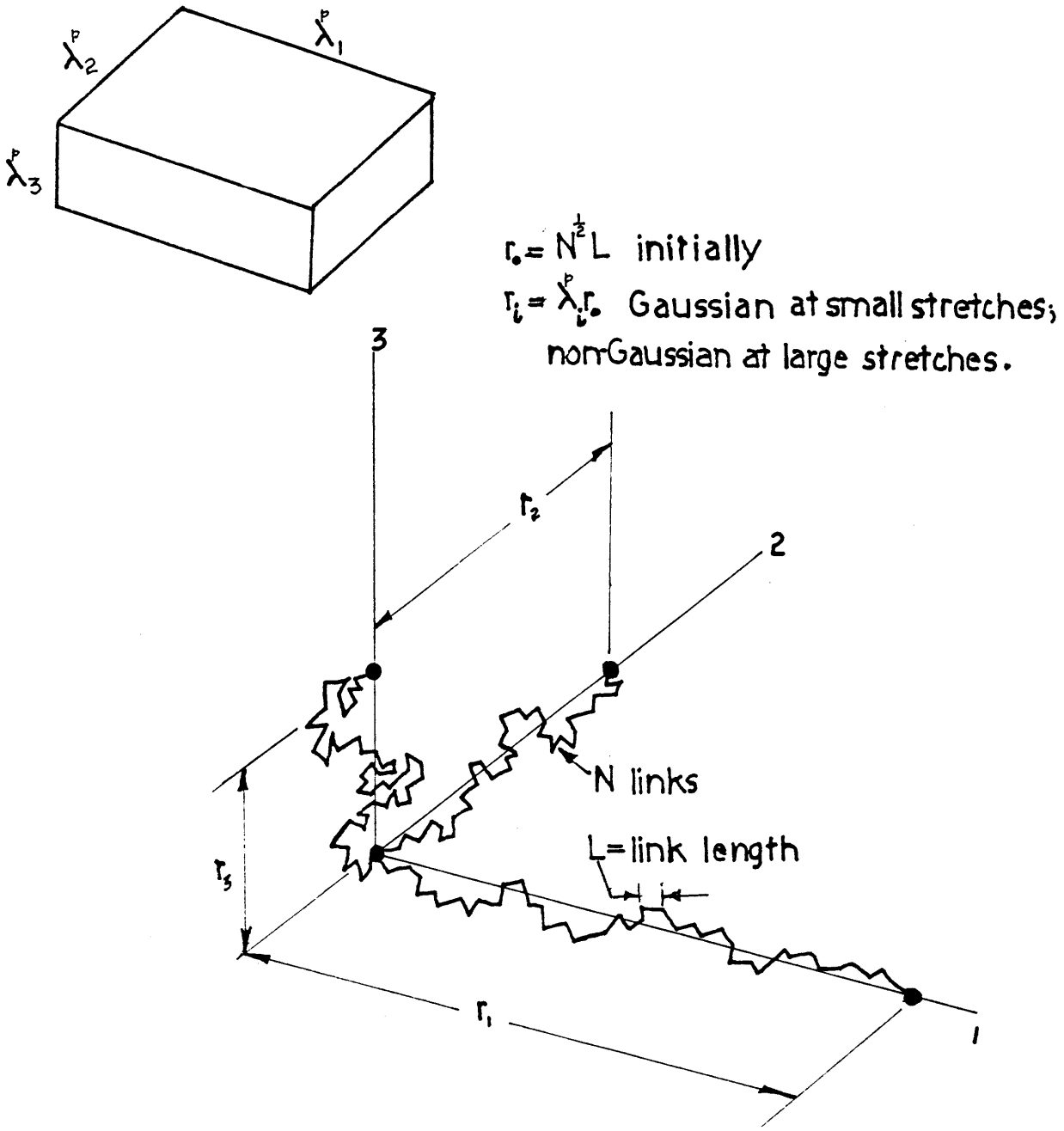

Figure 1.5 : The Three-Chain Model - affine deformations.

probability of finding a highly stretched chain diminishes, and finally, that of finding one fully stretched (ie. a stretched length of NL), is zero.

As a chain is stretched from r_o to r_i , its configurational entropy changes. The configurational entropy for a chain with the entanglement distance r , is

$$S = \mathrm{Ln}(P(r)) \qquad (1.4.3)$$

where P(r) is the probability of finding the entanglements of a chain, a distance r apart. Hence ,in stretching from r_o to r_i , a chain suffers a configurational entropy change of

$$\Delta S = \mathrm{Ln}(P(r_o)/P(r_i)) \qquad (1.4.4)$$

Thus, in the three-chain model we see the plastically deformed polymer as having three sets of chains whose entanglement distances are (r_1 , r_2 , r_3) along the principal plastic stretches ,

$$(\lambda_1^p , \lambda_2^p , \lambda_3^p)$$

1.5 Free Energy

In a thermodynamic system the Helmholtz free energy is

$$F = U - TS \ , \qquad (1.5.1)$$

where U is the internal energy, T, the absolute temperature in degrees Kelvin, and S, the entropy. Hence, for the plastic state described earlier, we have for free energy change,

$$\Delta F = U - S\Delta T - T\Delta S \quad . \qquad (1.5.2)$$

The change in internal energy between two plastically deformed states is usually negligible compared with the energy change due to the change in configurational entropy. This , however , may not be the case at stretches approaching the network stretch of the polymer . Hence at a constant temperature,

$$\Delta F \doteq - T\Delta S \quad . \qquad (1.5.3)$$

In a deforming rubber , the applied stresses are obtained as the gradient of free energy with strain. We have for the Rubbery Resistances in the plastic state above Tg , using Eq. 1.4.3 , as

$$\sigma_i^R = \frac{\partial F}{\partial \varepsilon_i^P}$$

$$= -T \lambda_i^P \frac{\partial S}{\partial \lambda_i^P} \qquad (1.5.4)$$

In a plastically deformed glassy polymer we have seen that chain configurations are changed . Hence the rubbery resistances in the plastic state <u>above</u> Tg , as in Eq. 1.5.4 , are taken to act <u>below</u> Tg as well.

In Appendix A we have derived expressions for the back stresses for the general case of the deformation of a glassy polymer , based on the above development. Thus, with plastic stretches

$$(\lambda_1^p, \lambda_2^p, \lambda_3^p)$$

we have the following for the back stresses , shown here in the deviatoric form :

$$\sigma_1^B = C^R \frac{\sqrt{N}}{3} \left(\lambda_1^p \mathcal{L}^{-1}\left(\frac{\lambda_1^p}{\sqrt{N}}\right) \cdot \frac{2}{3} - \left(\lambda_2^p \mathcal{L}^{-1}\left(\frac{\lambda_2^p}{\sqrt{N}}\right) + \lambda_3^p \mathcal{L}^{-1}\left(\frac{\lambda_3^p}{\sqrt{N}}\right) \right) \cdot \frac{1}{3} \right) \qquad (1.5.5)$$

where the modulus C^R has units of stress (see Appendix A).

Typical plots of σ_1^B vs. λ_1^p for two values of N are shown in Fig. 1.6 , for the case

$$\lambda_1^p = \frac{1}{(\lambda_2^p)^2} = \frac{1}{(\lambda_3^p)^2} \quad .$$

" Locking " behaviour ie., an upturn in the curve , is seen as we approach a limiting network stretch ,

$$\lambda_1^p \rightarrow \sqrt{N} \quad .$$

1.6 The Applied (Cauchy) Stresses

In Appendix B we have derived expressions for the applied Cauchy stresses, $\underline{\underline{\sigma}}$,

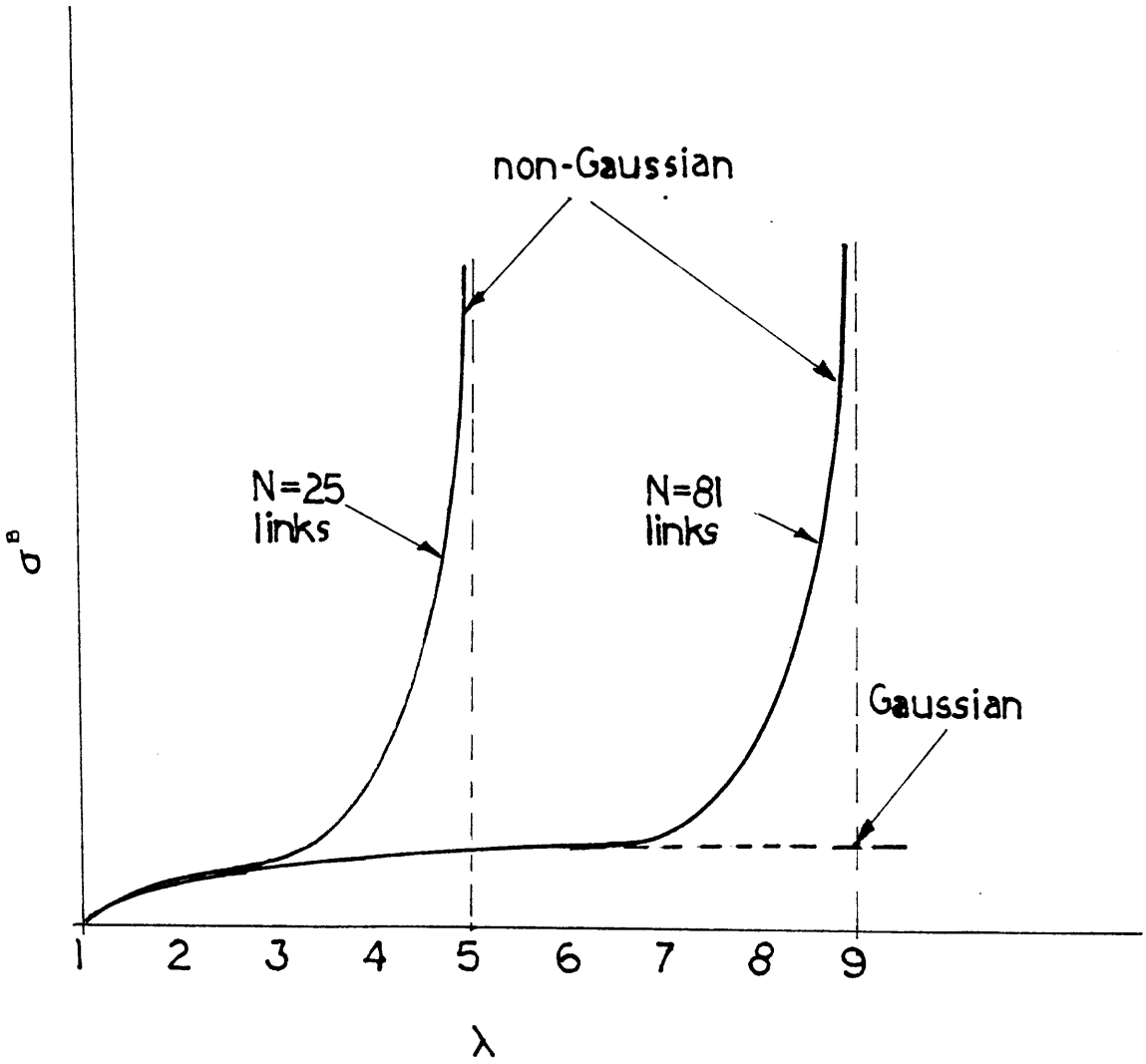

Figure 1.6 : The back stress vs. plastic stretch.

for the general case of the deformation of a glassy polymer. We can thus find the applied (Cauchy) stresses,

$$(\sigma_1 , \sigma_2 , \sigma_3) \quad ,$$

in terms of the elastic stretches (see Eq.1.2.2),

$$(\lambda^e_1 , \lambda^e_2 , \lambda^e_3) \quad ,$$

using logarithmic strain measures. Based on Appendix B, we have for principal elastic strains ,

$$\varepsilon^e_i = \mathrm{Ln}(\lambda^e_i) \qquad (1.6.1)$$

Thus the principal Cauchy stresses are

$$\sigma_i = \frac{E}{\lambda^e_1 \lambda^e_2 \lambda^e_3} \cdot \left\{ \frac{\varepsilon^e_i}{(1+\nu)} + \frac{\nu \cdot (\varepsilon^e_1 + \varepsilon^e_2 + \varepsilon^e_3)}{(1+\nu)(1-2\nu)} \right\} \qquad (1.6.2)$$

ie.,

$$\sigma_i = \frac{\tau_i}{\lambda^e_1 \lambda^e_2 \lambda^e_3}$$

where,

$$\underset{\sim}{\tau}$$

are the Kirchhoff stresses , and the small strain elastic constants are ,

$$E = \text{Young's modulus}$$

$$\nu = \text{Poisson ratio}$$

The stresses in Eq. 1.6.2 follow from the assumption that Kirchhoff stresses are work-conjugate to log-strains , up to moderate stretches of about 1.4 ,

(Anand , 1979).

1.7 The Net Result

We now assume that the material has a Mises type of flow resistance, remaining approximately constant with plastic deformation and, a rubbery resistance changing with plastic strains ie., with chain reorientation. Plastic deformation occurs when the magnitude of the applied stress to overcome both these resistances simultaneously , ie., when the difference between the applied stress and the rubbery resistance reaches a critical value .

Physically, this means that in uniaxial tension for example, the material would have a true-stress vs. stretch behaviour as represented in Fig. 1.7 . In this we see that the behaviour of the polymer (the net curve), is the " sum " of two curves : one representing elastic + perfectly-plastic behaviour, and the other, rubbery behaviour.

Further, we have seen from experiments the yield stress can be continually lowered by increasing the temperature up to Tg where the plastic resistance should disappear. At a temperature a little above Tg ,ideally no Mises resistance should remain, and the polymer should behave like a rubber. Thus Fig. 1.8 illustrates the constitutive behaviour of a polymer at two typical temperatures : one, a little below Tg , the other, a little above Tg . These two respectively represent the following behaviour : (1) linear-elastic + nonlinear- kinematically

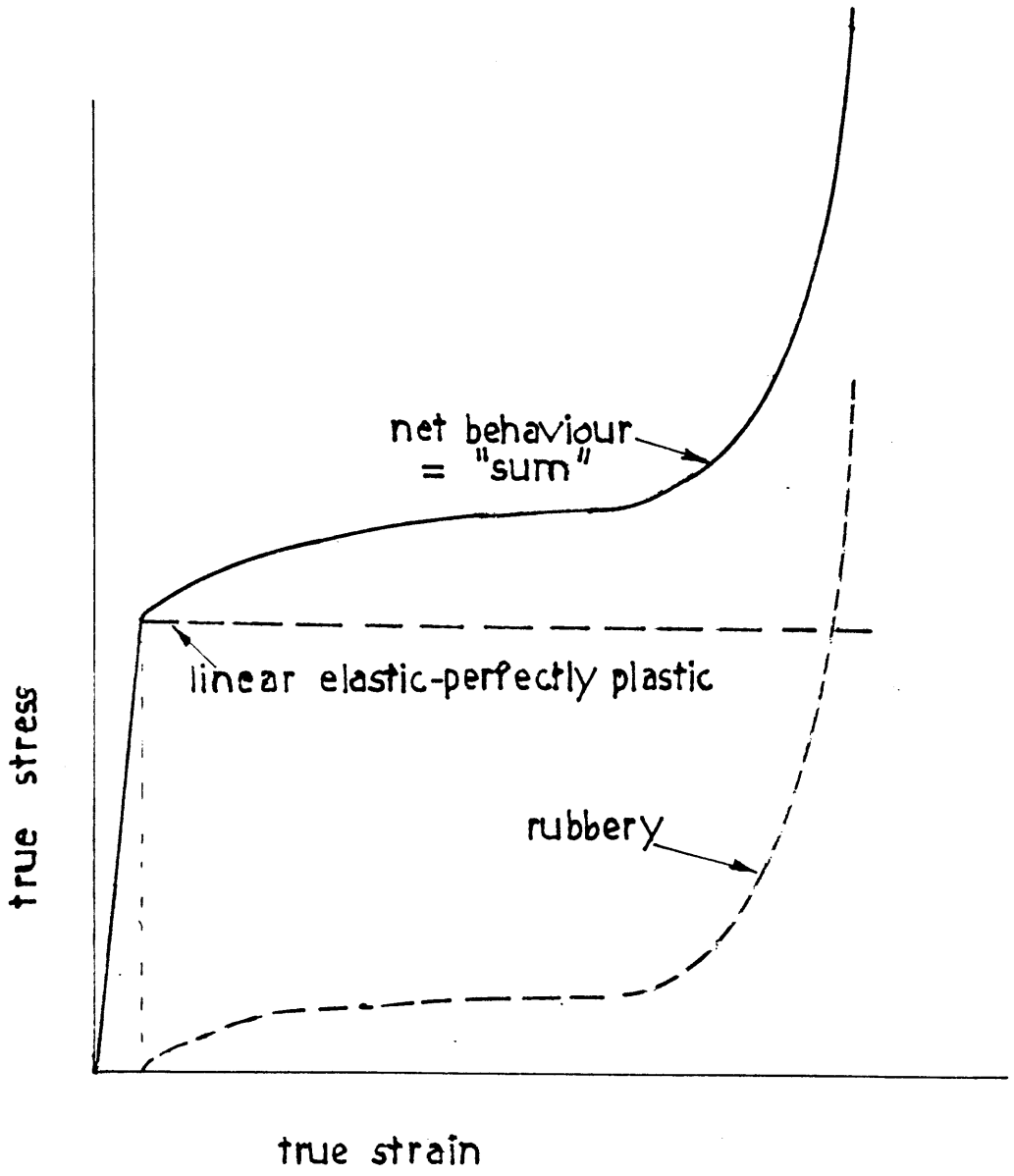

Figure 1.7 : The net true-stress vs. true-strain behaviour of glassy polymers .

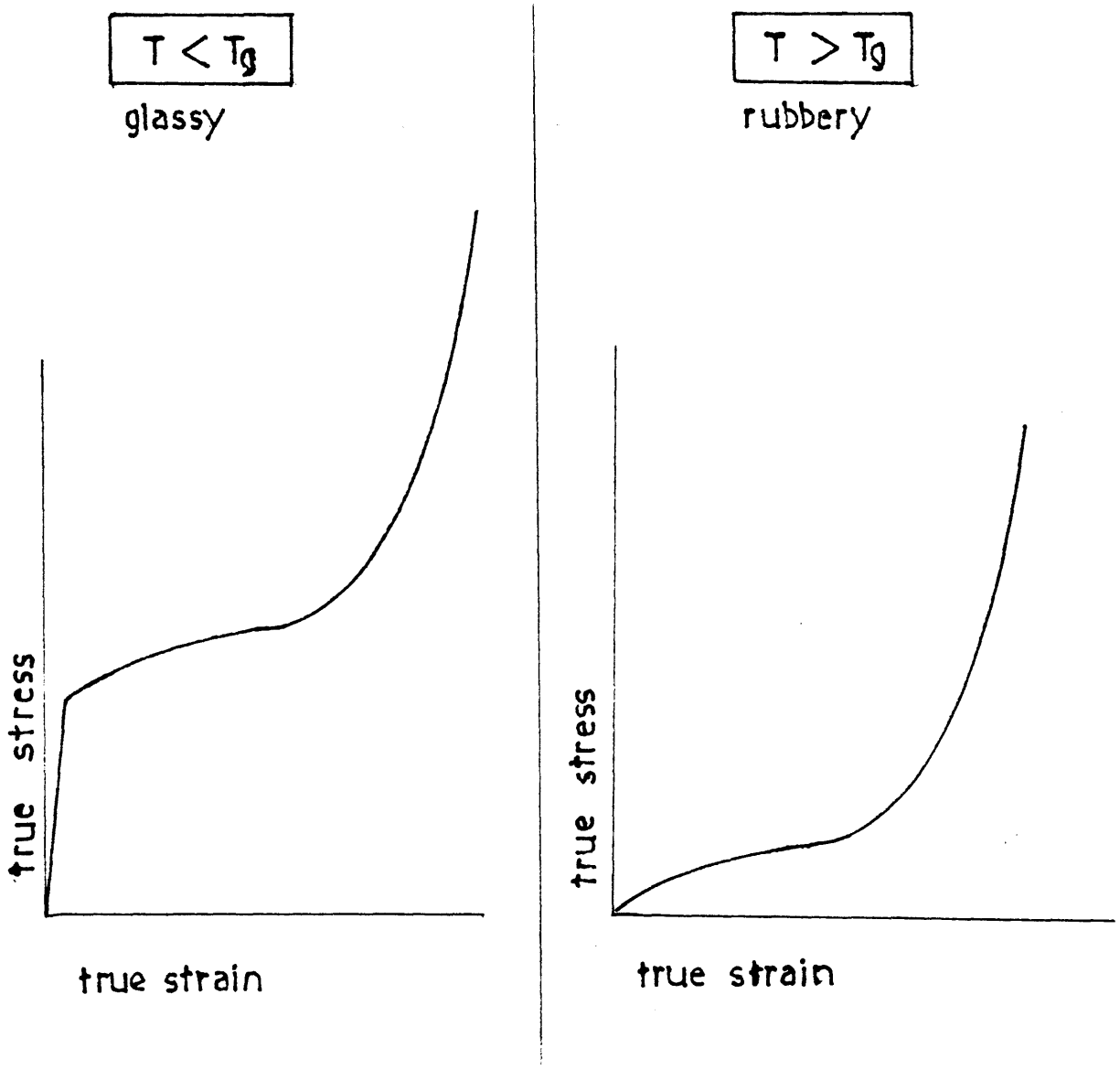

Figure 1.8 : The constituve behaviour of a glassy polymer in uniaxial tension, below Tg (left) and above Tg (right).

hardening plastic and ,(2) nonlinear-elastic or rubbery. The behaviour of a glassy polymer is idealized as the former.

Actual tests show that most polymers have a little rate-sensitivity at temperatures near or above Tg . Figure 1.9 shows the true-stress vs. stretch curve obtained in a load-unload experiment on polystyrene at 113 C (ie. about Tg + 15 C) , revealing a strong hysterisis effect . This is somewhat influenced by the loading rate that was employed and would change with it . At this temperature , however , instabilities are suppressed because , at all points on the stress-strain curve (in a one-dimensional Considere representation),

$$\frac{\partial \sigma}{\partial \varepsilon} > \sigma \qquad (1.7.1)$$

This is one reason why a test conducted at T < Tg will not give the true stress-stretch curve predicted in Fig. 1.8 , because necking instability would set in early in the test (at " b " in Fig. 1.1) , after which all the deformation would localize in the neck and shoulders as described in Ch. 1.1 . This is observed even at temperatures a little above Tg as is seen in Fig. 1.10 , in which we see the load vs. displacement curve for polystyrene at 105 C .

We can obtain the locus " C ", of instability points as defined by the inequality in Eq. 1.7.1 , with lowering yield stress (ie. increasing temperature from below Tg) as shown in Fig.1.11 . On any given curve we

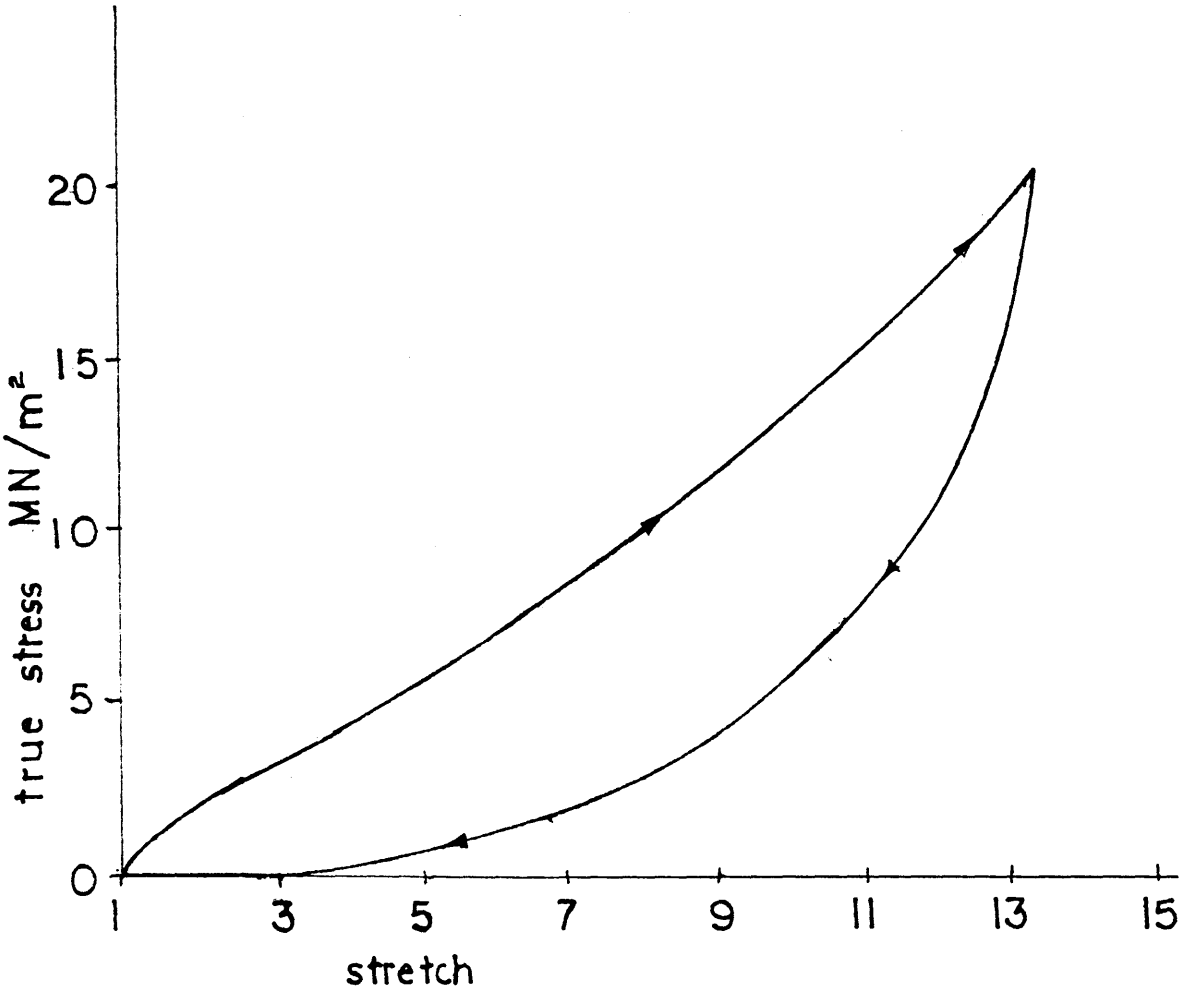

Figure 1.9 : Uniaxial tension test on polystyrene at 113°C .

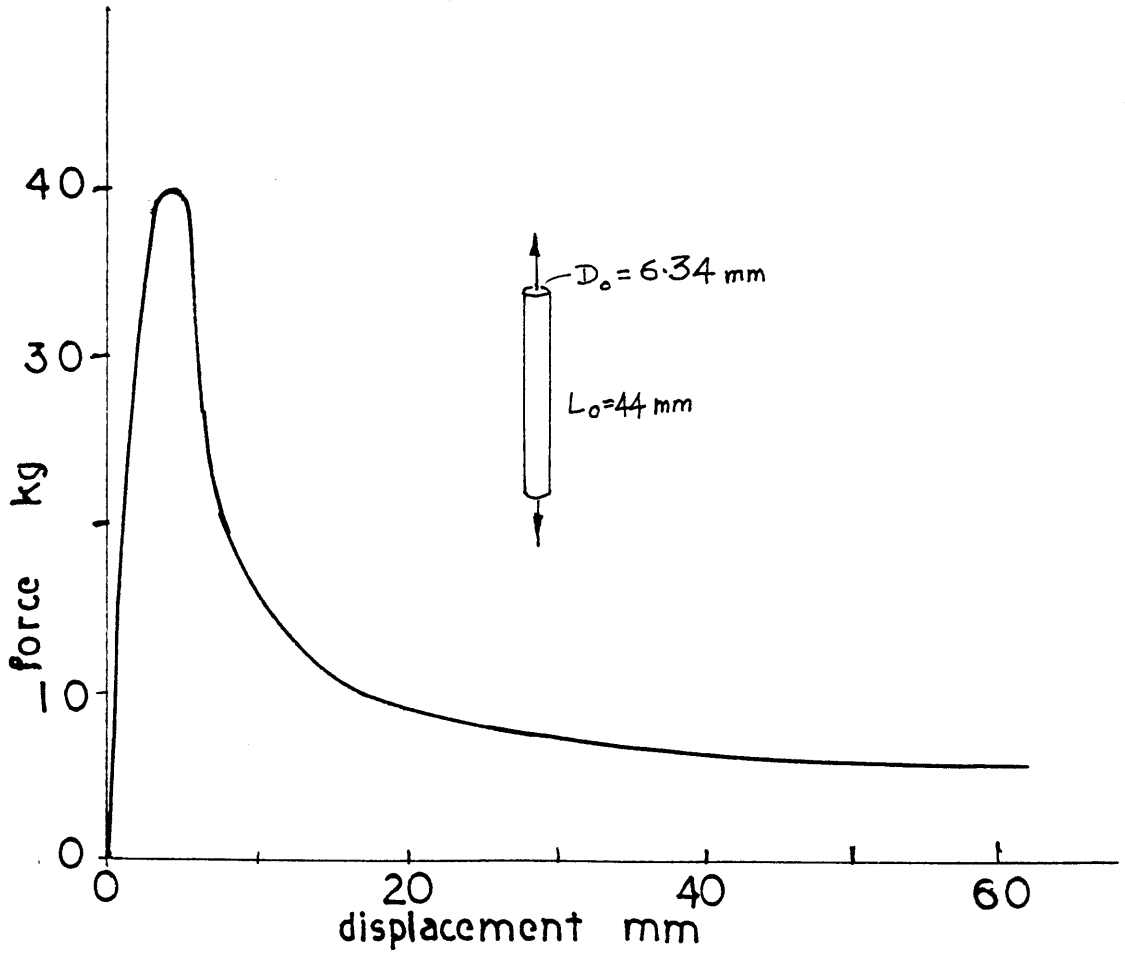

Figure 1.10 : Tension test on polystyrene at 105 C
-- load vs. extension .

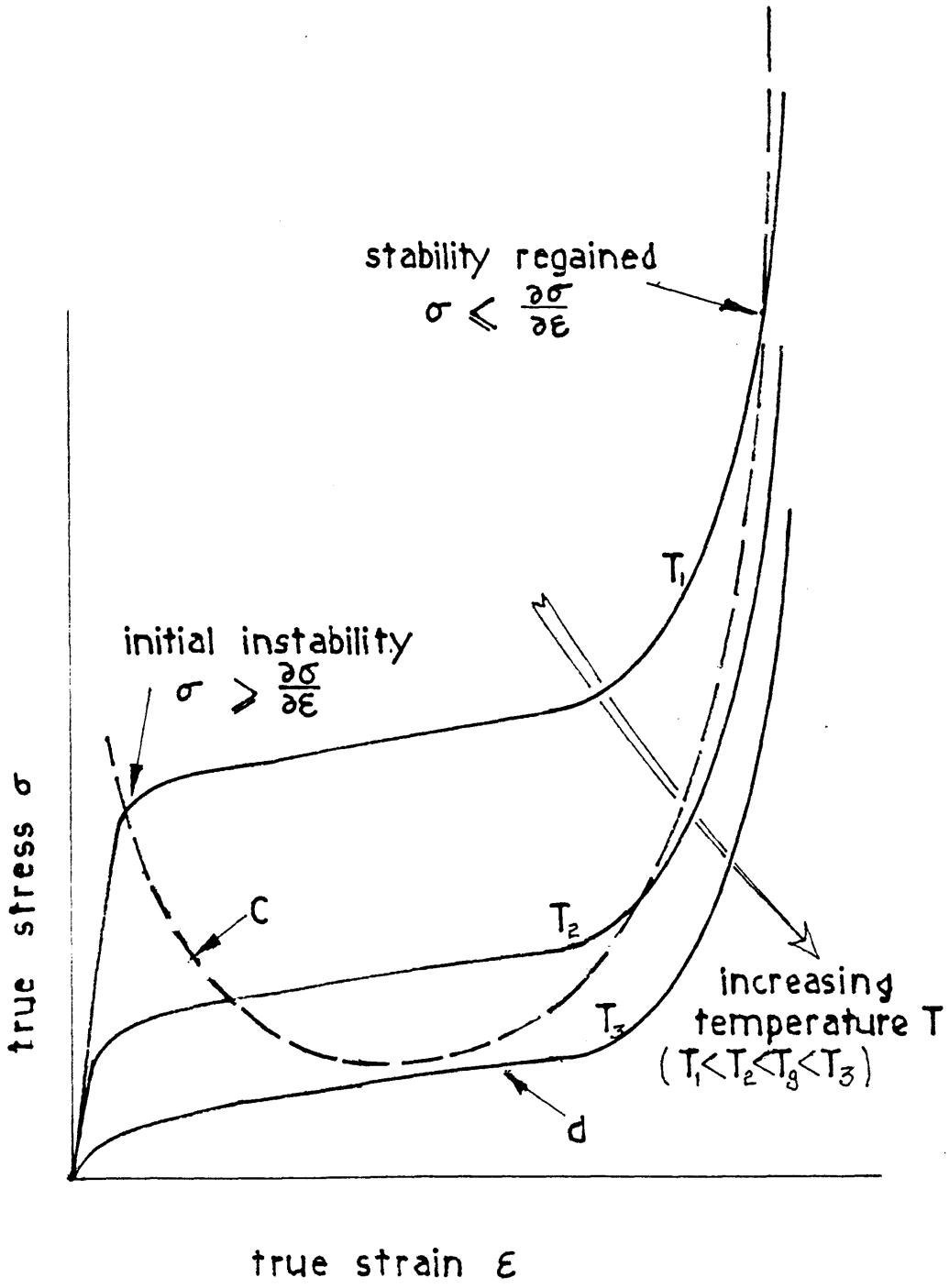

Figure 1.11 : Instability in tension tests on polymers .

have an initial point where instability is reached, and a final point where we regain stability , ie., when

$$\sigma \leq \frac{\partial \sigma}{\partial \varepsilon} \quad ,$$

because of the " locking " behaviour of polymers ie., the upturn in the stress-stretch curve . The curve in Fig. 1.9 was obtained from a test done at a temperature which lowered the yield stress , resulting in the true stress vs. stretch curve lying fully below the locus " C " as for example , curve " d " in Fig. 1.11 . We have avoided any necking instability necking , and thus in effect , obtained a truly uniaxial homogeneous stress field throughout the specimen for the entire duration of the test.

CHAPTER 2: FINITE STRAIN ANALYSIS -- TOTAL QUANTITIES

2.1 Kinematics

In Chapter 1 we saw the physics of deformation for the special case of principal stretches without rotations . Here we shall develop the mathematical equations to describe the most general case of deformations . Let us first define the following quantities (see Fig. 2.1):

$^{0}\underset{\sim}{x}$ = initial undeformed geometry (vector) at time = 0

$^{t}\underset{\sim}{x}$ = final deformed geometry (vector) at time = t

$^{t}\underset{\sim}{x}^{p}$ = plastically deformed geometry (vector) at time = t
ie. , this is the state elastically unloaded from $^{t}\underset{\sim}{x}$ without rotations

$^{t}\underset{\approx}{F}$ = deformation gradient (tensor) at time = t

$$= \frac{\partial\, ^{t}\underset{\sim}{x}}{\partial\, ^{0}\underset{\sim}{x}} \qquad (2.1.1)$$

Decomposition

Dropping the superscript " t " for clarity, let us use the following decomposition :

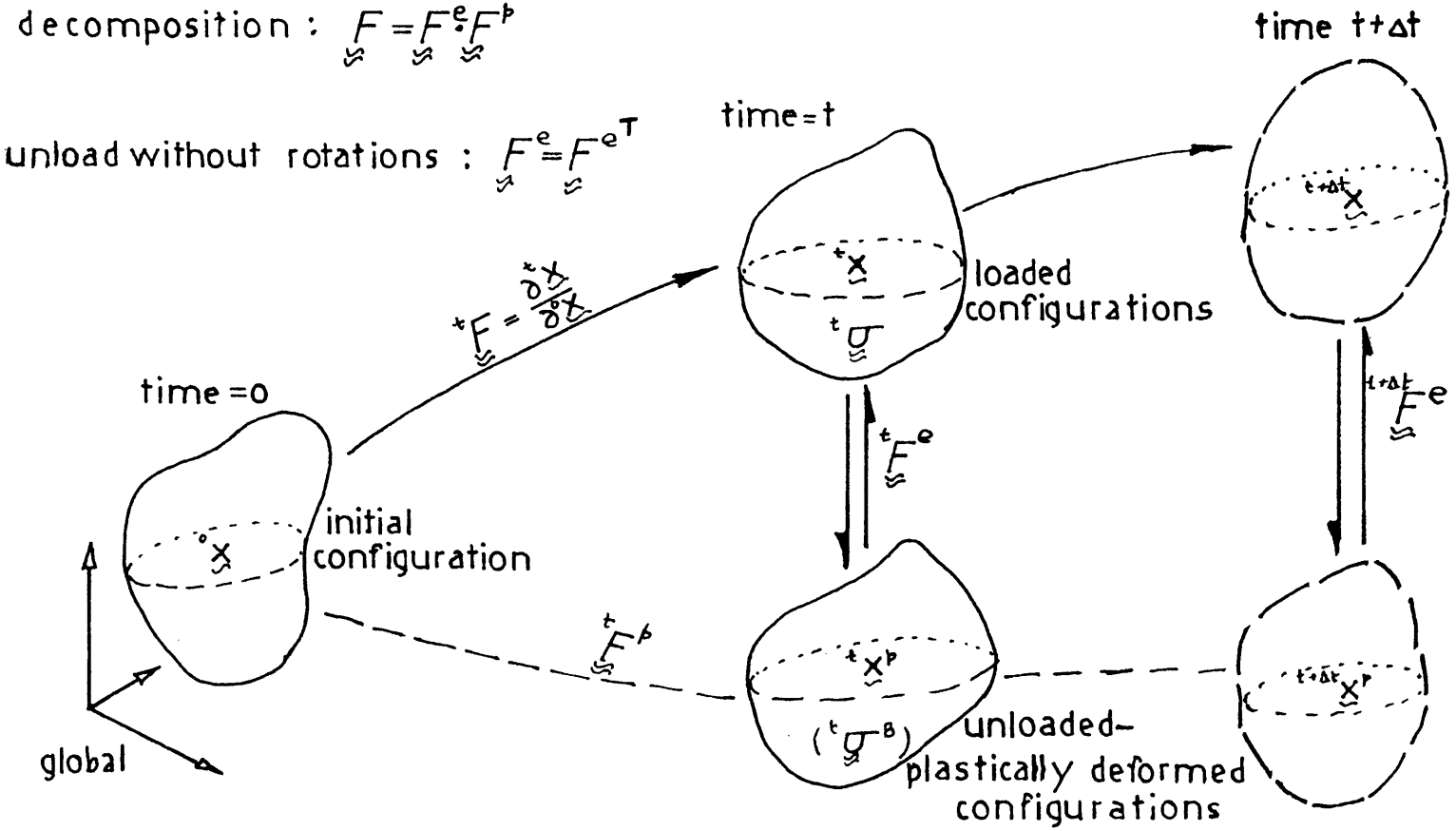

Figure 2.1 : Finite strain kinematics .

$$\underset{\sim}{F} = \underset{\sim}{F}^{e} \cdot \underset{\sim}{F}^{p} \qquad (2.1.2)$$

where

$$\underset{\sim}{F}^{e} = \underset{\sim}{F}^{e^{T}} \qquad (2.1.3)$$

is the (elastic) deformation gradient to bring a material point at state

$${}^{t}\underset{\sim}{x}^{p}$$

to the state

$${}^{t}\underset{\sim}{x}$$

Thus

$$\underset{\sim}{F}^{p} = \underset{\sim}{F}^{e^{-1}} \cdot \underset{\sim}{F} \qquad (2.1.4)$$

is the " plastic " deformation gradient and is not necessarily symmetric . However we choose it to satisfy the volume conservation condition, implying nondilational plasticity ,

$$\det(\underset{\sim}{F}^{p}) = 1 \qquad (2.1.5)$$

2.2 Constitutive Laws

Consider the states of deformation described in Fig. 2.1 (compare with Fig. 1.3 for physical interpretation) . All references are made to a global cartesian frame unless otherwise noted.

The initial state at a time 0 is deformed to the state at a time t carrying Cauchy stresses ,

$$ {}^{t}\underset{\sim}{\sigma} \quad . $$

The elastically unloaded (plastically deformed) configuration is

$$ {}^{t}\underset{\sim}{X}^{p} $$

where the " thought experiment " of unloading is done without rotations. This means that between the states

$$ {}^{t}\underset{\sim}{X}^{p} \quad \text{and} \quad {}^{t}\underset{\sim}{X} \quad , $$

we have pure (elastic) straining without any free-body rotations . As described in Section 1.2 , we note that we also have back stresses ,

$$ {}^{t}\underset{\sim}{\sigma}^{B} \quad , $$

associated the elastically unloaded , plastically deformed state .

Having described the kinematics of deformation at a time t , we can procede to obtain the Cauchy stresses ,

$$ {}^{t}\underset{\sim}{\sigma} \quad , $$

in terms of the elastic deformation gradient ,

$$ {}^{t}\underset{\sim}{F}^{e} $$

and the back stresses ,

$$ {}^{t}\underset{\sim}{\sigma}^{B} \quad , $$

in terms of the plastic deformation gradient ,

$$\underset{\sim}{F}^{p} \quad .$$

These are described in Appendices " B " and " A " respectively .

The Yield Function

Let us define a " Yield Radius " as follows

$$\underset{\sim}{\sigma}^{*\prime} = \underset{\sim}{\sigma}^{*} - \mathrm{tr}(\underset{\sim}{\sigma}^{*}) \cdot \frac{\underset{\sim}{I}}{3} \quad . \qquad (2.2.1)$$

The prime superscript ," $'$ ", indicates the deviatoric component ; " tr " indicates the trace ;

$$\underset{\sim}{I}$$

is the identity tensor . In Eq. 2.2.1 the following quantities are defined :

$$\underset{\sim}{\sigma}^{*} = \underset{\sim}{\sigma} - \hat{\underset{\sim}{\sigma}}^{B} \qquad (2.2.2)$$

with

$$\hat{\underset{\sim}{\sigma}}^{B} = (\underset{\sim}{F}^{e} \cdot \underset{\sim}{\sigma}^{B} \cdot \underset{\sim}{F}^{e}) \frac{1}{J} \qquad (2.2.3)$$

and

$$J = \det(\underset{\sim}{F}^{e}) \quad . \qquad (2.2.4)$$

Equation 2.2.2 uses all stress measures referred to the loaded configuration . Since we would like to include effects to the order of the elastic strain , the back

stress tensor ,

$$\underset{\sim}{\sigma}^{B}$$

that " lives " in the unloaded configuration is now transformed to a tensor ,

$$\hat{\underset{\sim}{\sigma}}^{B}$$

(as defined in Eq. 2.2.3) ,in the loaded configuration , since the (internal) tractions in one configuration would change with deformation .

We can now choose a Mises type of yield function representing kinematically hardening behaviour as illustrated in Fig 2.2 ,

$$Y = \underset{\sim}{\sigma}^{*\prime} : \underset{\sim}{\sigma}^{*\prime} - 2\tau_o^2 \leqslant 0 \qquad (2.2.5)$$

where " : " indicates a double contraction ie., the trace of the matrix product; and

$$\tau_o$$

is the yield strength in shear and is taken to be about 50.6 MPa for polystyrene (Argon and Bessonov, 1976);

Thus Eq. 2.2.5 can be written in index notation as

$$Y = \sigma_{ij}^{*\prime}\, \sigma_{ji}^{*\prime} - 2\tau_o^2 \leqslant 0 \quad .$$

There is an implicit assumption in our choice of yield function : that

$$\underset{\sim}{\sigma} \quad \text{and} \quad \underset{\sim}{\sigma}^{B}$$

Yield Function: $Y = \underset{\sim}{\sigma}^{*\prime} : \underset{\sim}{\sigma}^{*\prime} - 2\tau_o^2 \leq 0$

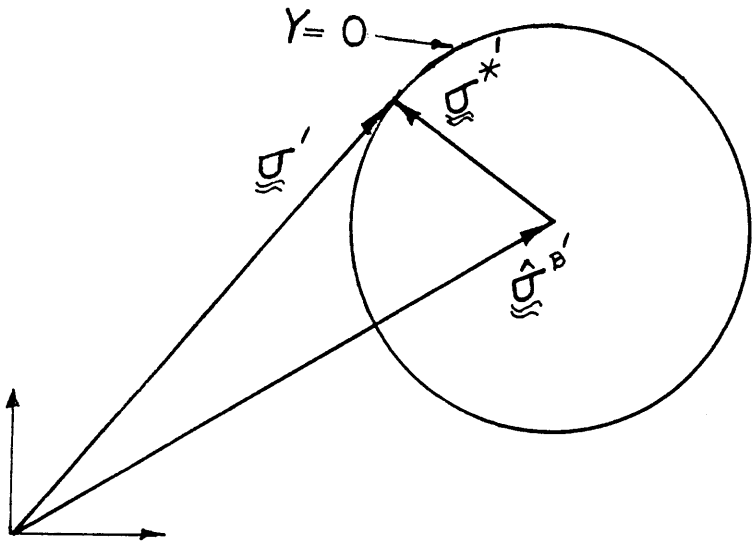

$\underset{\sim}{\sigma}^{*\prime} = (\underset{\sim}{\sigma}^{\prime} - \hat{\underset{\sim}{\sigma}}^{B\prime})$, the yield radius

$\hat{\underset{\sim}{\sigma}}^{B} = \frac{1}{J} \underset{\sim}{F}^{e} \cdot \underset{\sim}{\sigma}^{B} \cdot \underset{\sim}{F}^{e}$; $J = \det(\underset{\sim}{F}^{e})$

Figure 2.2 : Yield function representing kinematically hardening behaviour

always appear in the deviatoric form of their difference . In the yield function chosen above , we could also include the following effects often seen in polymers :

1) pressure sensitivity
2) temperature dependence of the yield strength
3) strain rate dependence of the yield strength .

Having defined all quantities relevant to the state at a time t , in Chapter 3 we will proceed to define incremental quantities , that will in effect help us update all variables to new values at atime $t + \Delta t$.

CHAPTER 3 : FINITE STRAIN ANALYSIS - INCREMENTAL QUANTITIES

3.1 Introduction

In order to update or integrate stresses , strains , state variables etc. from values at a time t to those at a time $t + \Delta t$, we have to evaluate all incremental quantities .

Consider the states of deformation represented in Fig. 2.1 ie. , say we know

$$ {}^{t}\underset{\sim}{x}, {}^{t}\underset{\sim}{x}^{p}, {}^{t}\underset{\approx}{F}, {}^{t}\underset{\approx}{F}^{p}, {}^{t}\underset{\approx}{\sigma} \quad etc. $$

at a time t , and ,

$$ {}^{t+\Delta t}\underset{\approx}{F} $$

at a time $t + \Delta t$. The scope of this chapter is to obtain expressions for

$$ {}^{t+\Delta t}\underset{\approx}{F}^{p} $$

having known all the variables at a time t , and having chosen the incremented state ,

$$ {}^{t+\Delta t}\underset{\sim}{x} \quad . $$

Hence, we can thereafter determine

$$ {}^{t+\Delta t}\underset{\approx}{\sigma} \quad , \quad {}^{t+\Delta t}\underset{\approx}{\sigma}^{B} $$

etc. and thus completely define the state at a time $t + \Delta t$.

3.2 Incremental kinematics

Here we shall develop expressions for increments of deformation in the loaded configuration ie., total increments , and for increments in the unloaded configuration ie., plastic increments .

Having known

$$ {}^{t}\underset{\sim}{x} \quad \text{and} \quad {}^{t+\Delta t}\underset{\sim}{x} $$

we can get expressions for

$$ {}^{t}\underset{\sim}{\underset{\sim}{F}} \quad \text{and} \quad {}^{t+\Delta t}\underset{\sim}{\underset{\sim}{F}} $$

(see Section 2.1) . Since elastic strains in polymers can be large , quantities such as vectors and tensors referred to the unloaded configuration could be different from the same referred to the loaded configuration .

Some definitions

The velocity gradient is defined as

$$ \underset{\sim}{\underset{\sim}{L}} = \dot{\underset{\sim}{\underset{\sim}{F}}} \cdot \underset{\sim}{\underset{\sim}{F}}^{-1} \qquad (3.2.1) $$

$$ = \underset{\sim}{\underset{\sim}{D}} + \underset{\sim}{\underset{\sim}{W}} \qquad (3.2.2) $$

where the rate of deformation is

$$\underset{\sim}{D} = \text{Sym}(\underset{\sim}{L})$$

$$= \frac{1}{2}(\underset{\sim}{L} + \underset{\sim}{L}^{T}) \qquad (3.2.3)$$

and the spin is

$$\underset{\sim}{W} = \text{Sk-Sym}(\underset{\sim}{L})$$

$$= \frac{1}{2}(\underset{\sim}{L} - \underset{\sim}{L}^{T}) \quad . \qquad (3.2.4)$$

In the above equations " Sym " and " Sk-Sym " respectively stand for the symmetric and the skew- symmetric components . In dealing with rate-kinematics , we essentially imply the following , for the time-rate of change of any quantity A

$$\dot{A} = Lt\Big|_{\Delta t \to 0} \frac{\Delta A}{\Delta t} \quad .$$

However , in a numerical procedure , small differences occuring over small increments in time can be cast into " effective " rate quantities . In a rate-dependent formulation the response to small imposed changes would depend on the time step over which these changes are imposed, and on these imposed changes themselves; in a rate-independent formulation , the response to small imposed changes would depend only on the imposed changes themselves , and not on the (small) time-step over which these changes occur .

Since ours is a rate-independent formulation, for changes occuring over a small time-step Δt , the entries in Eq. 3.2.1 are discretized as follows:

$$\dot{\underset{\sim}{F}} = \frac{\Delta \underset{\sim}{F}}{\Delta t} = \frac{{}^{t+\Delta t}\underset{\sim}{F} - {}^{t}\underset{\sim}{F}}{\Delta t} \quad , \qquad (3.2.5)$$

There are various ways of choosing an efective value for $\underset{\sim}{F}^{-1}$, for the increment.

$$\underset{\sim}{F}^{-1} = \frac{1}{2}\left({}^{t+\Delta t}\underset{\sim}{F}^{-1} + {}^{t}\underset{\sim}{F}^{-1}\right) \qquad (3.2.6)$$

(Parks, 1983)

or

$$\underset{\sim}{F}^{-1} = \frac{1}{2}\left({}^{t+\Delta t}\underset{\sim}{F} + {}^{t}\underset{\sim}{F}\right)^{-1} \qquad (3.2.7)$$

(Hughs and Winget, 1980)

or

$$\underset{\sim}{F}^{-1} = {}^{t}\underset{\sim}{F}^{-1} \quad . \qquad (3.2.8)$$

With small increments the differences amongst the above three diminish .

Increments in the Unloaaded Configuration

From Eqs. 2.1.2 , 3.2.1 and 3.2.2 we have

$$\underset{\sim}{L} = \dot{\underset{\sim}{F}}^{e}\underset{\sim}{F}^{e-1} + \underset{\sim}{F}^{e}\dot{\underset{\sim}{F}}^{p}\underset{\sim}{F}^{p-1}\underset{\sim}{F}^{e-1} \quad .$$

(3.2.9)

Then, with

$$\underset{\sim}{L}^{p} = \dot{\underset{\sim}{F}}^{p}\underset{\sim}{F}^{p-1}$$

$$\underset{\sim}{L}^{p} = \underset{\sim}{D}^{p} + \underset{\sim}{W}^{p} \quad , \qquad (3.2.10)$$

$$\underset{\sim}{D}^{p} = \mathrm{Sym}(\underset{\sim}{L}^{p}) \qquad (3.2.11)$$

can be interpreted as the rate of plastic deformation in the unloaded configuration (Onat,1981). We also have the quantity

$$\hat{\underset{\sim}{D}}^{p}$$

which is interpreted as the rate of plastic deformation in the loaded configuration , and is defined by the expressions

$$\hat{\underset{\sim}{D}}^{p} = \hat{\underset{\sim}{D}}^{pT} \qquad (3.2.12)$$

$$\underset{\sim}{D}^{p} = \frac{\underset{\sim}{F}^{e-1}\cdot\hat{\underset{\sim}{D}}^{p}\cdot\underset{\sim}{F}^{e} + \underset{\sim}{F}^{eT}\cdot\hat{\underset{\sim}{D}}^{p}\cdot\underset{\sim}{F}^{e-1}}{2} \; , \qquad (3.2.13)$$

Giving

$$D^{p}_{ij} = \mathcal{M}_{ikjL}\,\hat{D}^{p}_{kL} \qquad (3.2.14)$$

where

$$\mathcal{M}_{ikjL} = \frac{F^{e-1}_{ik}F^{e}_{jL} + F^{e}_{ik}F^{e-1}_{jL}}{2} \qquad (3.2.15)$$

is a fourth rank mapping function represented in index notation in Eq. 3.2.15 .

This development is based on power considerations and is described in detail in Appendix C .

It is found from a simple order of magnitude analysis , that a typical entry in $\underset{\sim}{F}^{e}$

is of order $(1 + \varepsilon^e)$ where ,

$$\varepsilon^e$$

is of the order of the elastic strains . Thus a typical entry in Eq. 3.2.15 is of order

$$(1 + \varepsilon^e) \times (1 - \varepsilon^e) \text{ ie., } (1 - \varepsilon^{e^2}) .$$

Hence , to order ε^e , we have

$$\underset{\sim}{D}^p \doteq \underset{\sim}{\hat{D}}^p \quad . \qquad (3.2.16)$$

Spin of the Unloaded State

From Eqs. 3.2.9 to 3.2.11 we have

$$\dot{\underset{\sim}{F}}^e = (\underset{\sim}{D} + \underset{\sim}{W}) \cdot \underset{\sim}{F}^e - \underset{\sim}{F}^e \cdot (\underset{\sim}{D}^p + \underset{\sim}{W}^p) \qquad (3.2.17)$$

and by Eq. 2.1.3 we also have

$$\dot{\underset{\sim}{F}}^e = \underset{\sim}{F}^e \cdot (\underset{\sim}{D} - \underset{\sim}{W}) - (\underset{\sim}{D}^p - \underset{\sim}{W}^p) \cdot \underset{\sim}{F}^e \quad . (3.2.18)$$

Hence, we have

$$(\underset{\sim}{W} - \underset{\sim}{W}^p) \cdot \underset{\sim}{F}^e + \underset{\sim}{F}^e \cdot (\underset{\sim}{W} - \underset{\sim}{W}^p) + (\underset{\sim}{D} + \underset{\sim}{D}^p) \cdot \underset{\sim}{F}^e - \underset{\sim}{F}^e \cdot (\underset{\sim}{D} + \underset{\sim}{D}^p) = \underset{\sim}{0} \quad .$$

(3.2.19)

Thus, the spin of the unloaded state is

$$\underset{\approx}{W}^{p} = \underset{\approx}{W} - \underline{\underline{\omega}} : (\underset{\approx}{D} + \underset{\approx}{D}^{p}) \qquad (3.2.20)$$

where ,

$$\underline{\underline{\omega}}$$

is a fourth rank linear mapping function of

$$\underset{\approx}{F}^{e}$$

that maps symmetric tensors into skew-smmetric ones. this tensor map is similar to the one in Eq. 3.2.13 . Appendix D has the detaled development of this map. We note that

$\underset{\approx}{W}^{p}$ is a little different from $\underset{\approx}{W}$

the spin of the loaded state . This would be the case if any incremental stretching occurs in a direction other than the principal elastic stretch directions at a time t . Further, we see that

$$\underline{\underline{\omega}}$$

has terms of order

$$(1 + \varepsilon^{e})$$

and cannot be neglected , unlike

$$\underline{\underline{M}}$$

in Eq. 3.2.13 . As an example in the two-dimensional case we have

$$W_{12}^{p} - W_{12} = \frac{(D_{12} + D_{12}^{p})(F_{11}^{e} - F_{22}^{e}) - (D_{11} + D_{11}^{p} - D_{22} - D_{22}^{p})F_{12}^{e}}{(F_{11}^{e} + F_{22}^{e})} \; .$$

(3.2.21)

The Flow rule

We can now define a flow rule : an obvious (but not necessarily unique) choice is , assuming nondilational incremental plasticity (using " yield radius " and the yield function as defined in Ch 2.2),

$$\underset{\sim}{D}^{p} \propto \frac{\partial Y}{\partial \underset{\sim}{\sigma}^{*\prime}} \qquad (3.2.22)$$

$$= \Lambda \underset{\sim}{\sigma}^{*\prime} \quad , \qquad (3.2.23)$$

where Λ is a scalar. Thus we have

$$\Lambda = \frac{\dot{\gamma}_e}{\mathcal{S}} \quad , \qquad (3.2.24)$$

where

$$\dot{\gamma}_e \quad \text{and} \quad \mathcal{S}$$

are developed in Appendix E. Note that , from Appendix E , we can express $\dot{\gamma}_e$ as

$$\dot{\gamma}_e = \underset{\sim}{Z} : \underset{\sim}{D} \quad , \qquad (3.2.25)$$

where $\underset{\sim}{Z}$ is evaluated in Appendix E4.

3.3 Updating the variables

Having defined all incremental quantities, we can now procede to integrate all variables from values at a time t ie.,

$$ {}^{t}\underset{\approx}{\sigma}, \; {}^{t}\underset{\approx}{\sigma}^{B} \quad \text{etc.} $$

to new values at a time $t + \Delta t$ ie.,

$$ {}^{t+\Delta t}\underset{\approx}{\sigma}, \; {}^{t+\Delta t}\underset{\approx}{\sigma}^{B} \quad \text{etc.} $$

In Eq. 3.2.10 we can define

$$ \dot{\underset{\approx}{F}}^{p} = \frac{{}^{t+\Delta t}\underset{\approx}{F}^{p} - {}^{t}\underset{\approx}{F}^{p}}{\Delta t} \qquad (3.3.1) $$

and

$$ \underset{\approx}{F}^{p-1} = \frac{1}{2}\left({}^{t+\Delta t}\underset{\approx}{F}^{p-1} + {}^{t}\underset{\approx}{F}^{p-1} \right) \qquad (3.3.2) $$

or

$$ \underset{\approx}{F}^{p-1} = \frac{1}{2}\left({}^{t+\Delta t}\underset{\approx}{F}^{p} + {}^{t}\underset{\approx}{F}^{p} \right)^{-1} \qquad (3.3.3) $$

or

$$ \underset{\approx}{F}^{p-1} = {}^{t}\underset{\approx}{F}^{p-1} , \qquad (3.3.4) $$

thus giving (using Eqs. 3.3.1 and 3.3.3)

$$ {}^{t+\Delta t}\underset{\approx}{F}^{p} = \left(\underset{\approx}{I} + 2\Delta t \underset{\approx}{L}^{p} \right) \cdot {}^{t}\underset{\approx}{F}^{p} \cdot \left(\underset{\approx}{I} - 2\Delta t \underset{\approx}{L}^{p} \right) . \qquad (3.3.5) $$

All quantities on the right side of Eq. 3.3.5 have been either defined or known (from Ch. 3.1 and Eqs. 3.2.10, 3.2.20 and 3.2.23). With the new value thus obtained, we have ,from the constraint in Eq. 2.1.2 ,

$$\overset{t+\Delta t}{\underset{\approx}{F}}{}^{e} = \overset{t+\Delta t}{\underset{\approx}{F}} \cdot \overset{t+\Delta t}{\underset{\approx}{F}}{}^{p-1} \qquad (3.3.6)$$

where the incremented final state ,

$$\overset{t+\Delta t}{\underset{\approx}{F}} \quad ,$$

has been chosen earlier .

With

$$\overset{t+\Delta t}{\underset{\approx}{F}}{}^{e} \quad \text{and} \quad \overset{t+\Delta t}{\underset{\approx}{F}}{}^{p}$$

known , we can get the new Cauchy stresses ,

$$\overset{t+\Delta t}{\underset{\approx}{\sigma}}$$

(from Appendix B) and the updated back stresses ,

$$\overset{t+\Delta t}{\underset{\approx}{\sigma}}{}^{B}$$

(from Appendix A) .

Since the integration process is discretized in finite steps , there is no assurance that the new state thus obtained will not violate the yield function defined by Eq. 2.2.5 . In Chapter 5 we will describe a method of converging to the " proper " solution that does not violate any of the constraints we have set , by employing a numerical " search " technique .

CHAPTER 4 : INVARIANCE UNDER RIGID-BODY ROTATIONS

In Chapter 3 we arrived at expressions for new stresses , state variables etc. , as we updated the state from

$$ {}^{t}\underset{\sim}{X} \tag{4.1} $$

at a time t to

$$ {}^{t+\Delta t}\underset{\sim}{X} \tag{4.2} $$

at a time $t + \Delta t$. If however , these two differed only by a rigid-body rotation between them ie., there were no strain increments , then we need only to suitably update the old variables at a time t to new ones with reference to the updated state at a time $t + \Delta t$, without any numerical integration ie., entirely via orthogonal transformations.

Hence for the most general case of deformation , given the states

$$ {}^{t}\underset{\sim}{X} \quad \text{and} \quad {}^{t+\Delta t}\underset{\sim}{X} $$

we can find an intermediate state

$$ {}^{*}\underset{\sim}{X} $$

which is a rotated , but unstretched version of the state

$$ {}^{t}\underset{\sim}{X} $$

The rigid-body rotation between the states

$$ {}^{t}\underset{\sim}{X} \quad \text{and} \quad {}^{*}\underset{\sim}{X} $$

is the same as between the states

$${}^{t}\underset{\sim}{X} \quad \text{and} \quad {}^{t+\Delta t}\underset{\sim}{X} \quad .$$

Hence , between the states

$${}^{*}\underset{\sim}{X} \quad \text{and} \quad {}^{t+\Delta t}\underset{\sim}{X} \quad ,$$

we have no rotations , but only strains . This procedure is illustrated in Fig. 4.1 .

Let the deformation gradients (defined by Eq. 2.1.1) at the states ,

$$({}^{t}\underset{\sim}{X} , {}^{*}\underset{\sim}{X} , {}^{t+\Delta t}\underset{\sim}{X})$$

be

$$({}^{①}\underset{\sim}{F} , {}^{*}\underset{\sim}{F} , {}^{②}\underset{\sim}{F}) \quad .$$

Our objective is to find

$${}^{*}\underset{\sim}{F}$$

given

$${}^{①}\underset{\sim}{F} \quad \text{and} \quad {}^{②}\underset{\sim}{F} \quad .$$

By polar decomposition (see Appendix A , for example , in which this is explained with reference to the plastic deformation gradient) , we have

$${}^{①}\underset{\sim}{F} = {}^{①}\underset{\sim}{V} \cdot {}^{①}\underset{\sim}{R} \tag{4.3}$$

and

$${}^{②}\underset{\sim}{F} = {}^{②}\underset{\sim}{V} \cdot {}^{②}\underset{\sim}{R} \tag{4.4}$$

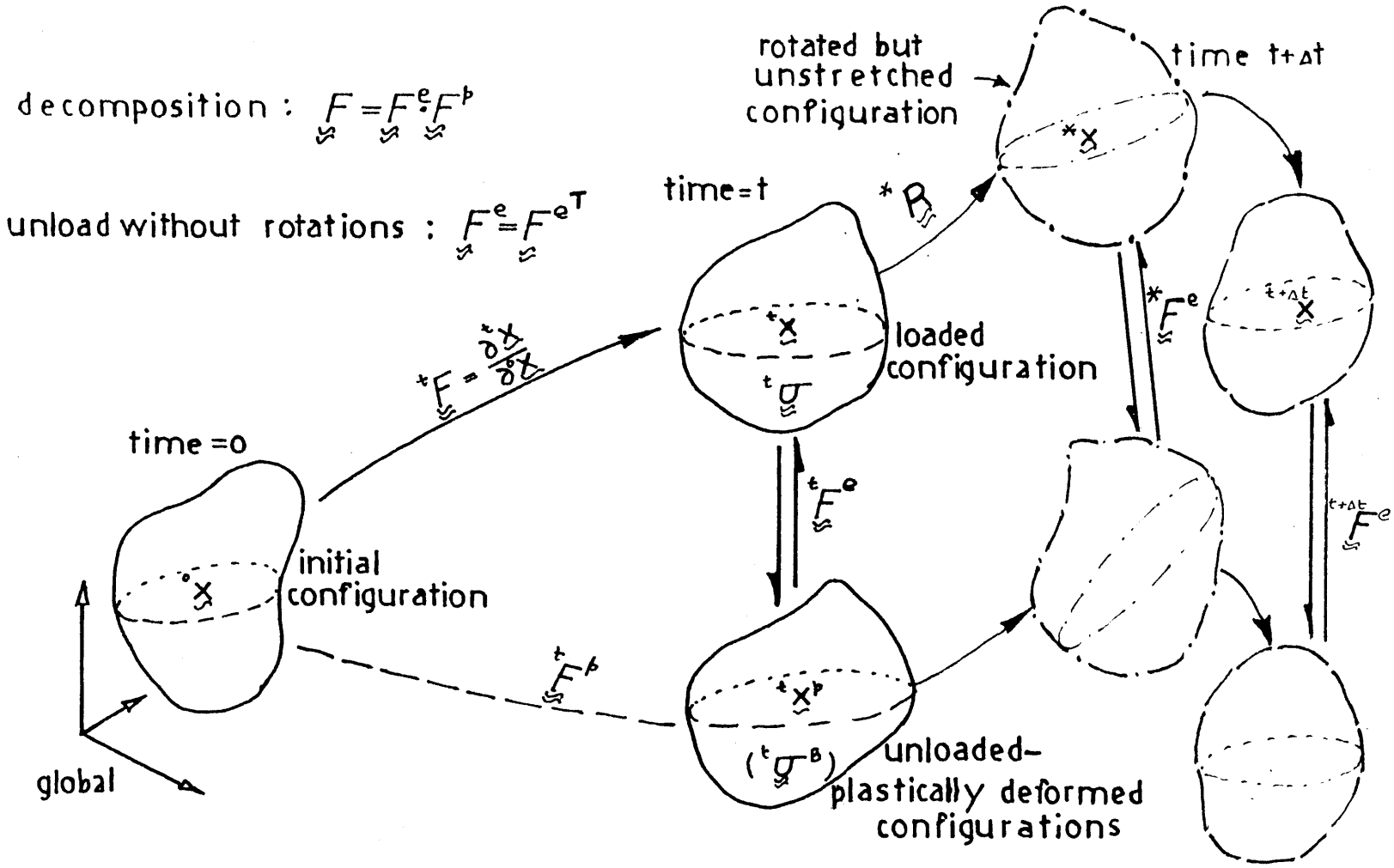

Figure 4.1 : Showing the " rotated but incrementally unstretched " intermediate state .

where

$$({}^{①}\underset{\approx}{V} , {}^{②}\underset{\approx}{V})$$

are the " left " finger stretch tensors , and

$$({}^{①}\underset{\approx}{R} , {}^{②}\underset{\approx}{R})$$

are the rotation tensors . By Eq. 2.1.2

$$ {}^{①}\underset{\approx}{F} = {}^{①}\underset{\approx}{F}^{e} \cdot {}^{①}\underset{\approx}{F}^{p} \qquad (4.5)$$

$$ {}^{②}\underset{\approx}{F} = {}^{②}\underset{\approx}{F}^{e} \cdot {}^{②}\underset{\approx}{F}^{p} \quad . \qquad (4.6)$$

From Eqs. 4.3 and 4.4 , let

$$ {}^{*}\underset{\approx}{R} = {}^{①}\underset{\approx}{R}^{T} \cdot {}^{②}\underset{\approx}{R} \qquad (4.7)$$

or , for axi-symmetric / plane strain cases , we could also write

$$ {}^{*}\underset{\approx}{R} = {}^{②}\underset{\approx}{R} \cdot {}^{①}\underset{\approx}{R}^{T} \quad . \qquad (4.8)$$

It is clearly seen that

$$ {}^{*}\underset{\approx}{R} $$

is the incremental rotation between the states at times " t " and " $t + \Delta t$ " , and is orthogonal .

Consider the deformation gradient

$$ {}^{*}\underset{\approx}{F} = {}^{*}\underset{\approx}{R} \cdot {}^{①}\underset{\approx}{F} \qquad (4.9)$$

which can be decomposed as follows :

$$ {}^{*}\underset{\sim}{F} = {}^{*}\underset{\sim}{F}^{e} \cdot {}^{*}\underset{\sim}{F}^{p} \tag{4.10} $$

where ,

$$ {}^{*}\underset{\sim}{F}^{e} = {}^{*}\underset{\sim}{R} \cdot {}^{\circ}\underset{\sim}{F}^{e} \cdot {}^{*}\underset{\sim}{R}^{T} \tag{4.11} $$

and

$$ {}^{*}\underset{\sim}{F}^{p} = {}^{*}\underset{\sim}{R} \cdot {}^{\circ}\underset{\sim}{F}^{p} \tag{4.12} $$

Thus, corresponding to the elastic deformation gradient in Eq. 4.11 , we have the Cauchy stresses

$$ {}^{*}\underset{\sim}{\sigma} = {}^{*}\underset{\sim}{R} \cdot {}^{\circ}\underset{\sim}{\sigma} \cdot {}^{*}\underset{\sim}{R}^{T} \tag{4.13} $$

where

$$ {}^{\circ}\underset{\sim}{\sigma} $$

corresponds to the elastic deformation gradient ,

$$ {}^{\circ}\underset{\sim}{F}^{e} $$

Corresponding to the plastic deformation gradient in Eq. 4.12 , we have the back stresses

$$ {}^{*}\underset{\sim}{\sigma}^{B} = {}^{*}\underset{\sim}{R} \cdot {}^{\circ}\underset{\sim}{\sigma}^{B} \cdot {}^{*}\underset{\sim}{R}^{T} \tag{4.14} $$

where

$$ {}^{\circ}\underset{\sim}{\sigma}^{B} $$

corresponds to the plastic deformation gradient ,

$$ {}^{\circ}\underset{\sim}{F}^{p} $$

Thus Eqs. 4.8 through 4.14 help determine the intermediate rotated but unstretched state .

Now , any deformation (straining) would be evident if

$$ {}^{*}\underset{\approx}{F} $$

as obtained were different from

$$ {}^{t+\Delta t}\underset{\approx}{F} $$

We can now use the procedure in Ch. 3 to integrate stresses , state variables etc. from values in the intermediate state to new values in the final state via a numerical integration procedure .

*The develpoment in this chapter was done in early January 1983, similar work has been done by Rolph (Rolph and Bathe, July 1983).

CHAPTER 5: A NUMERICAL SEARCH USING CONSTRAINED PERTURBATIONS

5.1 The concept of the " proper " solution

In Ch. 3 we arrived at expressions for stresses , state variables , etc. , as we incremented the geometry from the initial state at a time t to the final chosen state at a time $t + \Delta t$. Since we have discretized the process of integration via a forward Euler type of procedure , the values finally arrived at may not necessarily satisfy all the constraints .

The final geometry is fixed as chosen , ie., we know

$$\overset{t+\Delta t}{\underset{\approx}{F}} \tag{5.1.1}$$

at a time " $t + \Delta t$ " . Hence by Eqs. 2.1.2 and 2.1.5 , we have

$$\overset{t+\Delta t}{\underset{\approx}{F}} = \overset{t+\Delta t}{\underset{\approx}{F}}{}^{e} \cdot \overset{t+\Delta t}{\underset{\approx}{F}}{}^{p} \tag{5.1.2}$$

and

$$\det\left(\overset{t+\Delta t}{\underset{\approx}{F}}{}^{e}\right) = \det\left(\overset{t+\Delta t}{\underset{\approx}{F}}\right) \tag{5.1.3}$$

Hence from Eq. 2.1.3

$$\overset{t+\Delta t}{\underset{\approx}{F}}{}^{e} = \overset{t+\Delta t}{\underset{\approx}{F}}{}^{e^{T}} \tag{5.1.4}$$

By Eq. 2.2.5 we can write the yield function as

$$Y\left({}^{t+\Delta t}\underset{\approx}{F}^{e},\ {}^{t+\Delta t}\underset{\approx}{F}^{p}\right) \leqslant 0 \qquad (5.1.5)$$

By the procedure described in Ch. 3 , we automatically satisfy the constraints in Eqs. 5.1.1 through 5.1.4 , but not necessarily Eq. 5.1.5 . It should be noted , however , that the first estimate of the solution will not be " far " from the exact solution satisfying all of the above mentioned constraints .

Let

$$\left({}^{t+\Delta t}\underset{\approx}{F}^{e}_{①},\ {}^{t+\Delta t}\underset{\approx}{F}^{p}_{①}\right) \qquad (5.1.6)$$

be the first estimate of the solution arrived at in Ch. 3 . Our objective is to determine the corrections to the solution in Eq. 5.1.6 , such that the second estimate thus arrived at , ie., the solution ,

$$\left({}^{t+\Delta t}\underset{\approx}{F}^{e}_{②},\ {}^{t+\Delta t}\underset{\approx}{F}^{p}_{②}\right) \qquad (5.1.7)$$

will satisfy all the constraints , Eqs. 5.1.1 through 5.1.4 and the constraint in Eq. 5.1.5 to a closer tolerance than was achieved with the first estimate (Eq. 5.1.6) . Convergence is achieved to an acceptable tolerance , by repeating the above procedre , to susequent estimates of the solution .

5.2 The " Constrained Perturbation " procedure

Here we seek new elastic , and plastic deformation gradients to give the chosen (fixed) total deformation gradient . In Fig. 5.1 we see a physical interpretation of this , in which we have , for a (fixed) final configuration at a time $t + \Delta t$, several " close " solutions that satisfy the constraints in Eqs. 5.1.4 through 5.1.4 . By successively arriving at new estimates , we can get to, (within a tolerance) , satisfy Eq. 5.1.5 aswell .

For convenience let us drop off the superscripts $t + \Delta t$. Since we are perturbing variables about the " just found " first estimate of the solution , we do have increments in deformation , rotation etc. Eq. 5.1.4 implies that

$$\underset{\approx}{\dot{F}}^{e} = \underset{\approx}{\dot{F}}^{e^{T}} \qquad (5.2.1)$$

Since the final configuration is fixed as chosen , the total increments in deformation , rotation etc., are absent during any perturbation , ie. ,the velocity gradient

$$\underset{\approx}{L} = \underset{\approx}{D} + \underset{\approx}{W} = \underset{\approx}{0} \qquad (5.2.2)$$

(see Eq. 3.2.1) . But the plastic deformation rate and spin ,

$$\underset{\approx}{D}^{p}, \underset{\approx}{W}^{p}$$

need not necessarily be $\underset{\approx}{0}$.

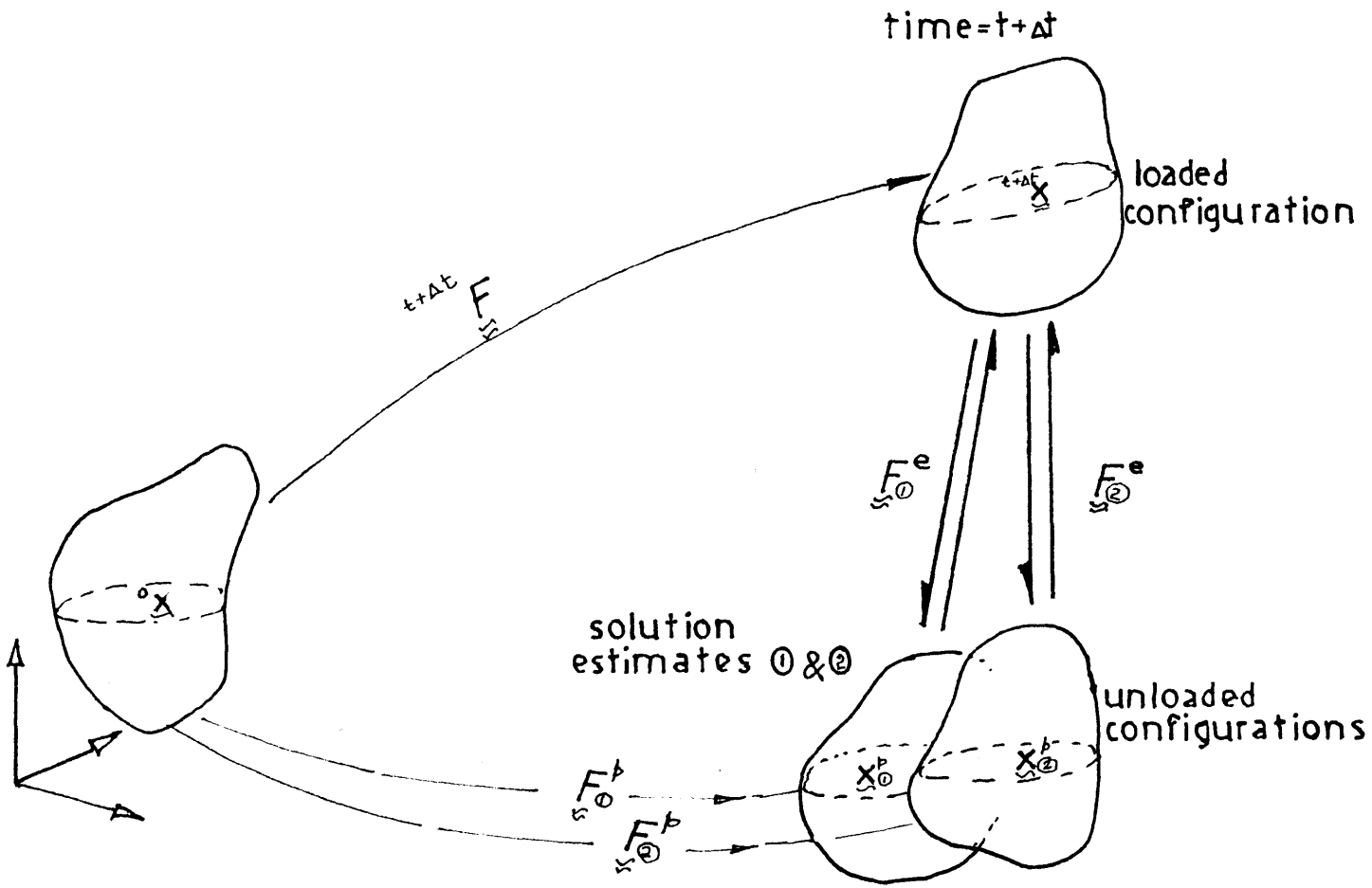

Figure 5.1 : Physical interpretation of the constrained perturbations during the numerical search

From Eq. C.4 in Appendix C , we have for the rate of the elastic Cauchy-Green tensor , using Eq. 5.2.2 ,

$$\dot{\underset{\approx}{B}} = -2\underset{\approx}{F}^{e}_{\textcircled{1}}\cdot\underset{\approx}{D}^{p}\cdot\underset{\approx}{F}^{e}_{\textcircled{1}} \tag{5.2.3}$$

From Eq. C.3 we have

$$\underset{\approx}{D}^{p} = -\frac{1}{2}\left(\underset{\approx}{F}^{e^{-1}}_{\textcircled{1}}\cdot\dot{\underset{\approx}{F}}^{e} + \dot{\underset{\approx}{F}}^{e}\cdot\underset{\approx}{F}^{e^{-1}}_{\textcircled{1}}\right) \tag{5.2.4}$$

or in index notation ,

$$D^{p}_{ij} = -\frac{1}{2}\left(F^{e^{-1}}_{\textcircled{1}\,im}\delta_{jn} + F^{e^{-1}}_{\textcircled{1}\,jn}\delta_{im}\right)\dot{F}^{e}_{mn} \tag{5.2.5}$$

or

$$\underset{\approx}{D}^{p} = -\frac{1}{2}\underset{\approx}{\underset{=}{S}}:\dot{\underset{\approx}{F}}^{e} \tag{5.2.6}$$

in which

$$S_{imjn}$$

is a fourth rank tensor mapping function , relating the local rate of the elastic deformation gradient to the local rate of plastic deformation , during a constrained perturbation . In Table 5.1 , we have a representation of Eq. 5.2.6 , in which

$$F^{e^{-1}}_{ij}$$

are the corresponding entries in the inverse of the elastic deformation gradient matrix ,

$$\underset{\approx}{F}^{e^{-1}}_{\textcircled{1}}$$

From Eqs. 5.2.2 and 3.2.20 we have

$$\underset{\approx}{W}^{p} = -\underset{\approx}{\underset{=}{\omega}}:\underset{\approx}{D}^{p} \tag{5.2.7}$$

TABLE 5.1: matrix representation of Eq 5.2.6

$$
\begin{bmatrix} D_{11}^{p} \\ D_{22}^{p} \\ D_{33}^{p} \\ D_{12}^{p} \\ D_{23}^{p} \\ D_{31}^{p} \end{bmatrix}
= -\frac{1}{2}
\begin{bmatrix}
2F_{11}^{e^{-1}} & & & F_{12}^{e^{-1}} & & F_{13}^{e^{-1}} \\
& 2F_{22}^{e^{-1}} & & F_{12}^{e^{-1}} & F_{23}^{e^{-1}} & \\
& & 2F_{33}^{e^{-1}} & & F_{23}^{e^{-1}} & F_{31}^{e^{-1}} \\
F_{12}^{e^{-1}} & F_{12}^{e^{-1}} & & (F_{11}^{e^{-1}}+F_{22}^{e^{-1}})^{\frac{1}{2}} & & \\
& F_{23}^{e^{-1}} & F_{23}^{e^{-1}} & & (F_{22}^{e^{-1}}+F_{33}^{e^{-1}})^{\frac{1}{2}} & \\
F_{13}^{e^{-1}} & & F_{13}^{e^{-1}} & & & (F_{33}^{e^{-1}}+F_{11}^{e^{-1}})^{\frac{1}{2}}
\end{bmatrix}
\begin{bmatrix} \dot{F}_{11}^{e} \\ \dot{F}_{22}^{e} \\ \dot{F}_{33}^{e} \\ 2\dot{F}_{12}^{e} \\ 2\dot{F}_{23}^{e} \\ 2\dot{F}_{31}^{e} \end{bmatrix}
$$

and using Eq. 5.2.6 , we have in index notation ,

$$W^{p}_{ij} = \frac{1}{2}\, \omega_{ijmn}\, S_{mknl}\, \dot{F}^{e}_{kl} \qquad (5.2.8)$$

The rate of change of yield status is found from Appendix E , Eq. E.12 ,

$$\dot{\gamma}_e = \frac{2}{J}\left(\underset{\approx}{\alpha} : \dot{\underset{\approx}{\tau}} - \underset{\approx}{\beta} : \dot{\underset{\approx}{\sigma}}^{B}\right) \qquad (5.2.9)$$

From Eq. E.23 we have

$$\dot{\gamma}_e = \frac{2}{J}\Big[\alpha_{ij}\,\dot{\tau}_{ji} - \beta_{ij}\big(\mathcal{L}^{R}_{ijkl}\, D^{p}_{kl} - \sigma^{B}_{pj}\,\omega_{ipkl}\, D^{p}_{kl} + \sigma^{B}_{ip}\,\omega_{pjkl}\, D^{p}_{kl}\big)\Big] \qquad (5.2.10)$$

From Appendix B , Eqs. B.2 , B.3 and B.6 we have the elastic strain tensor ,

$$\underset{\approx}{\xi}^{e} = \mathrm{Ln}\left(\underset{\approx}{F}^{e}\right) \qquad (5.2.11)$$

$$= \underline{\underline{C}} : \underset{\approx}{\tau} \qquad (5.2.12)$$

where ,

$$C_{ijkl}$$

is the compliance tensor (see Eq. E2.3 in Sub-Appendix E2) Thus for linear elastic materials , we have

$$\left.\begin{aligned} \dot{\underset{\sim}{\tau}} &= \underset{\sim\sim}{\mathcal{L}}^{e} : \dot{\underset{\sim}{\xi}}^{e} \\ \dot{\underset{\sim}{\xi}}^{e} &= \underset{\sim\sim}{C} : \dot{\underset{\sim}{\tau}} \end{aligned}\right\} \quad , \qquad (5.2.13)$$

From Eq. 5.1.3 ,

$$\begin{aligned} J &= \det(\underset{\sim}{F}_{\odot}^{e}) \\ &= \det(\underset{\sim}{F}_{\odot}) \\ &= \text{constant, for chosen final state .} \end{aligned} \qquad (5.2.14)$$

Hence , the pressure ,

$$\operatorname{tr}\left(\frac{\underset{\sim}{\tau}_{\odot}}{J}\right) = \text{constant} \qquad (5.2.15)$$

Hence from Eqs. 5.2.14 and 5.2.15 we have

$$\dot{J} = 0 \qquad (5.2.16)$$

and

$$\frac{d}{dt}\operatorname{tr}\left(\frac{\underset{\sim}{\tau}_{\odot}}{J}\right) = 0 \qquad (5.2.17)$$

We finally get

$$\operatorname{tr}(\dot{\underset{\sim}{\tau}}) = 0 \qquad (5.2.18)$$

ie., any increments in Kirchhoff stress during a constrained perturbation will be purely deviatoric .

5.3 Relating $\dot{\underset{\sim}{\sim}}{}^{e}$ to $\dot{\underset{\sim}{\sim}}$

From Eq. 5.2.11 we have

$$\underset{\sim}{\sim}{}^{e}_{\Phi} = \exp(\underset{\sim}{\sim}{}^{e}_{\Phi}) = \underset{\sim}{\sim}{}^{I} + \underset{\sim}{\sim}{}^{e}_{\Phi} + \frac{\underset{\sim}{\sim}{}^{e}_{\Phi}\underset{\sim}{\sim}{}^{e}_{\Phi}}{2!} + \frac{\underset{\sim}{\sim}{}^{e}_{\Phi}\underset{\sim}{\sim}{}^{e}_{\Phi}\underset{\sim}{\sim}{}^{e}_{\Phi}}{3!} + \cdots\cdots \tag{5.3.1}$$

or,

$$\dot{\underset{\sim}{\sim}}{}^{e} = \frac{\dot{\underset{\sim}{\sim}}{}^{e}}{1} + \frac{\dot{\underset{\sim}{\sim}}{}^{e}\underset{\sim}{\sim}{}^{e}_{\Phi} + \underset{\sim}{\sim}{}^{e}_{\Phi}\dot{\underset{\sim}{\sim}}{}^{e}}{2} + \frac{\dot{\underset{\sim}{\sim}}{}^{e}\underset{\sim}{\sim}{}^{e}_{\Phi}\underset{\sim}{\sim}{}^{e}_{\Phi} + \underset{\sim}{\sim}{}^{e}_{\Phi}\dot{\underset{\sim}{\sim}}{}^{e}\underset{\sim}{\sim}{}^{e}_{\Phi} + \underset{\sim}{\sim}{}^{e}_{\Phi}\underset{\sim}{\sim}{}^{e}_{\Phi}\dot{\underset{\sim}{\sim}}{}^{e}}{6} + \cdots \tag{5.3.2}$$

Hence , from Eqs. 5.2.13 and 5.2.18 we have

$$\dot{\underset{\sim}{\sim}}{}^{e} = \dot{\underset{\sim}{\sim}} \frac{E}{1+\nu} \tag{5.3.3}$$

Thus , to order $\underset{\sim}{\sim}{}^{e^2}$, in Eq. 5.3.2 we have

$$\dot{F}^{e}_{ij} = \frac{1+\nu}{E}\left\{\delta_{ir}\delta_{js} + \frac{1}{2}\left(\varepsilon^{e}_{\Phi}{}_{ir}\delta_{js} + \delta_{ir}\varepsilon^{e}_{\Phi}{}_{js}\right) + \frac{1}{6}\left(\delta_{ir}\varepsilon^{e^2}_{\Phi}{}_{js} + \varepsilon^{e^2}_{\Phi}{}_{ir}\delta_{js} + \varepsilon^{e}_{\Phi}{}_{ir}\varepsilon^{e}_{\Phi}{}_{js}\right)\right\}\dot{\tau}_{rs} \tag{5.3.4}$$

We could write Eq. 5.3.4 as

$$\dot{\underset{\sim}{F}}^{e} = \underline{\underline{H}} : \dot{\underset{\sim}{\tau}} \quad , \tag{5.3.5}$$

and is represented in Table 5.2 .

5.4 The final correction

In Eq. 5.2.10 , using Eqs. 5.2.6 and 5.3.5 we get , for the rate of change of the yield function ,

$$\dot{Y} = \frac{2}{J}\Big[\alpha_{ij}\dot{\tau}_{ij} + \frac{1}{2}\beta_{ij}\big(\mathcal{L}^{R}_{ijkl} S_{kmln} + \sigma^{B}_{ip} W_{pjkl} S_{kmln} - \sigma^{B}_{pj} W_{ipkl} S_{kmln}\big) H_{mnrs}\dot{\tau}_{rs}\Big] \tag{5.4.1}$$

Equation 5.4.1 can be written as

$$\delta Y = \underset{\sim}{\underset{\sim}{K}} : \delta\underset{\sim}{\tau} \tag{5.4.2}$$

We can now choose the correction to the Kirchhoff stress as follows :

$$\delta\underset{\sim}{\tau} = Q\,\mathrm{sym}(\underset{\sim}{\underset{\sim}{K}})' \tag{5.4.3}$$

where the scalar Q is to be determined . From Eq. 5.4.2 we have for the incremental change in yield status ,

TABLE 5.2: matrix representation of Eq. 5.3.5

$$
\begin{bmatrix} \dot{F}^e_{11} \\ \dot{F}^e_{22} \\ \dot{F}^e_{33} \\ \dot{F}^e_{12} \\ \dot{F}^e_{23} \\ \dot{F}^e_{31} \end{bmatrix}
= \frac{1+\nu}{E}
\begin{bmatrix}
1+\varepsilon^e_{11}+\frac{1}{2}\varepsilon^{e^2}_{11} & \frac{1}{6}\varepsilon^{e^2}_{12} & \frac{1}{6}\varepsilon^{e^2}_{13} & \frac{1}{2}\varepsilon^e_{12}+\frac{1}{6}\varepsilon^e_{12}+\frac{1}{6}\varepsilon^e_{11}\varepsilon^e_{12} & \frac{1}{6}\varepsilon^e_{12}\varepsilon^e_{13} & \frac{1}{2}\varepsilon^e_{13}+\frac{1}{6}\varepsilon^e_{13}+\frac{1}{6}\varepsilon^e_{11}\varepsilon^e_{13} \\
 & 1+\varepsilon^e_{22}+\frac{1}{2}\varepsilon^{e^2}_{22} & \frac{1}{6}\varepsilon^{e^2}_{23} & \frac{1}{2}\varepsilon^e_{12}+\frac{1}{6}\varepsilon^e_{12}+\frac{1}{6}\varepsilon^e_{12}\varepsilon^e_{22} & \frac{1}{2}\varepsilon^e_{32}+\frac{1}{6}\varepsilon^e_{32}+\frac{1}{6}\varepsilon^e_{32}\varepsilon^e_{22} & \frac{1}{6}\varepsilon^e_{21}\varepsilon^e_{23} \\
 & & 1+\varepsilon^e_{33}+\frac{1}{2}\varepsilon^{e^2}_{33} & \frac{1}{6}\varepsilon^e_{31}\varepsilon^e_{32} & \frac{1}{2}\varepsilon^e_{32}+\frac{1}{6}\varepsilon^e_{32}+\frac{1}{6}\varepsilon^e_{32}\varepsilon^e_{33} & \frac{1}{2}\varepsilon^e_{13}+\frac{1}{6}\varepsilon^e_{13}+\frac{1}{6}\varepsilon^e_{13}\varepsilon^e_{33} \\
 & & & \frac{1}{2}+\frac{1}{4}\varepsilon^e_{11}+\frac{1}{4}\varepsilon^e_{22}+\frac{1}{12}\varepsilon^e_{11}\varepsilon^e_{22}+\frac{1}{12}\varepsilon^{e^2}_{12} & \frac{1}{4}\varepsilon^e_{13}+\frac{1}{12}\varepsilon^{e^2}_{13} & \frac{1}{4}\varepsilon^e_{23}+\frac{1}{12}\varepsilon^{e^2}_{23} \\
 & & & +\frac{1}{12}\varepsilon^e_{11}\varepsilon^e_{22}+\frac{1}{12}\varepsilon^{e^2}_{12} & +\frac{1}{12}\varepsilon^e_{12}\varepsilon^e_{23}+\frac{1}{12}\varepsilon^e_{12}\varepsilon^e_{22} & +\frac{1}{12}\varepsilon^e_{13}\varepsilon^e_{21}+\frac{1}{12}\varepsilon^e_{11}\varepsilon^e_{13} \\
 & & & & \frac{1}{2}+\frac{1}{4}\varepsilon^e_{22}+\frac{1}{4}\varepsilon^e_{33}+\frac{1}{12}\varepsilon^e_{22}+\frac{1}{12}\varepsilon^{e^2}_{33} & \frac{1}{4}\varepsilon^e_{12}+\frac{1}{12}\varepsilon^{e^2}_{12} \\
 & & & & +\frac{1}{12}\varepsilon^e_{32}\varepsilon^e_{33}+\frac{1}{12}\varepsilon^{e^2}_{23} & +\frac{1}{12}\varepsilon^e_{32}\varepsilon^e_{23}+\frac{1}{12}\varepsilon^e_{23}\varepsilon^e_{31} \\
 & & & & & \frac{1}{2}+\frac{1}{4}\varepsilon^e_{33}+\frac{1}{4}\varepsilon^e_{11}+\frac{1}{12}\varepsilon^e_{33}+\frac{1}{12}\varepsilon^{e^2}_{11} \\
 & & & & & +\frac{1}{12}\varepsilon^e_{11}\varepsilon^e_{33}+\frac{1}{12}\varepsilon^{e^2}_{13}
\end{bmatrix}
\begin{bmatrix} \dot{\tau}_{11} \\ \dot{\tau}_{22} \\ \dot{\tau}_{33} \\ 2\dot{\tau}_{12} \\ 2\dot{\tau}_{23} \\ 2\dot{\tau}_{31} \end{bmatrix}
$$

(symmetric)

$$\delta Y = Q \underset{\approx}{K} : (\mathrm{sym}(\underset{\approx}{K}')) \qquad (5.4.4)$$

Hence , if the new yield status is not to violate the yield function , we have

$$Y_{①} + \delta Y = 0 \qquad (5.4.5)$$

giving

$$Q = \frac{-Y_{①}}{\underset{\approx}{K} : (\mathrm{sym}(\underset{\approx}{K}'))} \qquad (5.4.6)$$

Thus the second estimate of the solution is obtained from

$$\underset{\approx}{\tau}_{②} = \underset{\approx}{\tau}_{①} + \delta \underset{\approx}{\tau} \qquad (5.4.7)$$

in which the increment in Kirchhoff stress ie., the correction is completely determined from Eqs. 5.4.3 and 5.4.6 .

We can now get the elastic deformation gradient corresponding to the state of stress in Eq. 5.4.7 ie.,

$$\underset{\approx}{F}^{e}_{②} = \underset{\approx}{F}^{e}_{②}(\underset{\approx}{\tau}_{②}) \qquad (5.4.8)$$

following a procedure similar to the one in Appendix B .

All other variables such as ,

$$\underset{\approx}{F}^{P}_{②} , \quad \underset{\approx}{\sigma}^{B}_{②} , \quad \underset{\approx}{\sigma}_{②} \text{ etc.}$$

can thus be found using constraint Eq. 5.1.2 , Appendix A etc.

The second estimate of the solution will be found to satisfy all the constraints , Eqs. 5.1.1 through 5.1.5 to the extent that Eq. 5.4.5 closely represents the Eq. 5.1.5 , ie. ,

$$Y(\tilde{F}^{t+\Delta t}_{e}, \tilde{F}^{t+\Delta t}_{p}) \leq 0 \qquad (5.4.9)$$

The procedure can be repeated successively till a suitably converged solution is reached .

CHAPTER 6: IMPLEMENTATION IN THE FEM PROGRAMME , AND RESULTS

6.1 Verifying the Constitutive Model

The constitutive model developed in the previous chapters was coded-up into a computer programme . Several simple cases of homogeneous deformation were tried, to confirm that the code truly reflected the mathematical logic used in developing the model.

The case of a pseudo-shear deformation is one of many cases used to demonstrate the above mentioned. Figure 6.1 shows the response of the coded programme for this case , clearly showing a " locking " behaviour . We also see that , due to the very large strains and the inherent non-linearity , we develop normal stresses such as σ_{11} shown.

6.2 Finite Element Method (FEM) Implementation

The constitutive model developed was linked to the FEM programme ABAQUS , by suitably coding up the linking subroutines for compatability .

We investigated the behaviour of two polymeric materials - polycarbonate (Pc) and polystyrene (Ps) , in two problems of large deformation:

a) the formation and propagation of necks in round bars in tension ; and

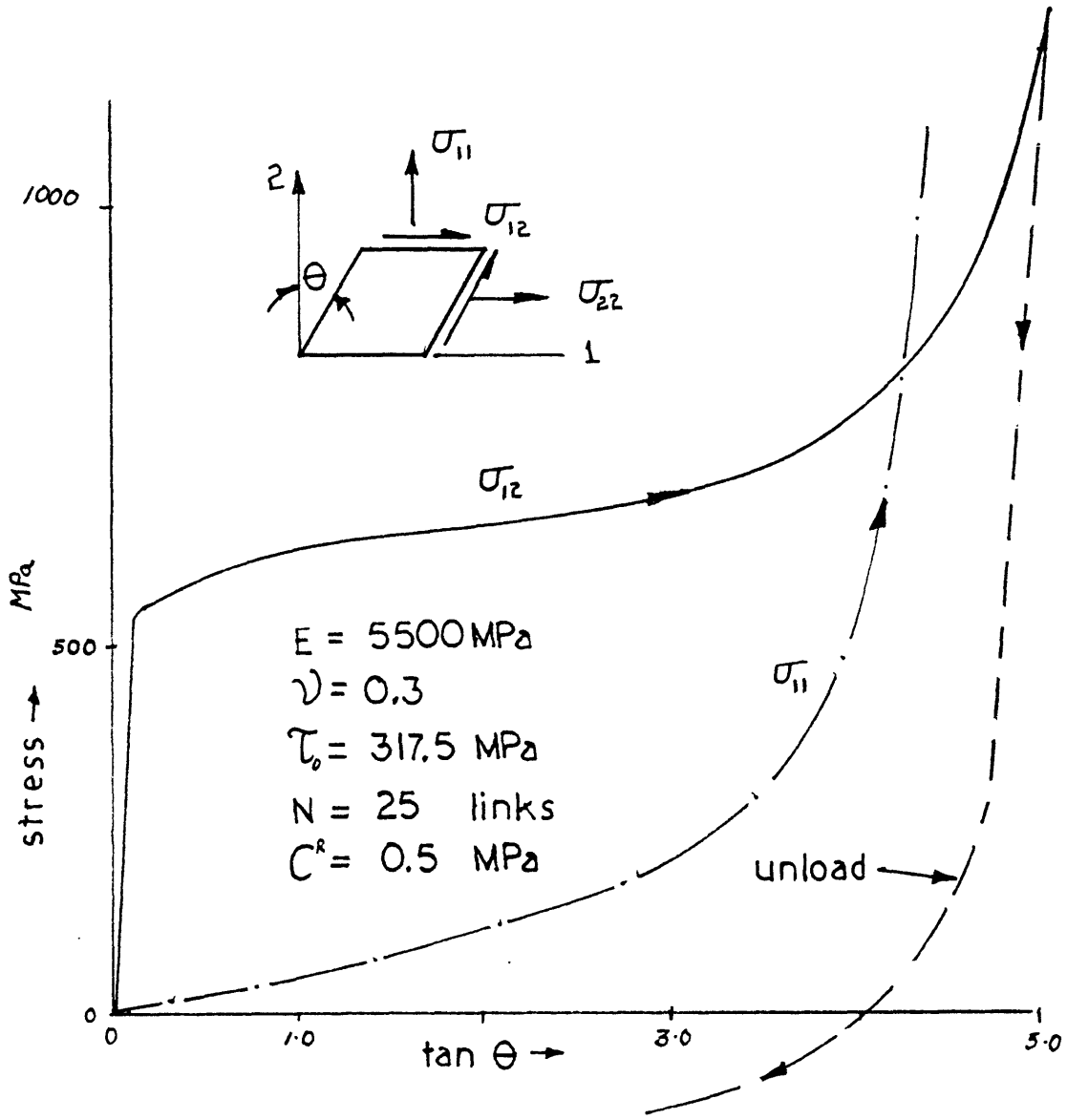

Figure 6.1 : Large strain " pseudo shear " deformation : Results of the coded computer programmme

b) the drawing of round polymer tufts out of a half-space , thus modelling the drawing of craze-tufts outlined in Chapter 1.

In all of the cases we used eight-noded axi-symmetric elements , and employed a reduced integration procedure .

The mechanical properties used are as follows:

Polystyrene

The Young's modulus, $E = 3250$ MPa

The yield stress in shear, $\tau_o = 50.625$ MPa Argon, (1976)

Poisson's ratio, $\nu = 0.3$

Number of polymer links between entanglements, $N = 25$ (This is based on stretches of about 5 observed in craze-tufts by Kramer , 1983 .)

The pre-multiplier rubber modulus, $C_{PS}^{R} = 0.75$ MPa (This is based on a test done above Tg, see Appendix A .)

Polycarbonate

E = 2350 MPa Bauwens-Crowet, (1972)

ν = 0.3

τ_o = 35.14 MPa (from a test, explained later in the text)

N = 3

$$C_{PC}^{R} = \left(\frac{\rho}{M_e}\right)_{PC} \times \left(\frac{M_e}{\rho}\right)_{PS} \times C_{PS}^{R}$$

$$\doteq 2.25 \text{ MPa}$$

6.3 Necking and Plastic Drawing of Round Bars in Tension

The problem of necking in glassy polymers was investigated for both the materials , polystyrene and polycarbnate , by the finite element method . A simple-tension experiment was also done on a round polycarbonate sample (- diameter , D = 5.5 mm ; length , L = 23.3 mm) at room temperature. The sample used had been heat-treated to 165 C and then quenched in ice . In Fig. 6.2 we have the load vs. normalized displacement curve obtained from the test.

The yield stress based on peak load in the test is about 60 Mpa , giving

$$\tau_o = 35.14 \text{ Mpa} = 60/\sqrt{3}$$

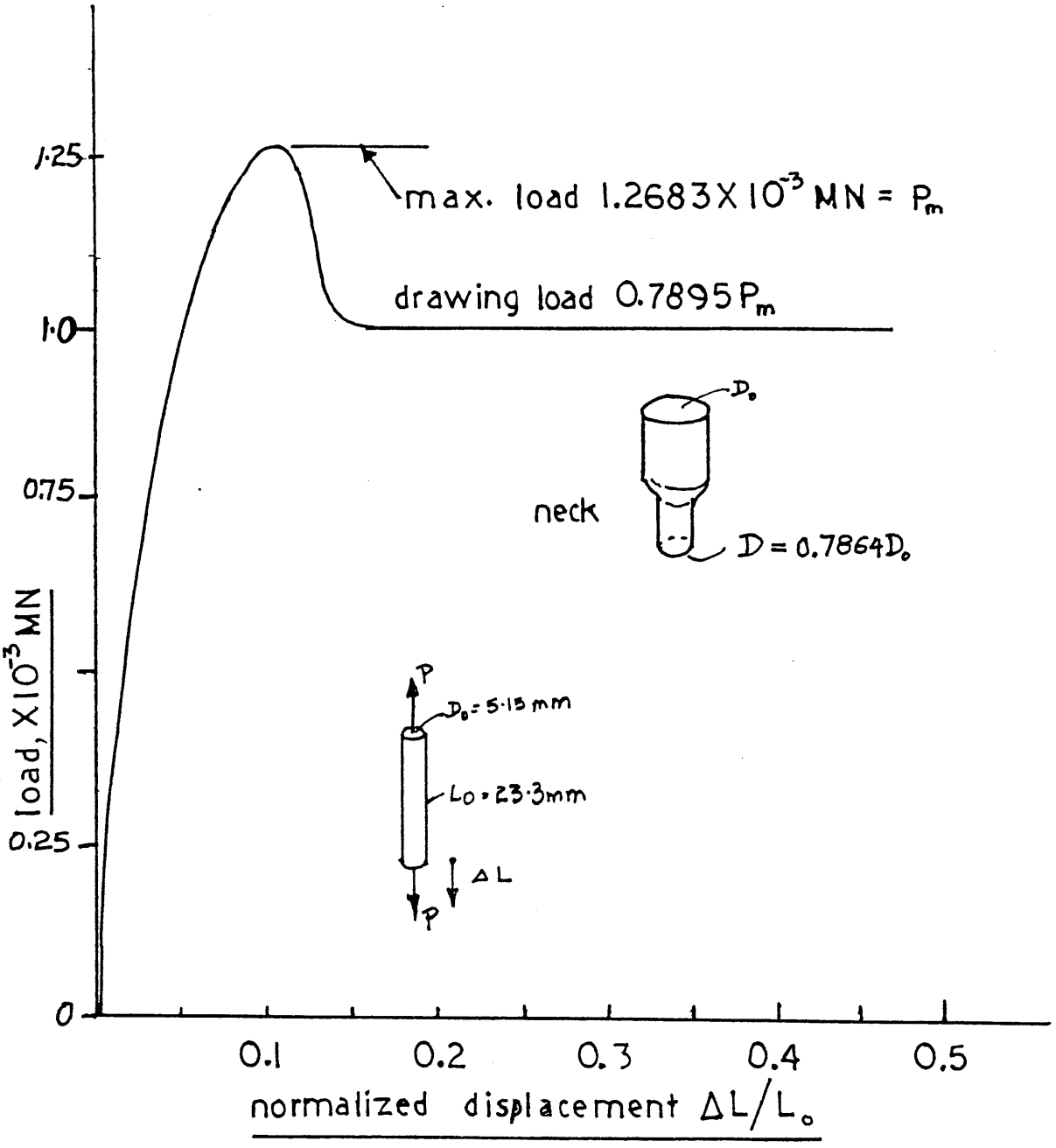

Figure 6.2 : The load vs. normalized displacement curve from a uniaxial tension test on a polycarbonate sample quenched in ice after being heat-treated to 165 °C .

The number of links between entanglements is taken to be

$$N = 3 \quad ,$$

based on ratio of the un-necked to the necked areas meaured to be about 1.62 . This ratio is usually very close to the network-stretch for a polymer ie., $\sqrt{N}$.

6.3.1 Results from the Finite Element Analysis

Polycarbonate Neck

The initial (undeformed) mesh is shown in Fig. 6.3 , showing the imposed displacement boundary condition . In Fig. 6.4 we have the plots of the normalized load vs. normalized displacement , both from the experiment and from the FEM analysis . For the experimental curve the load has been normalized with respect to the peak load ; in the computational case , the normalization is with respect to yield load based on the initial area, A_o of the undeformed mesh . The displacements are normalized with respect to the initial length, L_o of the specimen and the undeformed mesh respectively .

In Fig.6.5 we see a comparison of the unloaded profiles from the test and the FEM analysis ; the agreement is remarkable . In Fig. 6.6 we see the deformed meshes during the stages of formation and propagation of the neck . The profile on unloading is also shown .

From Fig. 6.4 we note that the drawing load of approximately 0.85 times the peak from the FEM analysis , is about 7.5 % higher than the corresponding

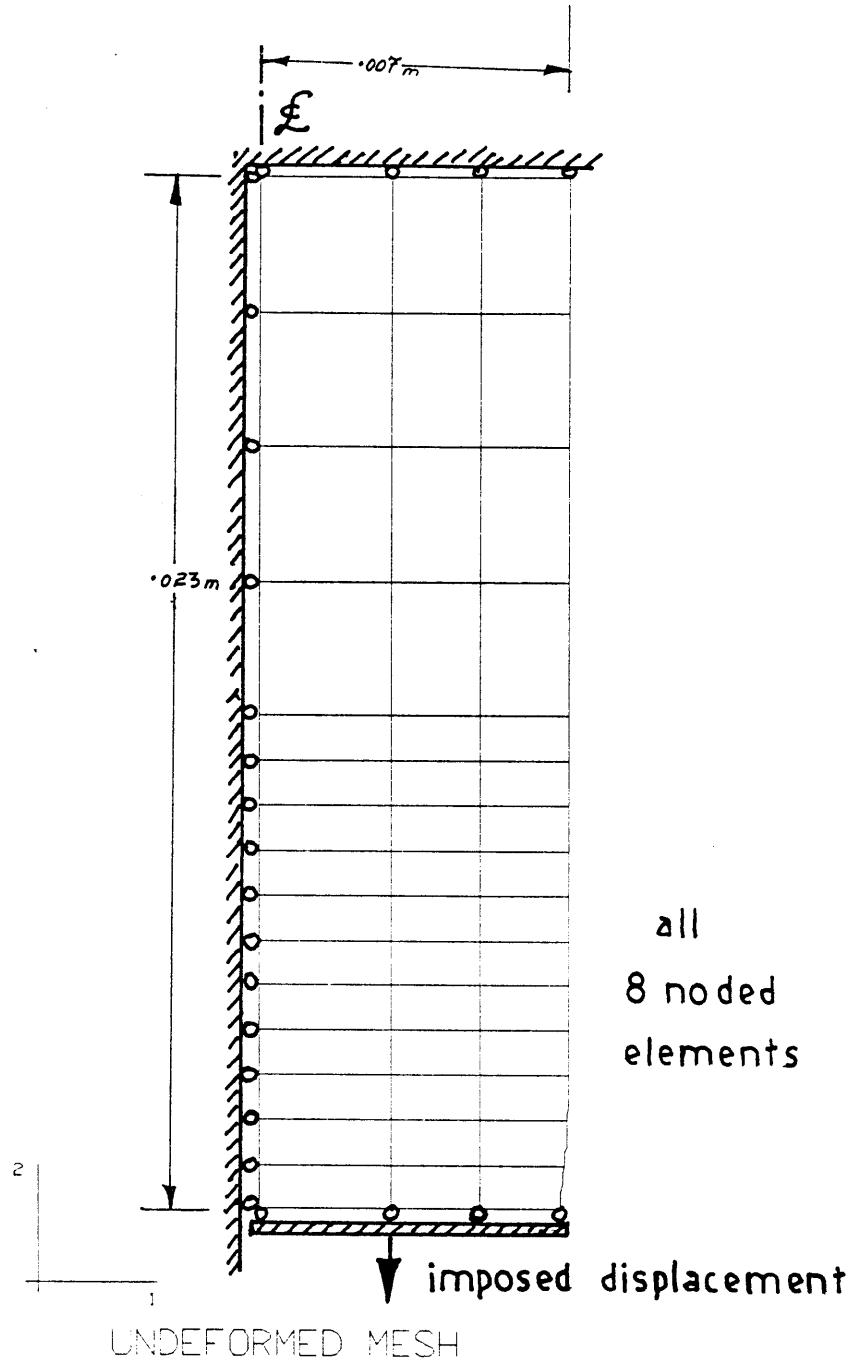

Figure 6.3 : Initial axi-symmetric FEM mesh used for the polycarbonate neck problem .

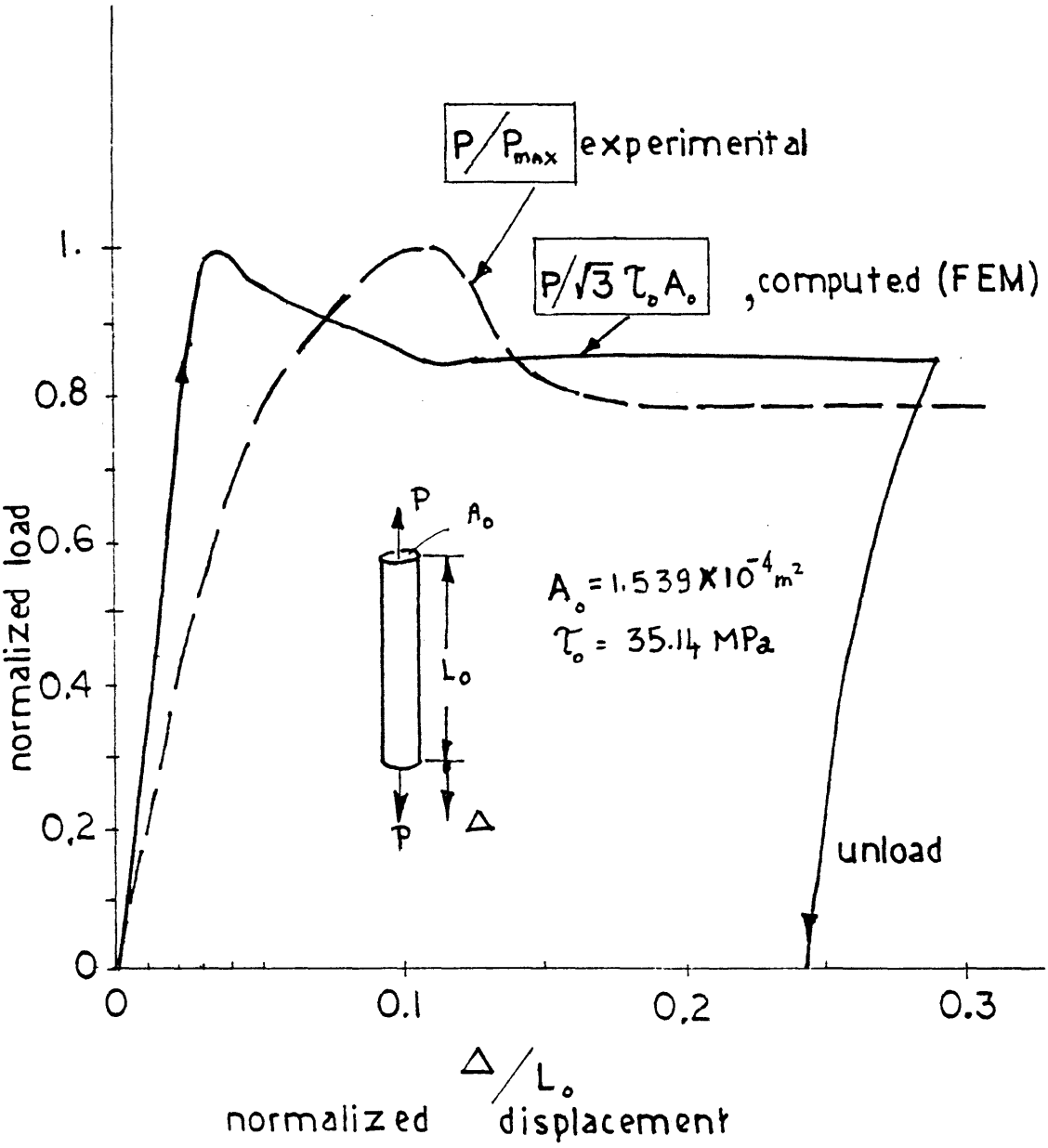

Figure 6.4 : Normalized load vs. normalized displacement from a FEM analysis of the polycarbonate neck problem , compared with the experimental curve.

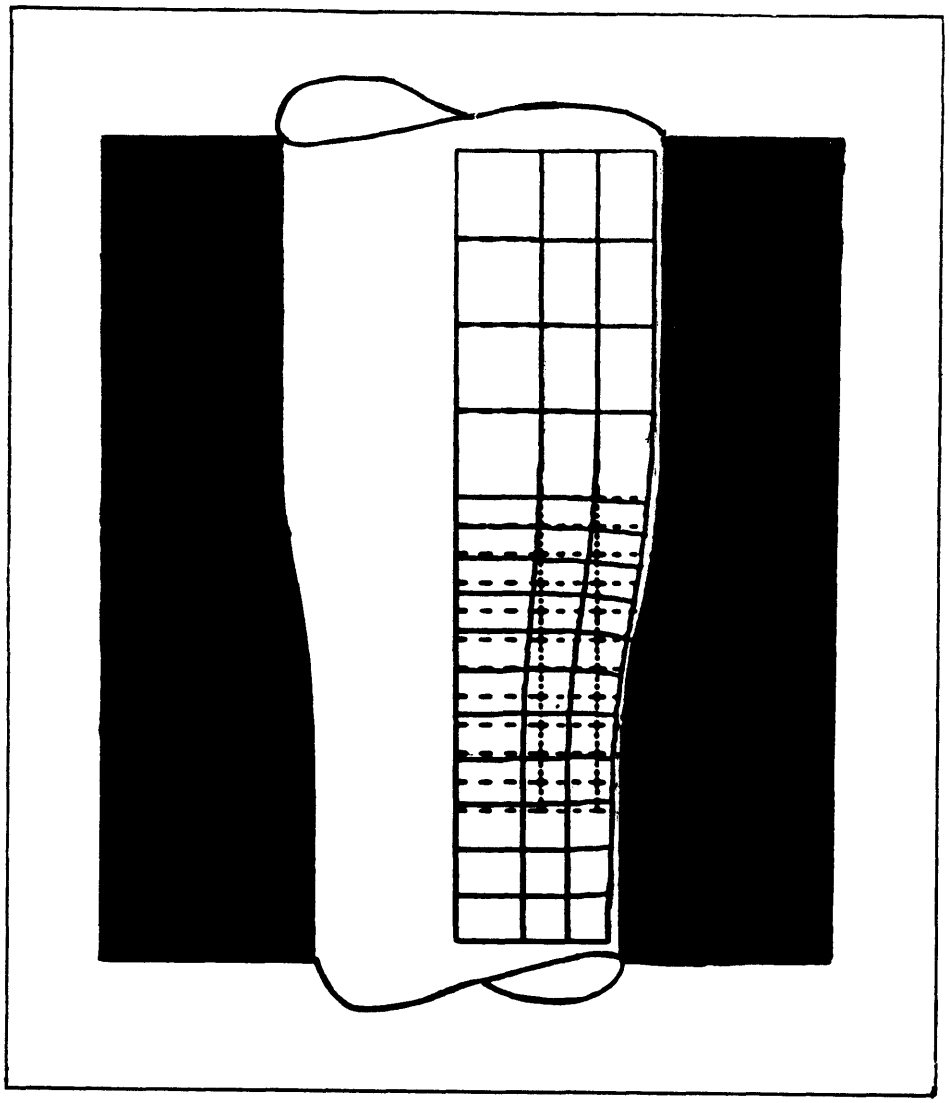

Figure 6.5 : Comparison of the experimental neck profile with the computed one (shown nested a little off centre for clarity) for polycarbonate .

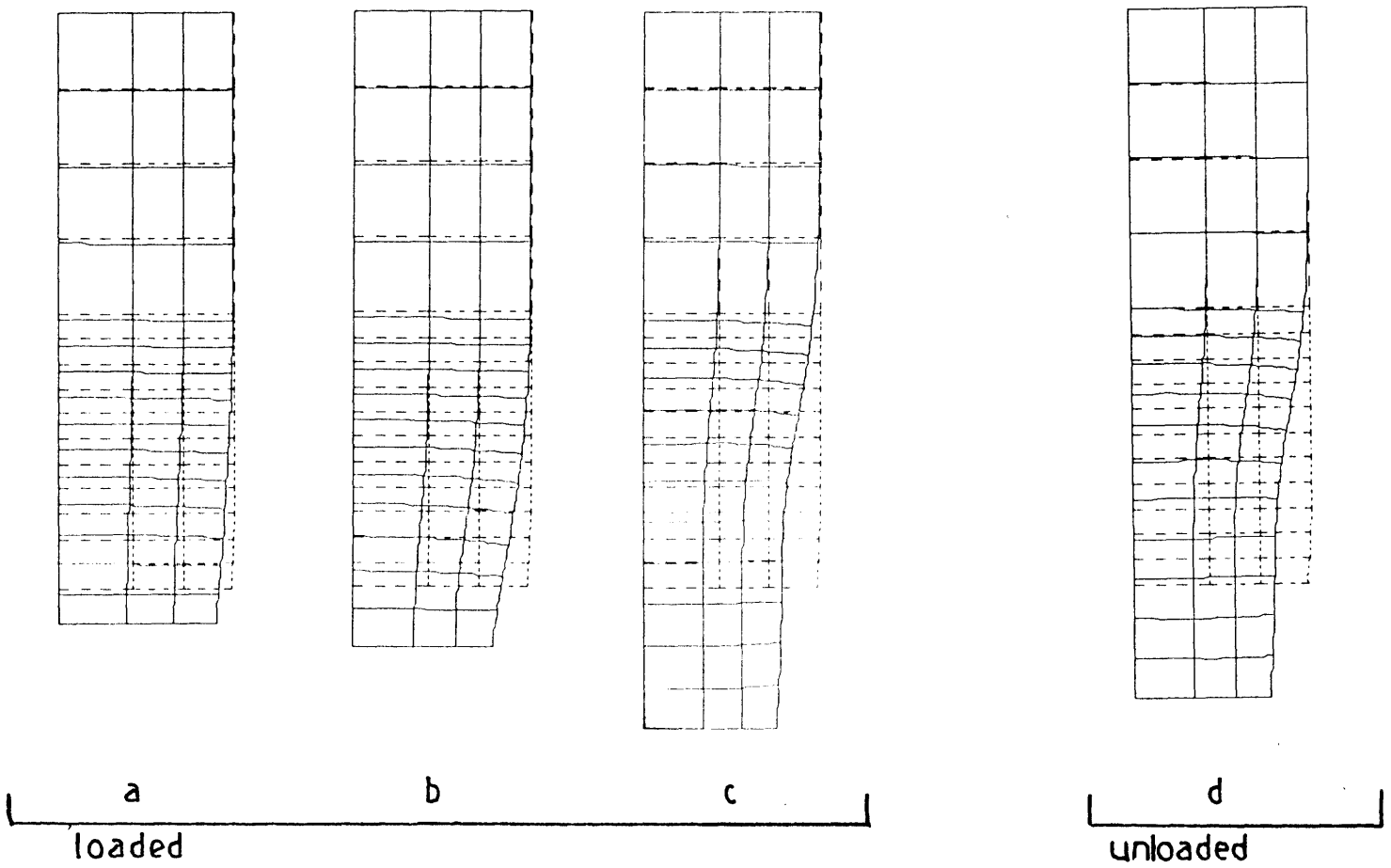

Figure 6.6 : Deformed meshes from computational analysis corresponding to the stages of formation and propagation of a neck -- polycarbonate case ; d is the configuration unloaded from c .

load from the test (- found to be about 0.789 times the peak). One reason for this disparity may be that polycarbonate could have a material instability or yield drop represented schematicall in Fig.6.7 (Spitzig and Richmond, 1979). This would cause the load to drop further.

We could also expect a larger yield drop if we took into consideration the pressure dependence of the yield stress . Bauwens (1972) found that , for polycarbonate , the yield stress in compression is about 1.307 times that in tension at room temperature . In Figs. 6.8 and 6.9 we see contours of the hydrostatic pressure , p ie., of

$$p = -\frac{tr(\underset{\sim}{\sigma})}{3} \qquad (6.3.1)$$

in the loaded and in the unloaded states . In Fig. 6.10 we see contours of incremental plastic strain ,

$$\sqrt{\underset{\sim}{D}^p : \underset{\sim}{D}^p}$$

in which we can see a central region where maximum flow is occuring flanked , above and below, by zones of lower incremental plastic deformation . The zone above is seen to be approaching the main body which is only elastically deforming and hence has no flow occuring . The zone below approaches the neck which has reached steady-state proportions and is not deforming further . A close examination of Figs. 6.8 and 6.10 reveals that close to the region of maximum plastic flow , we also have the maximum negetive pressure . In this zone we see an average pressure of about -30 MPa (ie., about 1.5 times the average pressure at peak load) . Hence ,based on the pressure-dependence of the yield stress , we could have an effective yield stress of about 32.8 MPa ie., about 6.5 %

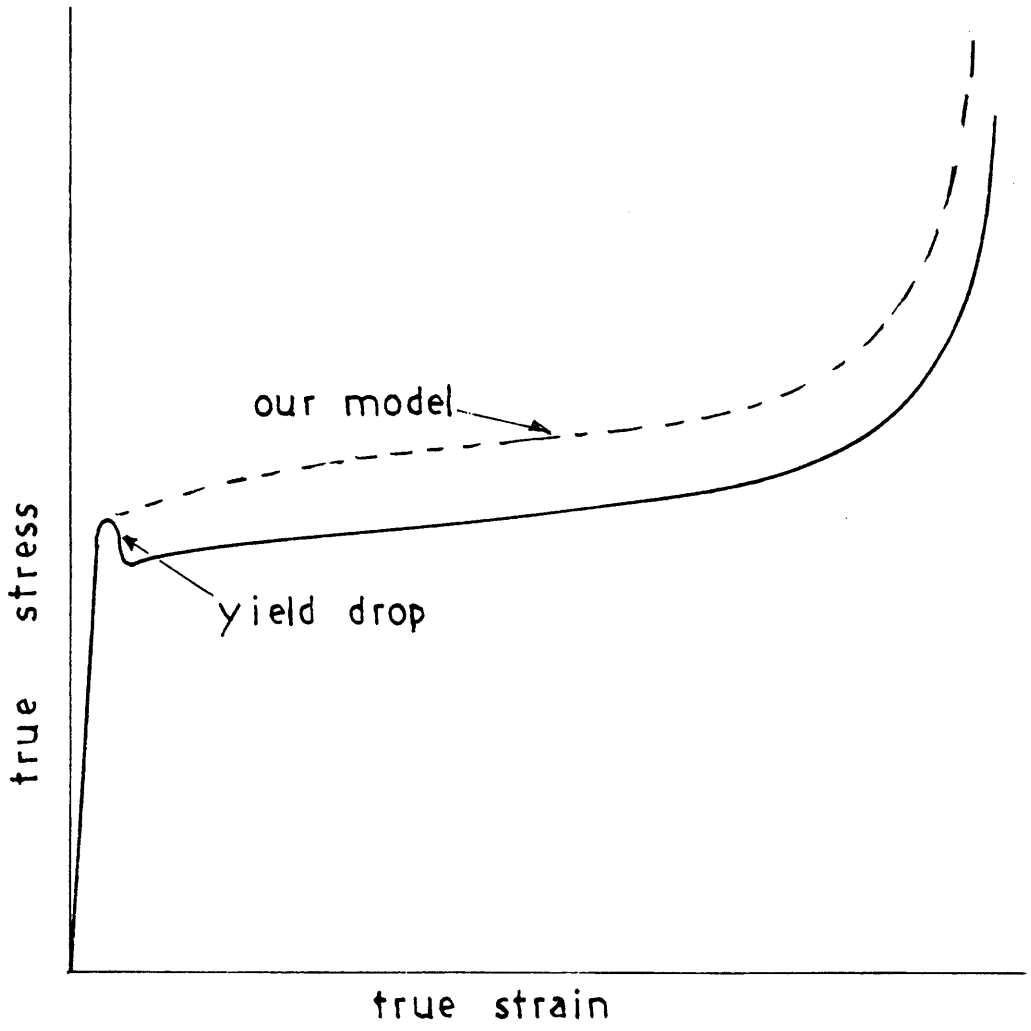

Figure 6.7 : Schematic representation of a true stress vs. true strain curve with a small material instability (yield drop) .

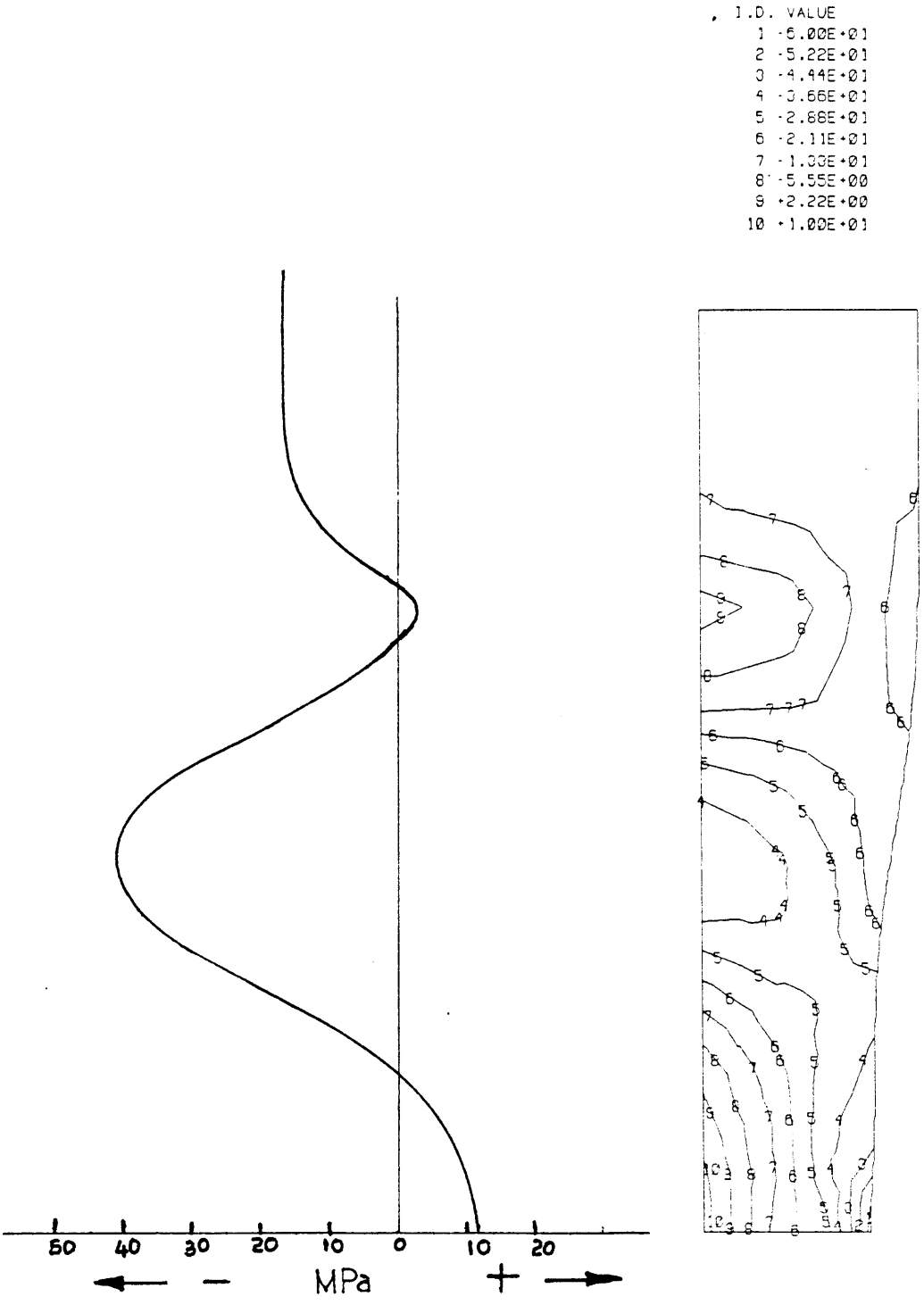

Figure 6.8 : Polycarbonate neck : hydrostatic pressure (in MPa) contours shown on the deformed, loaded configuration ; the variation along the axis is plotted on the left .

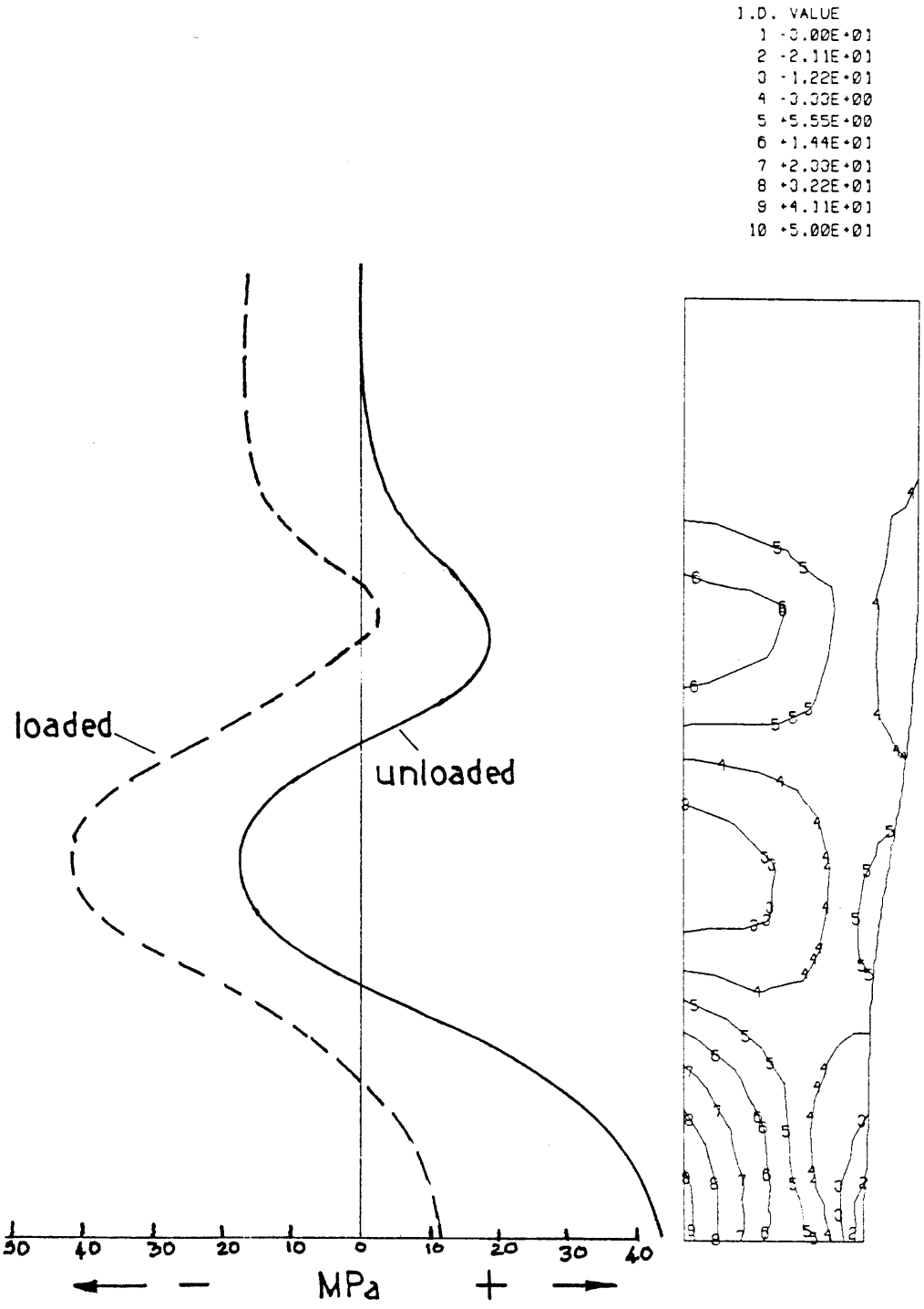

Figure 6.9 : Polycarbonate neck : hydrostatic pressure (in MPa) contours shown on the deformed, unloaded configuration ; the variation along the axis is plotted on the left .

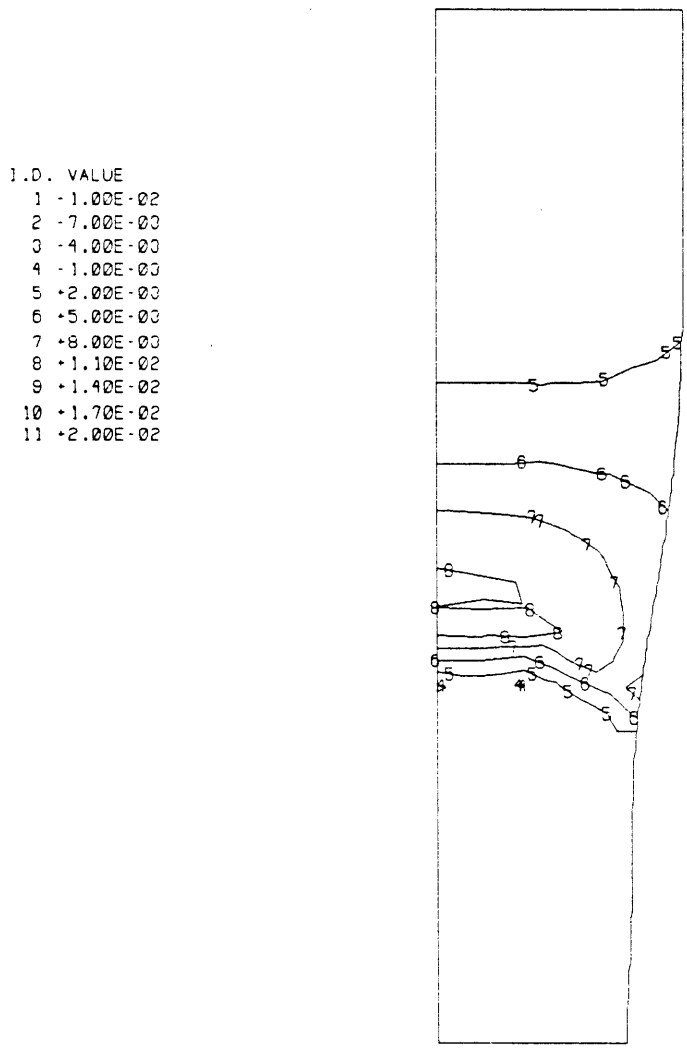

Figure 6.10 : Polycarbonate neck : contours showing the range of incremental plastic strain in the yielding zone .

lower than used in the yield function (see Chapter 2) . Incorporating this effect would result in a drawing load much closer to the experimentally observed one .

Changes in chain configuration in a plastically deformed polymer specimen bear a direct relationship to the birefringence patterns observed when such a specimen is tested (Andrews, 1965) . There is however , to a much lesser degree the photoelstic effect due to elastic strains . The two effects may clash in regions of low plastic strains ; but close to the necked region , for example , where plastic strains are orders of magnitude higher than elastic strains , the birefringence patterns observed would predominently relate to the changes in chain configuration ie., to the contours of differences in principal plastic stretches shown in Fig. 6.11 .

Some Observations :

We note that , even though having reached steady-state proportions under an external tensile load , the necked region is not under a state of uniaxial tensile stress . Each material element in the un-necked region of the main body at a typical distance from the load-axis suffers a unique strain history as it sequentially " passes " through the shoulder , and then , into the neck. A material element closer to the outer edge of the bar suffers far greater hoop stress than does an element close to the axis of symmetry .

Hence , as seen in Fig. 6.9 for example , the pressure along the axis in the unloaded configuration drops to zero in the main body which has not plastically deformed

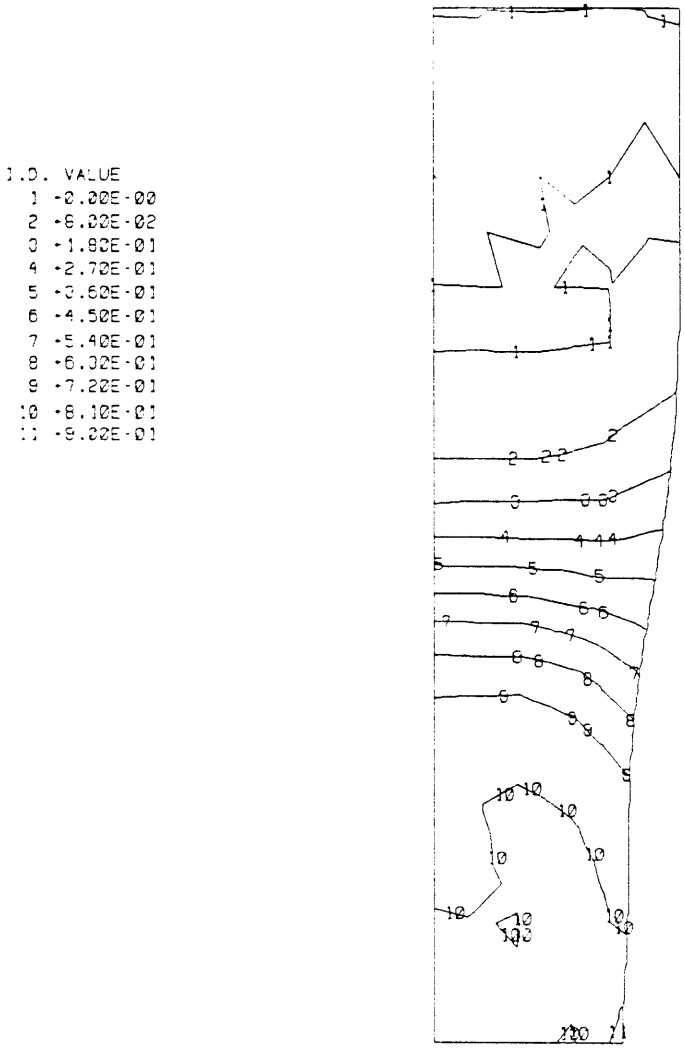

Figure 6.11 : Polycarbonate neck : contours of the differences in the principal plastic stretches .

at all ; but in the necked region we see a residual stress, and the pressure does not drop to zero . However, the integrated effect of the stresses across any cross-section in the unloaded state will yield a net zero load .

At steady state we can thus expect that all gradients along the load-axis alone will vanish ; we could however, have radial gradients ie., normal to the axis . Lee, Mallett and McMeeking, (1977), have made similar observations in the extrusion problem they studied.

Polystyrene Neck

When a polystyrene rod is tested in tension below its Tg (about 100 C) , it does not result in a neck because crazing, followed by fracture intervene . None the less , a FEM analysis of the polystyrene neck problem provides insight for the understanding of large strain drawing processes , such as in textile fibres .

The initial mesh for the polystyrene neck problem is shown in Fig. 6.12 . All the material properties used are as indicated earlier . except for the yield stress in shear ; the value , 89.1 MPa was used for the polystyrene neck problem . This was later revised for the polystyrene craze-tuft problem , for which the value of 50.625 MPa was used .

Figure 6.13 is a plot of the normalized load vs. normalized displacement , showing a much larger load drop than seen in the polycarbonate case . In Fig. 6.14 we see the deformed meshes during stages of formation and propagation of the neck, and of the unloaded configuration.

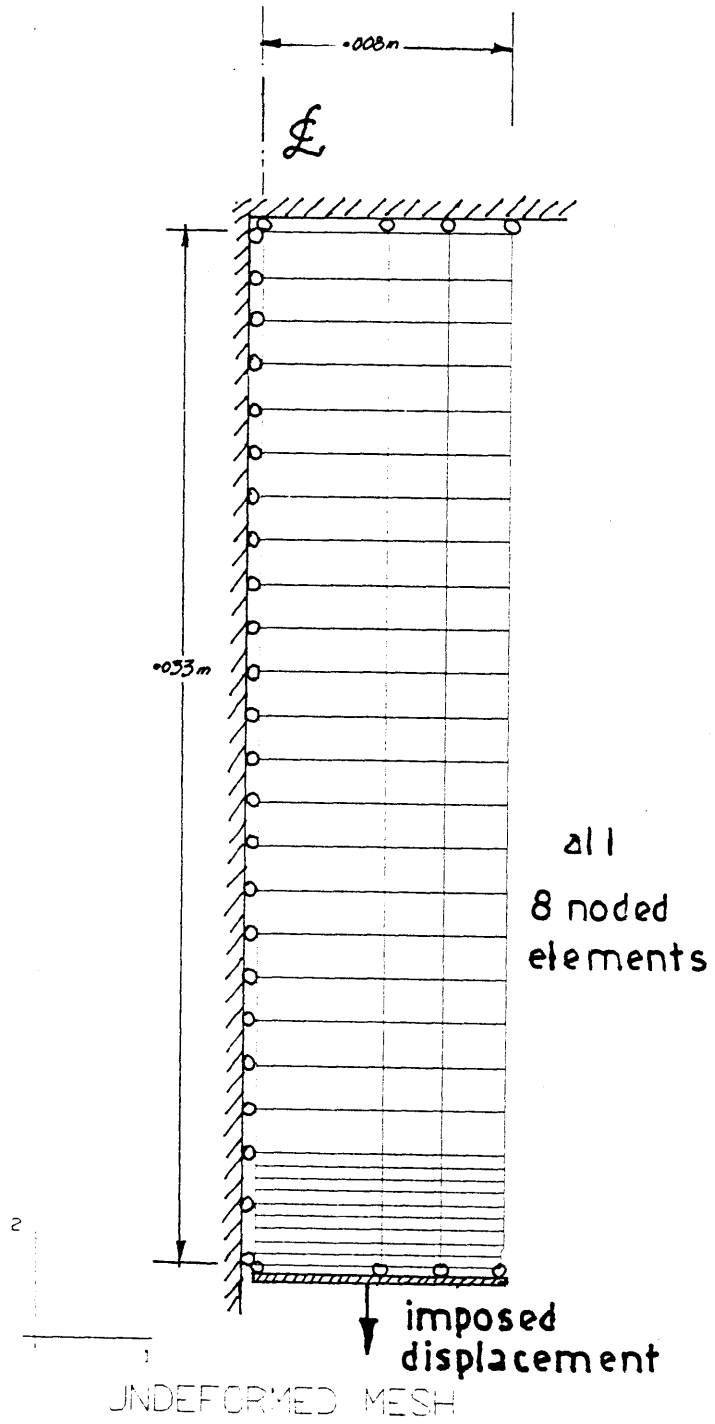

Figure 6.12 : Initial axi-symmetric FEM mesh used for the polystyrene neck problem .

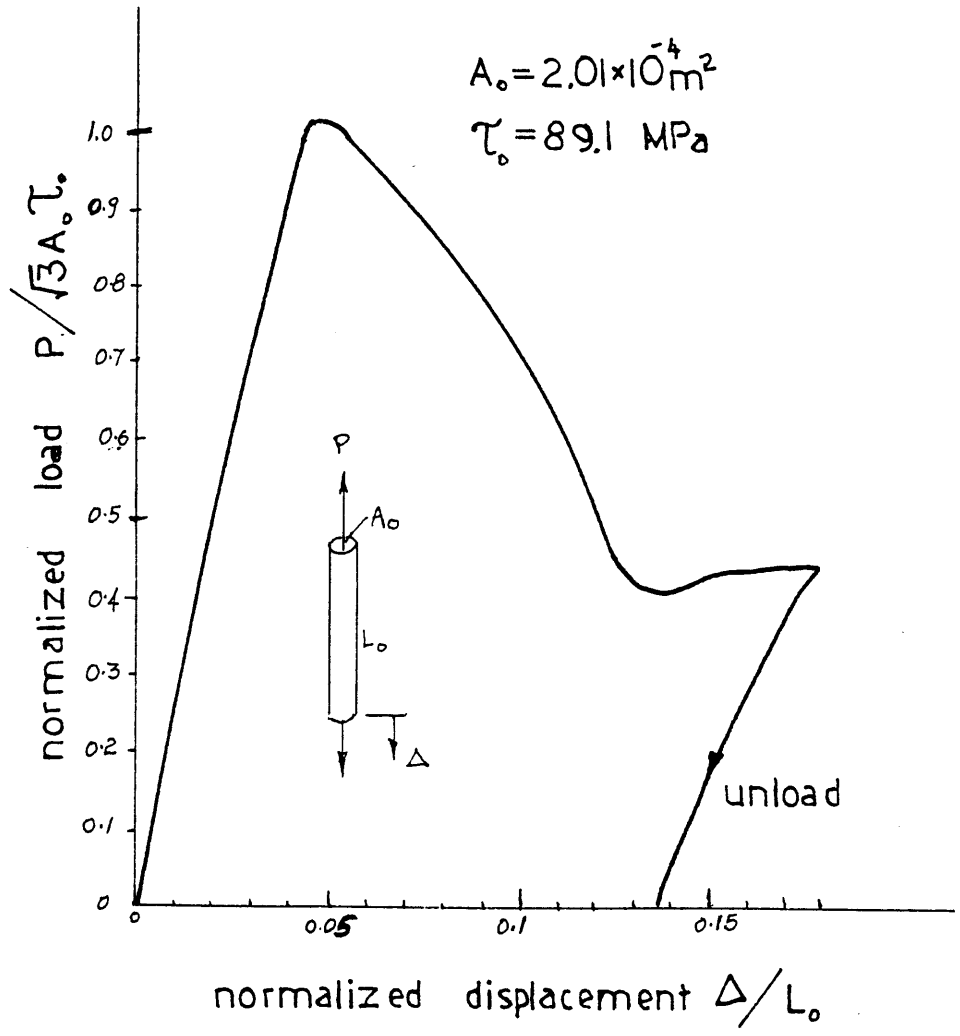

Figure 5.13 : Normalized load vs. normalized displacement from a FEM analysis of the polystyrene neck problem .

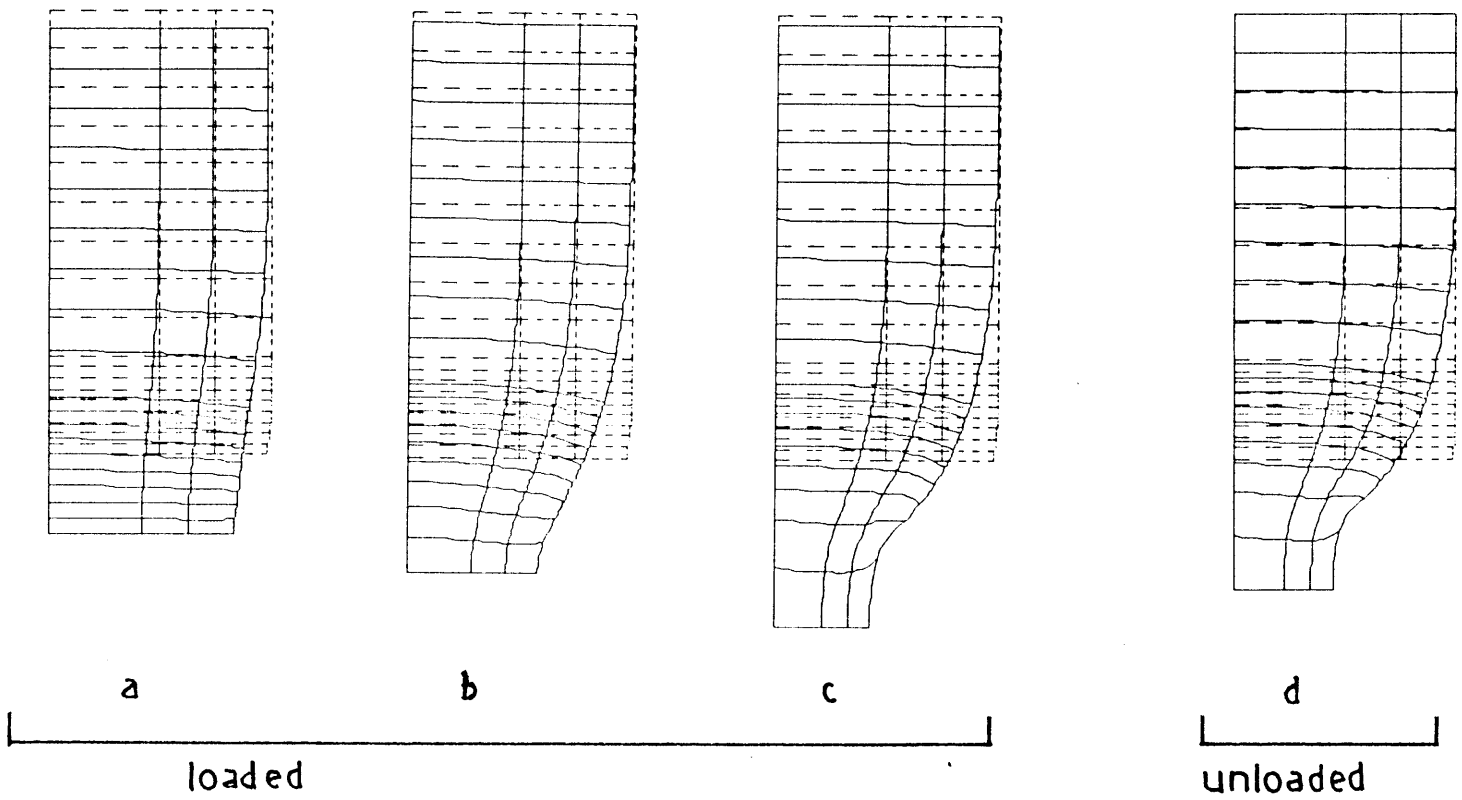

Figure 6.14 : Deformed meshes from computational analysis corresponding to the stages of formation and propagation of a neck -- polystyrene case ; d is the configuration unloaded from c .

We clearly see that the necked section suffers an axial stretch of the order 4.95 , much larger than, about 1.62 seen in the polycarbonate case . We also note that this stretch (of 4.95) is about equal to the ratio of the un-necked to the necked areas , and also , to the square root of the number of chain links, N (= 25) . Hence , this serves as a useful method of obtaining an approximate measure of the number of links , N . The same is observed in the polycarbonate case described earlier , in which we assumed a value for N based on the experimentally determined area ratio ; the area ratio that we finally got from the FEM analysis is remarkably close to the actually observed one (see Fig. 6.5).

Figures 6.15 and 6.16 show contours of hydrostatic pressure in the loaded and in the unloaded configurations. In Figure 6.17 we see the yield zone of incremental plastic deformation. Figure 6.18 shows contours of differences in principal plastic stretches , and would correspond to those observed in birefringence measurements.

6.4 Plastic Drawing of a Polymer Tuft out of a Half-Space

In this section we will try to model a polystyrene craze-tuft. There is no obvious initial undeformed mesh configuration that can be used in order to arrive at a final shape that would resemble a drawn craze-tuft under steady state conditions . The choice of the undeformed mesh shown in Fig. 6.19 is motivated by the following observations of crazes :

Geometrically , where the tuft departs from the half-space ie., the craze-flank , we expect to see the

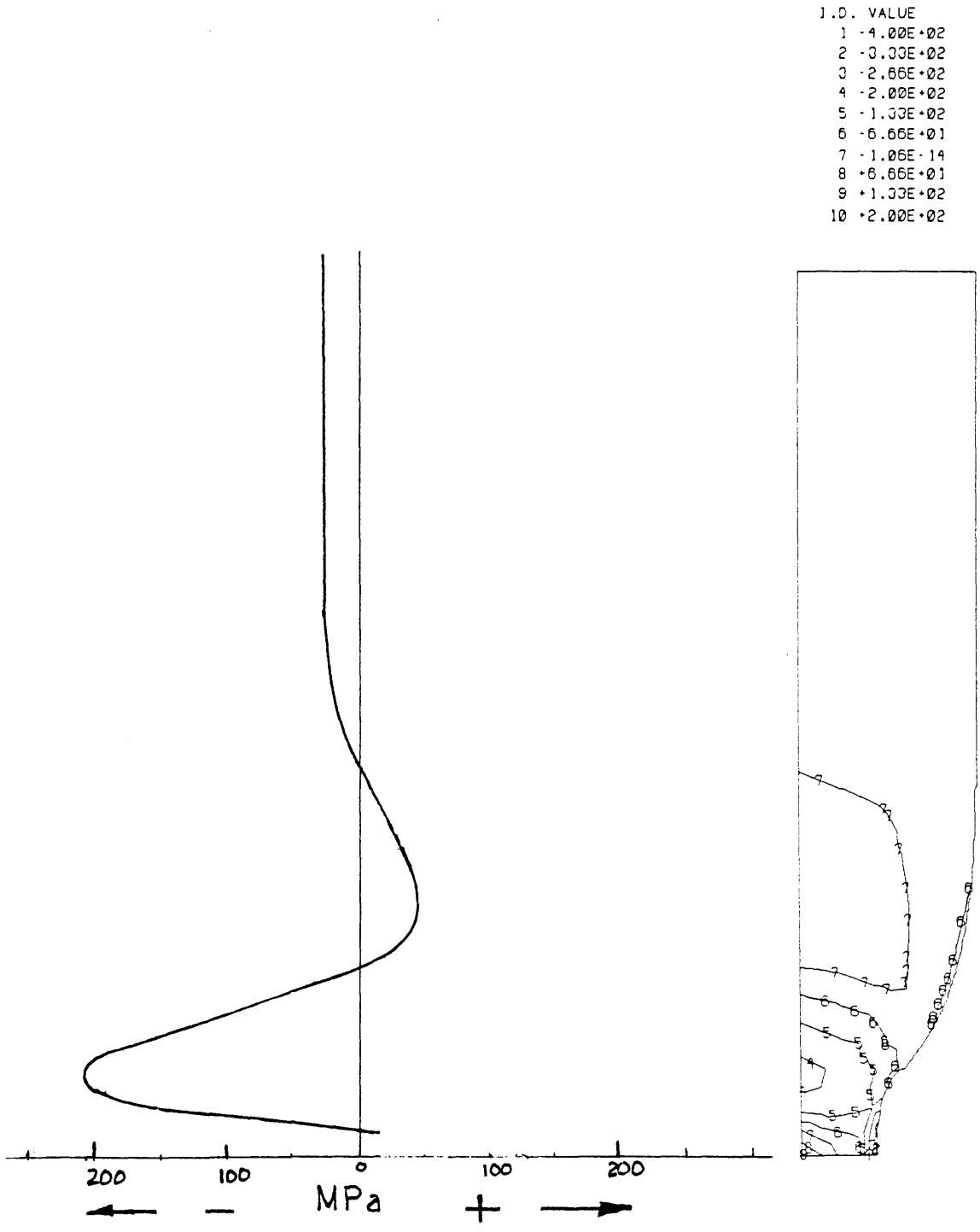

Figure 6.15 : Polystyrene neck : hydrostatic pressure (in MPa) contours shown on the deformed, loaded configuration ; the variation along the axis is plotted on the left .

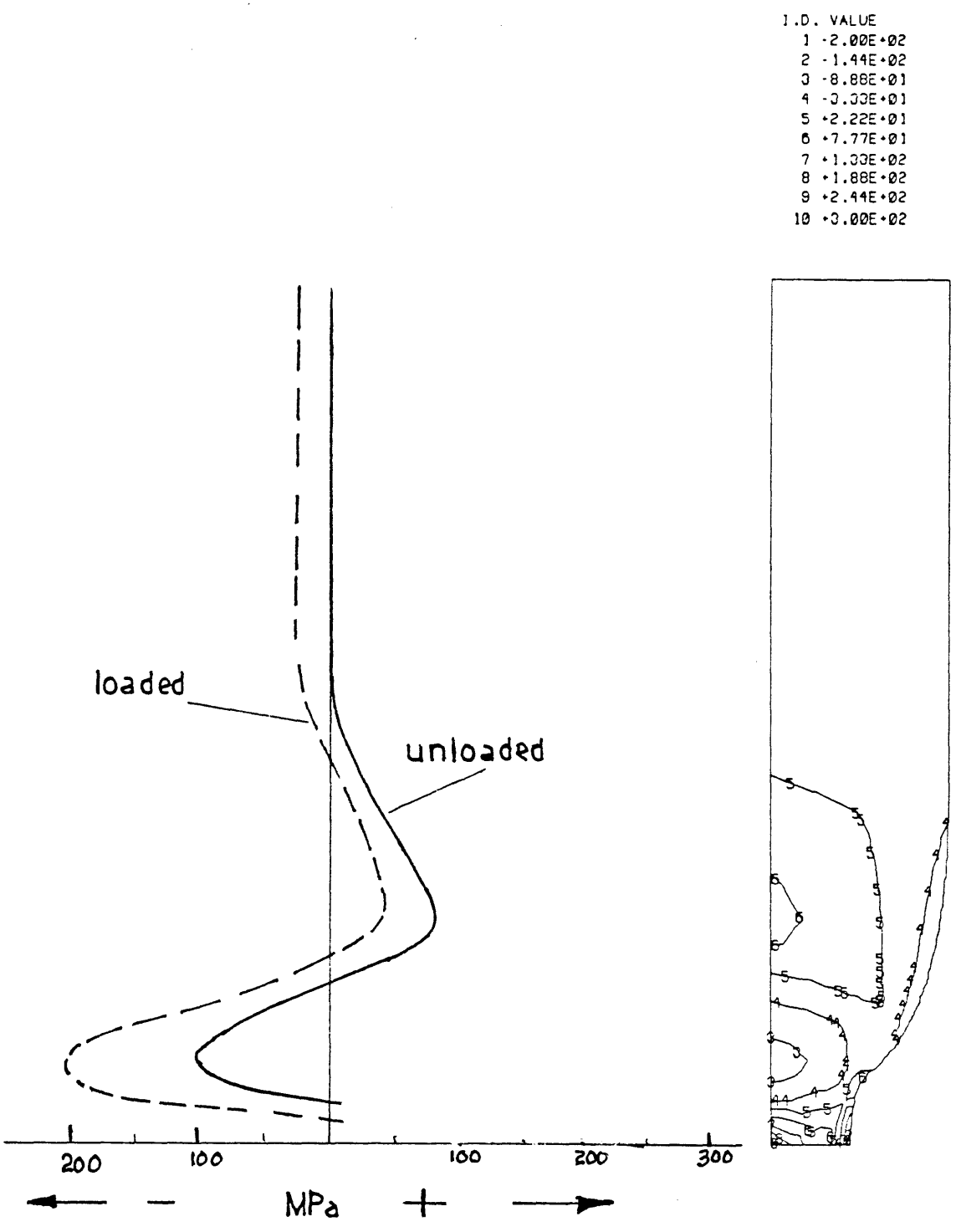

Figure 6.16 : Polystyrene neck : hydrostatic pressure (in MPa) contours shown on the deformed, unloaded configuration ; the variation along the axis is plotted on the left .

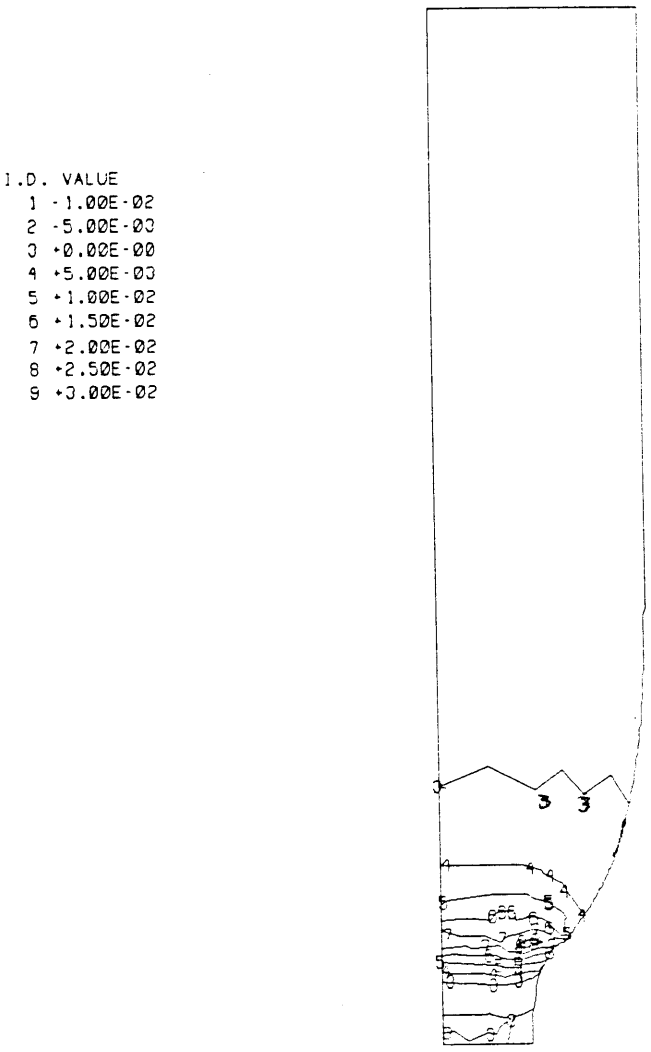

Figure 6.17 : Polystyrene neck : contours showing the range of incremental plastic strain in the yielding zone .

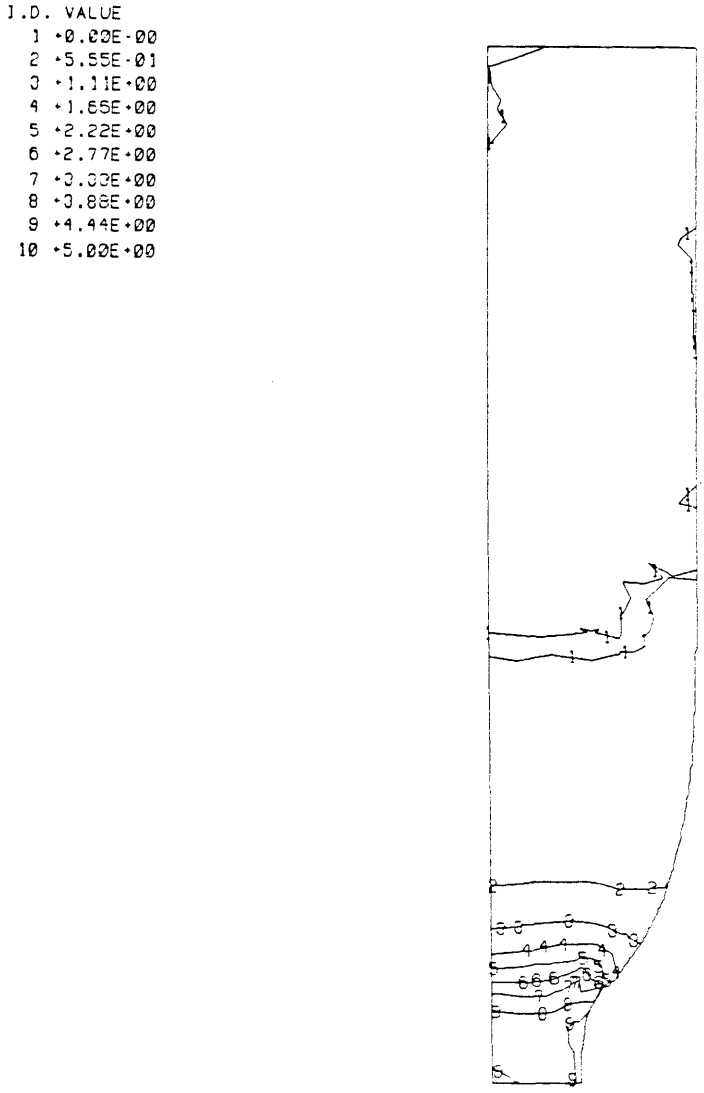

Figure 6.18 : Polystyrene neck : contours of the differences in the principal plastic stretches .

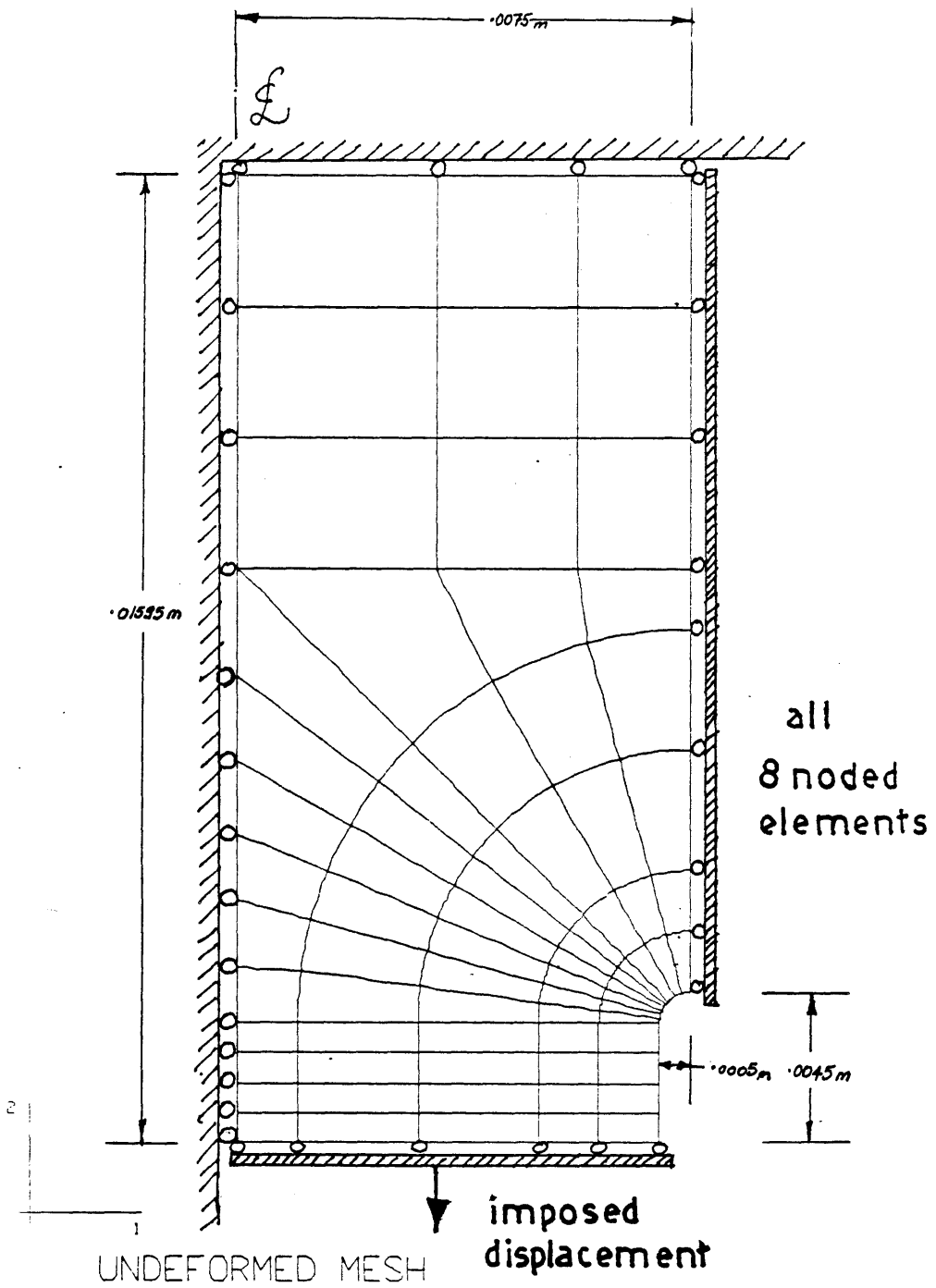

Figure 6.19 : Initial axi-symmetric FEM mesh used for the polystyrene craze problem .

tuft-contour to blend with the edge of the half-space. A notch is hence introduced in the initial configuration . Further , the edge condition imposed on the outer rim (Fig. 6.19) implies, no net radial traction ; this would mean that in an array of craze-tufts extending at steady state , we expect no net radial traction imposed by any one tuft on its neighbouring tufts . There could however be steep gradients in radial stress along the outer rim, as we shall see later.

The analysis is made under imposed displacement. In Fig. 6.20 we see the load vs. displacement curve obtained from the FEM analysis, with corresponding deformed meshes during stages of formation of the tuft shown in Fig. 6.21 . Figures 6.22 and 6.23 show the hydrostatic pressure contours in the loaded and the unloaded configurations. In Figs. 6.24 and 6.25 we see contours of radial stress distribution in the loaded and the unloaded configurations ; the variation along the outer edge is also plotted . Figure 6.26 shows contours of incremental plastic strain in the yield zone. Lastly , in Fig. 6.27 we see contours of differences in principal plastic stretches and would correspond to contours seen in a birefringence test.

6.5 Closing Remarks

We see that the constitutive model developed based on the physical processes occuring in a deforming polymer , when applied to a few boundary value problems yields interesting results . Most of the results seem to be intuitively sound . In the case of polycarbonate , for which some experimental investigation was done , some agreement is seen with the computed results. Experiments done above Tg

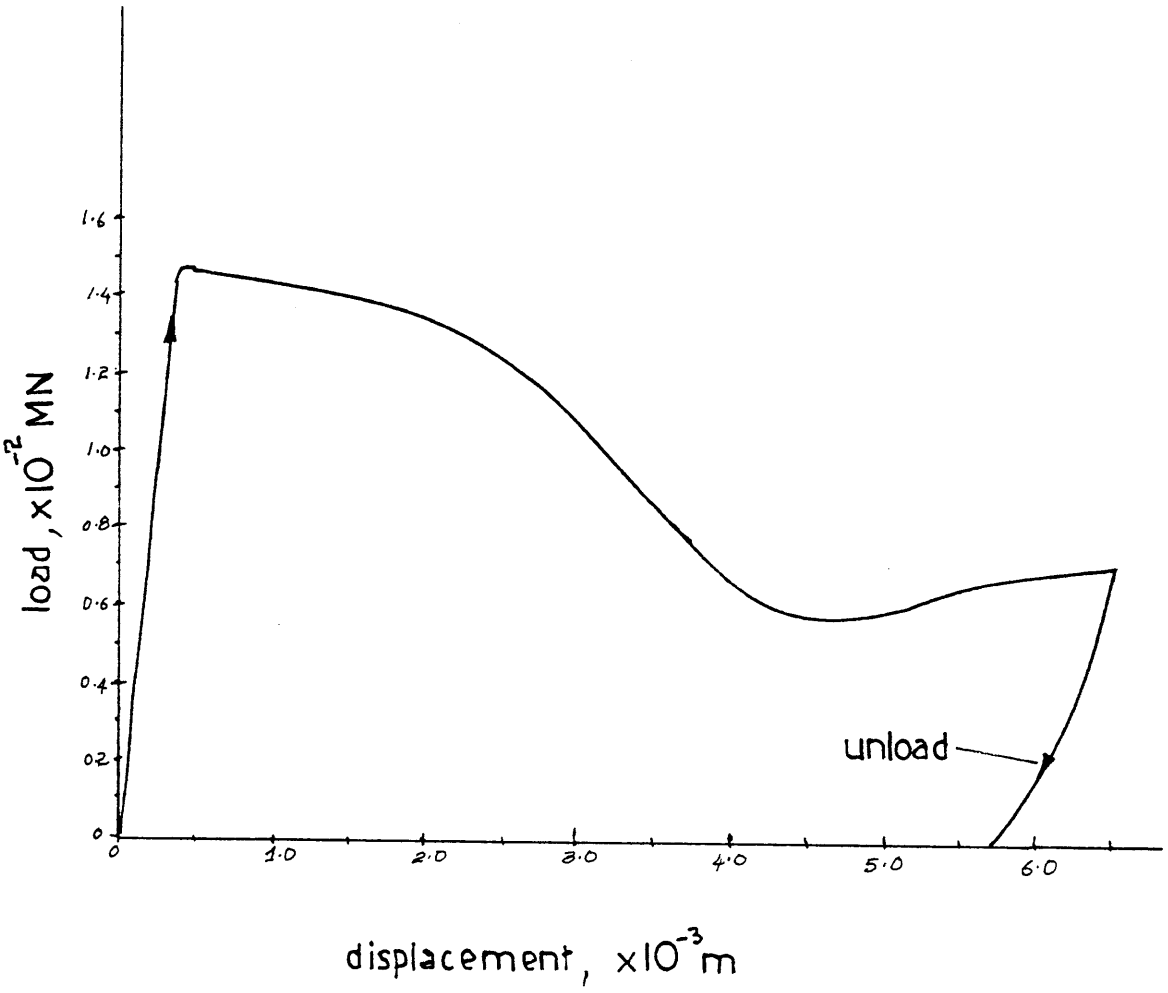

Figure 6.20 load vs. displacement from a FEM analysis of the polystyrene craze problem .

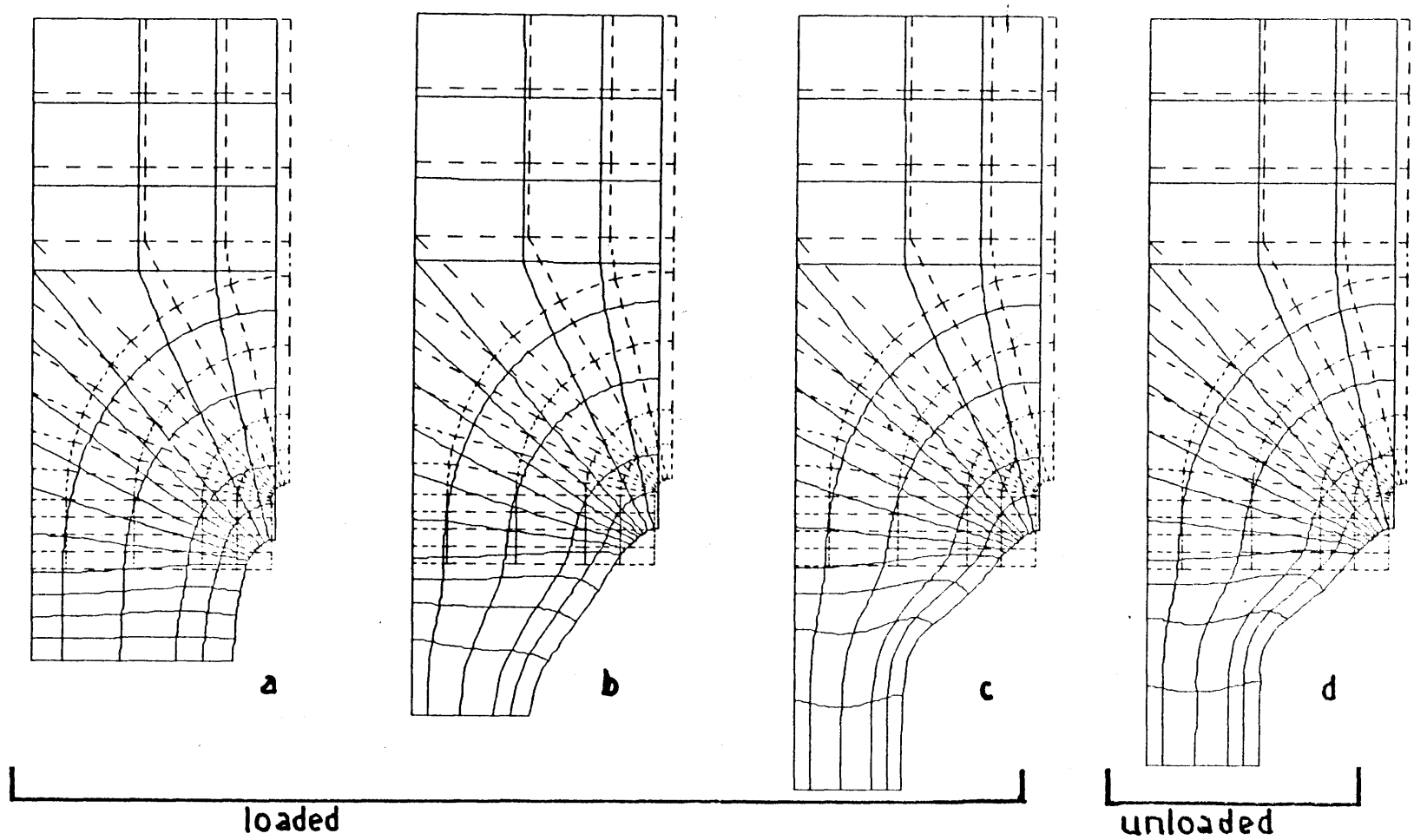

Figure 6.21 : Deformed meshes from computational analysis corresponding to the stages of formation of a polystyrene craze tuft; d is the configuration unloaded from c .

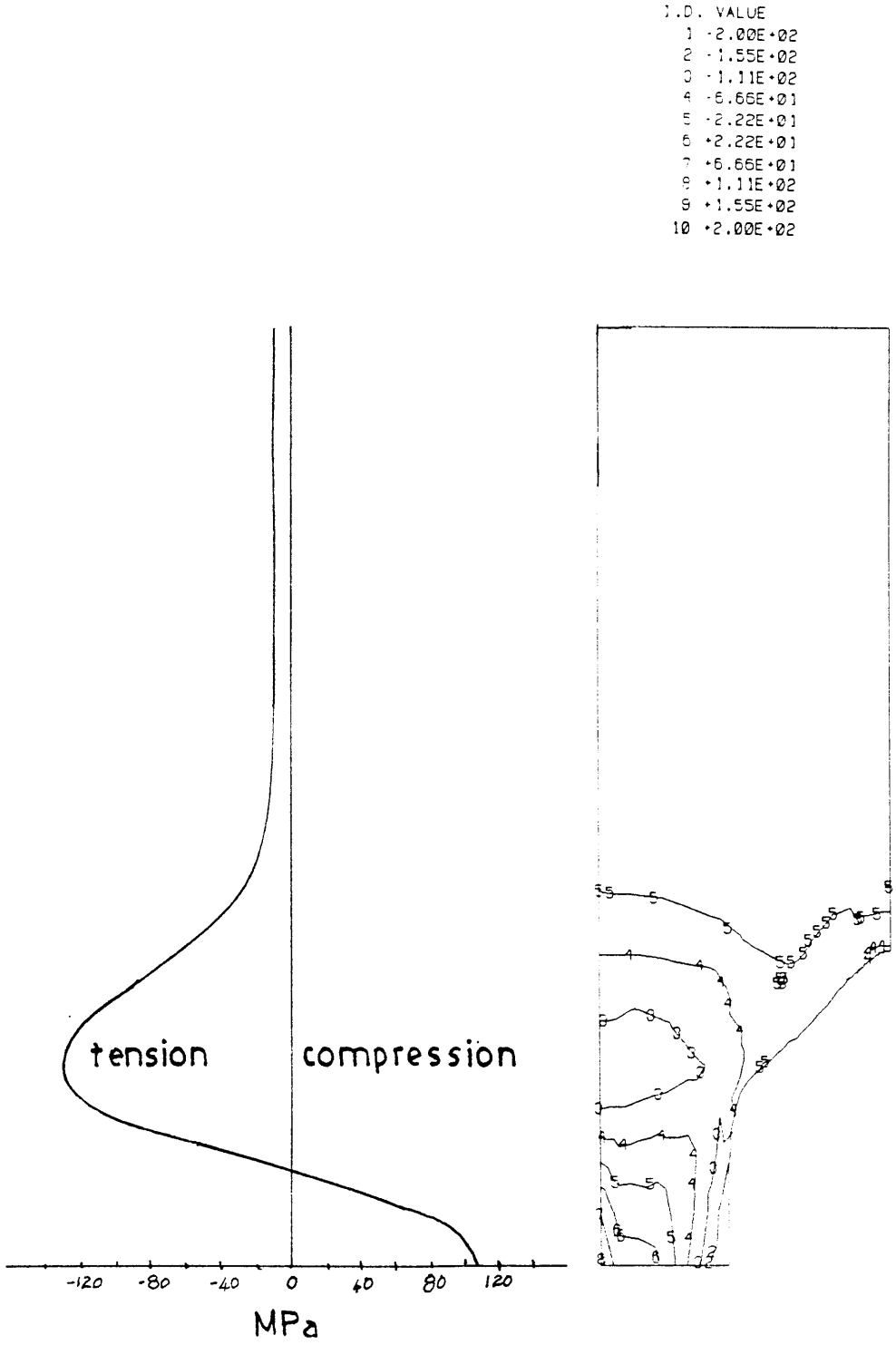

Figure 6.22 : Polystyrene craze : hydrostatic pressure (in MPa) contours shown on the deformed, loaded configuration ; the variation along the axis is plotted on the left .

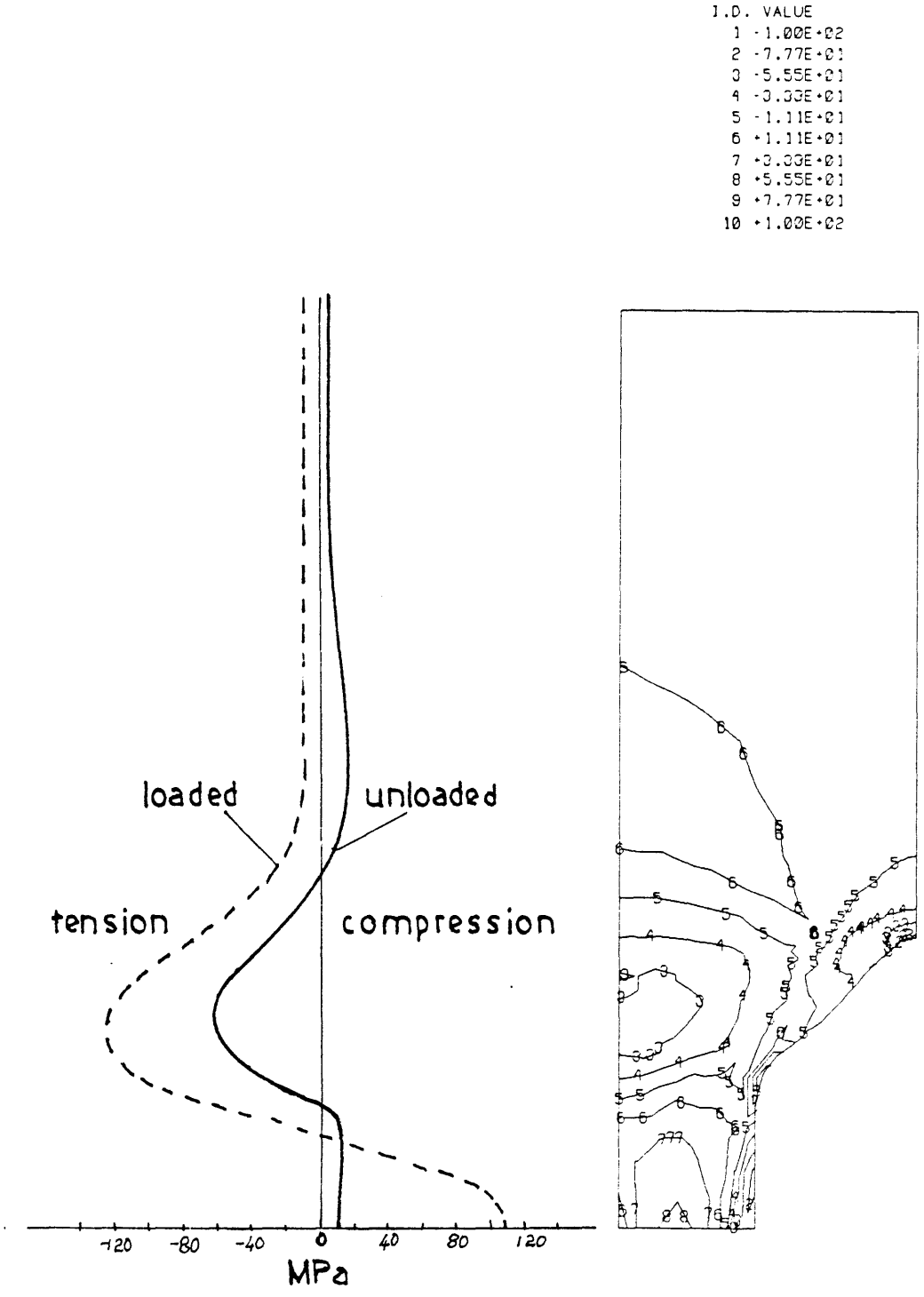

Figure 6.23 : Polystyrene craze : hydrostatic pressure (in MPa) contours shown on the deformed, unloaded configuration ; the variation along axis is plotted on the left .

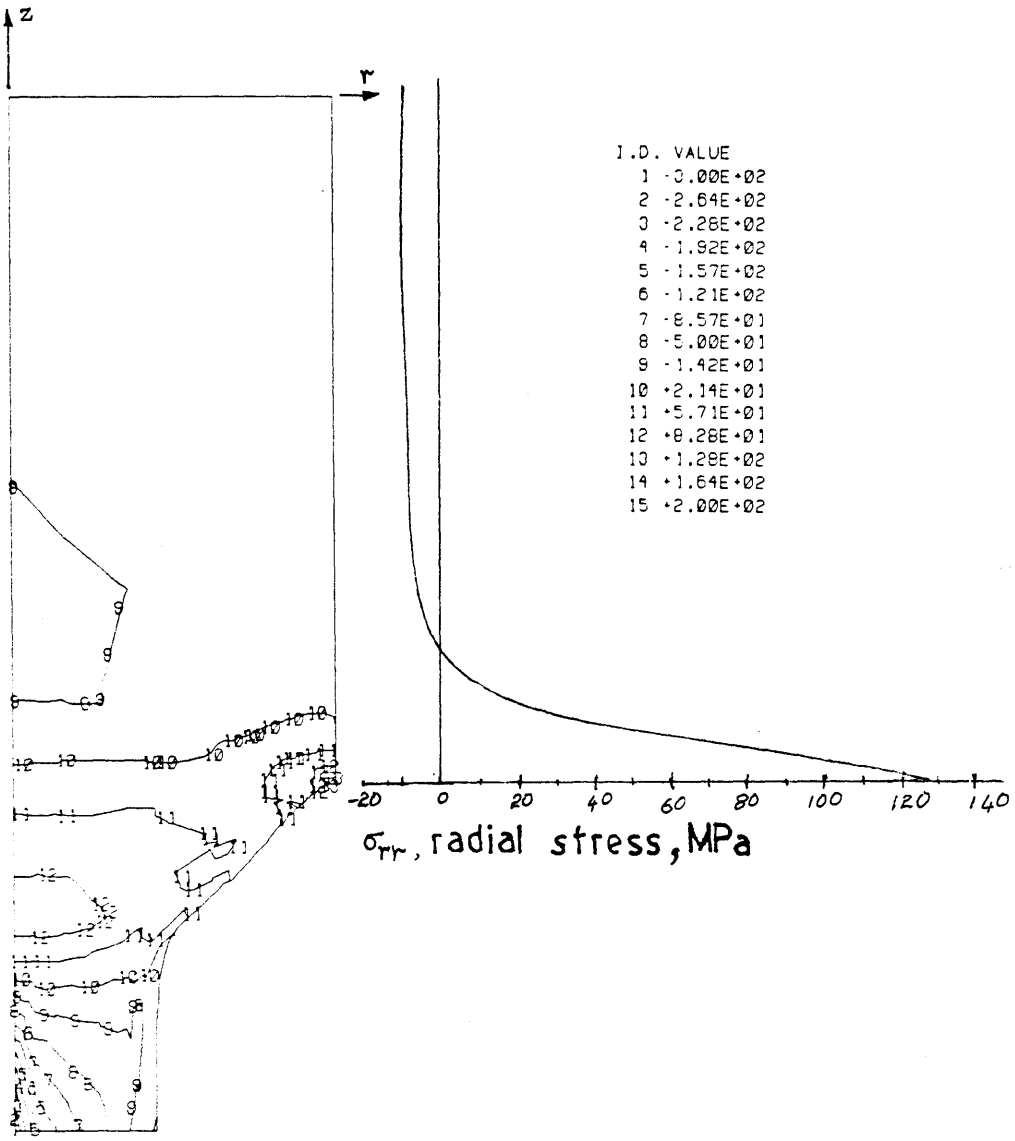

Figure 6.24 : Polystyrene craze : radial stress contours (in MPa) shown on the deformed , loaded configuration ; the variation along the outer rim is plotted on the right.

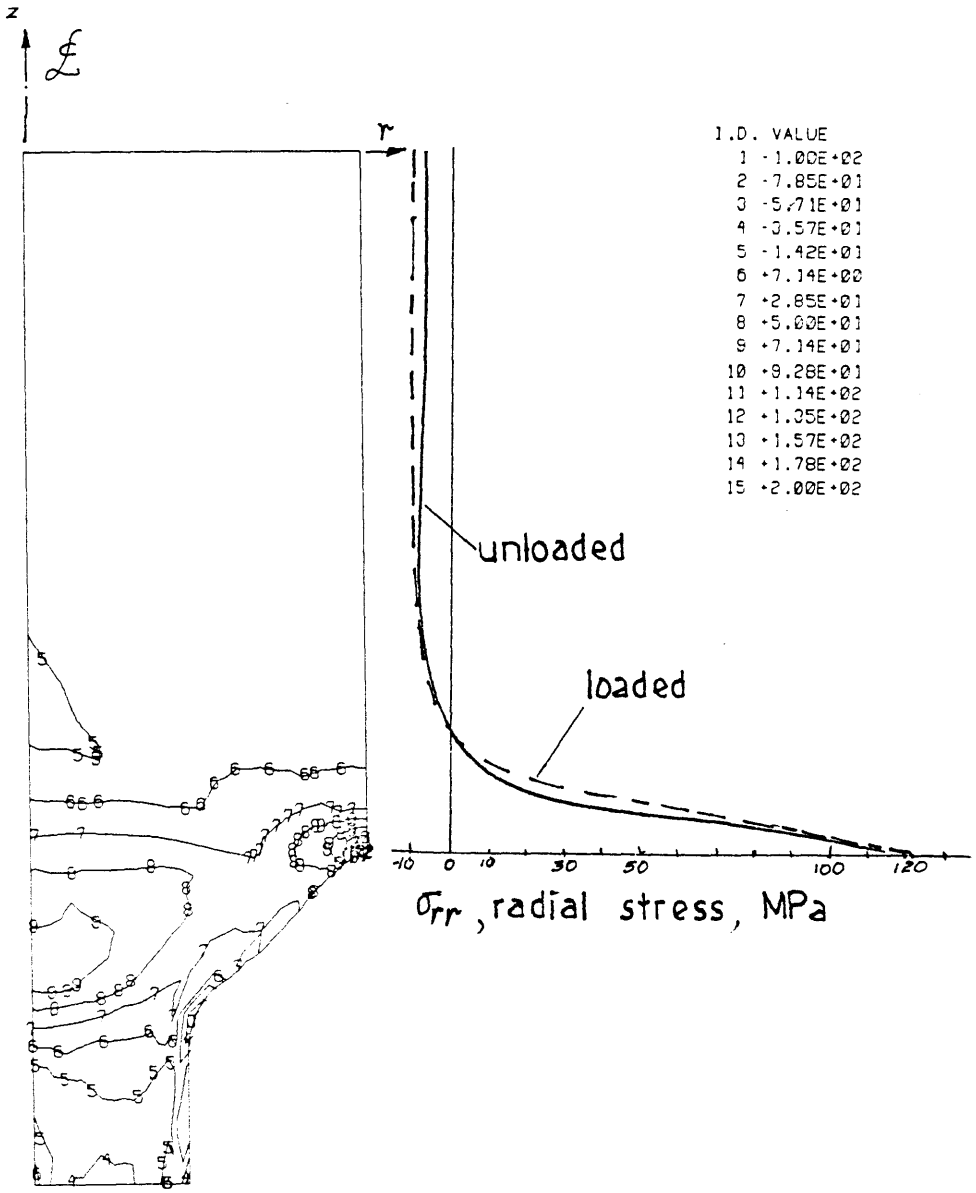

Figure 6.25 : Polystyrene craze : radial stress contours (in MPa) shown on the deformed , unloaded configuration ; the variation along the outer rim is plotted on the right.

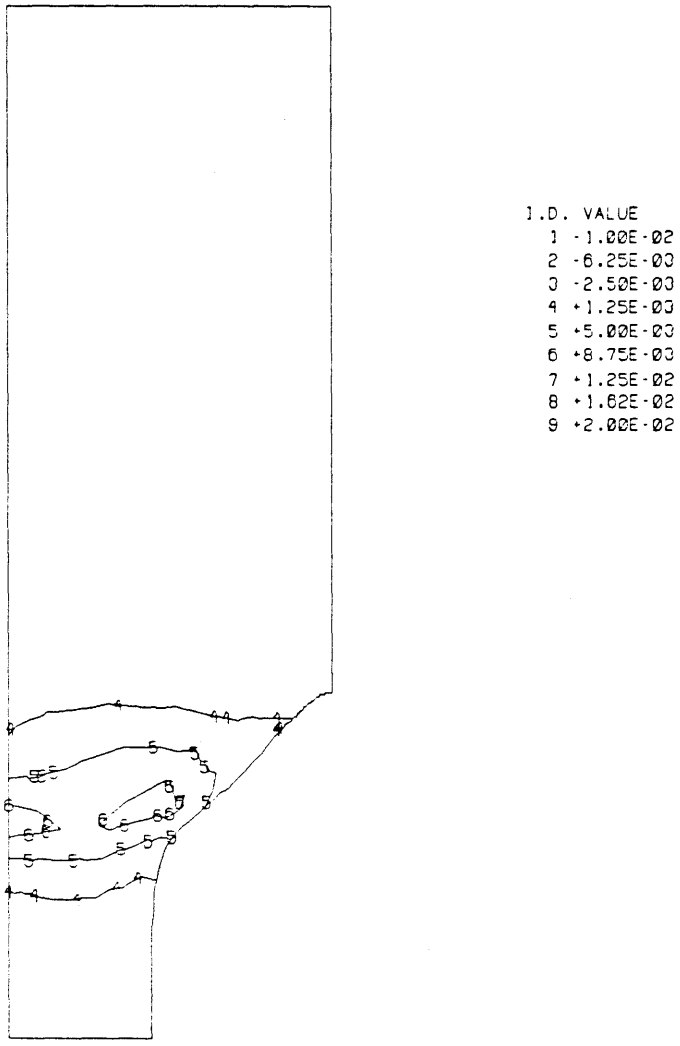

Figure 6.26 : Polystyrene craze : contours showing the range of incremental plastic strain in the yielding zone .

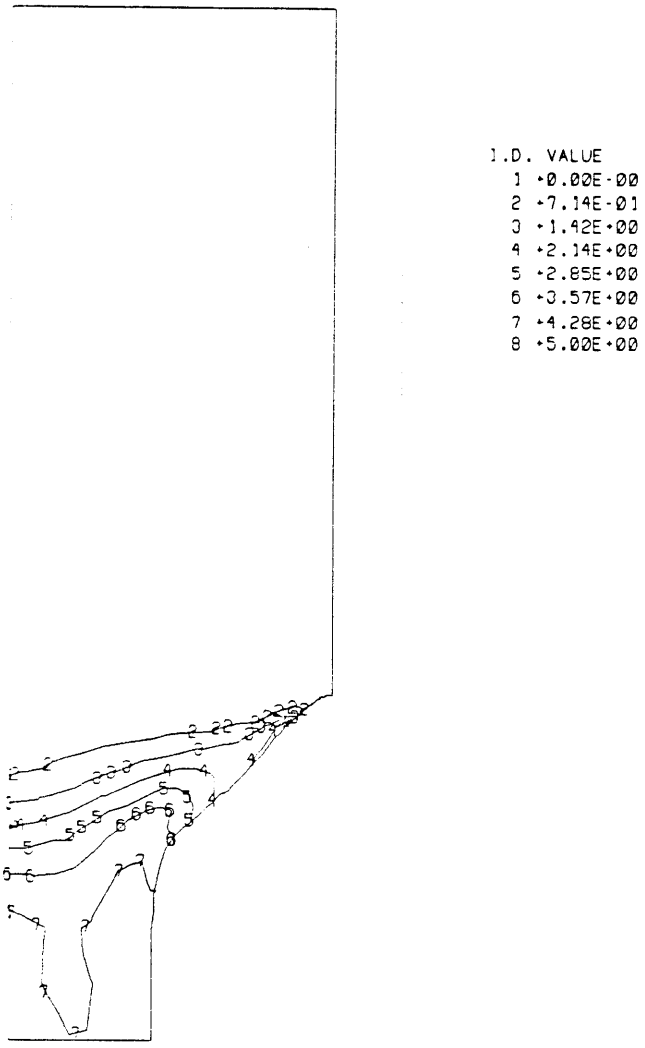

Figure 6.27 : Polystyrene craze : contours of the differences in the principal plastic stretches .

on polystyrene showed strong hysterisis effects ; they however , did confirm the rubbery nature of polymers above Tg .Further experimentation would strengthen the validity of the model.

A few changes in the model would perhaps yield more agreable results in some cases. As was seen in the polycarbonate case , a pressure-sensitive yield function will yield better results. Since most polymers are sensitive to loading rates even at temperatures below Tg , we could have a rate-sensitive formulation.

APPENDIX : A

Back Stresses in Terms of the Plastic Deformation Gradient

For a given plastic deformation gradient,

$$\underset{\sim}{F}^{p}$$

at any time , we have (by polar decomposition) :

$$\underset{\sim}{F}^{p} = \underset{\sim}{V} \cdot \underset{\sim}{R}^{p} \qquad (A.1)$$

where ,

$$\underset{\sim}{R}^{p}$$

is the (plastic) rotation matrix and

$$\underset{\sim}{V} = \underset{\sim}{\bar{R}}^{p} \cdot \underset{\sim}{\bar{V}}^{T} \cdot \underset{\sim}{\bar{R}}^{p} \qquad (A.2)$$

is the " Left " Finger-Stretch tensor and has the (diagonal) matrix of eigen values

$$\underset{\sim}{\bar{V}}$$

whose diagonal entries are the principal plastic stretches

$$(\bar{V}_1 , \bar{V}_2 , \bar{V}_3)$$

and the (orthogonal) matrix of eigen vectors

$$\underset{\sim}{\bar{R}}^{p} \quad .$$

Hence by Eq. 2.1.5 we have

$$\bar{V}_1 \, \bar{V}_2 \, \bar{V}_3 = 1 \qquad (A.3)$$

Based on The Three-Chain Model discussed in Section 1.2 , the expression for free energy based on contributions entirely from the configurational entropy change due to plastic strains ,(Treloar ,1975) is

$$F = C - \sum_{i=1}^{3} C^R \frac{\sqrt{N}}{3}\left(\frac{\bar{V}_i}{\sqrt{N}}\beta_i + \mathrm{Ln}\left(\frac{\beta_i}{\sinh\beta_i}\right)\right) \qquad (A.4)$$

where ,

C = an additive constant

C^R = nkT MPa (units of stress)
= 0.1948 MPa at 387 K
as calculated for polystyrene ;

k = 1.38×10^{-23} Nm/ K-molecule
= Boltzmann's constant
= R/An ,

R = Universal Gas Constant

An = Avogadro's Number
= 6.02×10^{23} molecules/mole

n = number of chain segments / volume
= (ρ An)/Me
= 365×10^{23} molecules/m^3 for polystyrene ;

ρ = mass density
= 1.0491×10^{6} g/m^{3} for polystyrene

Me = entanglement molecular weight,
≐ Critical molecular weight(Mc)/2
(Ferry, 1970),
= 17,300 g/mole for polystyrene ,
= 6.500 g/mole for polycarbonate;

N = number of chain links
between entanglements,
= about 25 for polystyrene

T = temperature , K
= (114 + 273) = 387 K in our test

$\bar{V}_i$ = the principal plastic stretches ,

$\mathcal{L}(\beta_i)$ = " Langevin β_i "

$= \mathrm{Coth}(\beta_i) - 1/\beta_i$

$= \bar{V}_i/\sqrt{N}$

Hence ,

β_i = " Langevin-inverse ($\bar{V}_i/\sqrt{N}$) "

$= \mathcal{L}^{-1}(\bar{V}_i/\sqrt{N})$

We thus have, for the principal back stresses (see Eq. 1.5.4),

$$\bar{\sigma}_i^B = \bar{V}_i \frac{\partial F}{\partial \bar{V}_i} \qquad \text{(no sum)}$$

$$= C^R \frac{\sqrt{N}}{3} \mathcal{L}^{-1}(\bar{V}_i/\sqrt{N}) \cdot \bar{V}_i \qquad \text{(A.5)}$$

Since by our assumption plastic deformation occurs non-dilationally , and since any dilational free energy is attributable to elastic deformations , we can take the back stresses to be deviatoric . Thus,

$$\bar{\sigma}_i^B = C^R \frac{\sqrt{N}}{3} \left(\bar{V}_i \mathcal{L}^{-1}\left(\frac{\bar{V}_i}{\sqrt{N}}\right) - \frac{1}{3} \sum_{i=1}^{3} \bar{V}_i \mathcal{L}\left(\frac{\bar{V}_i}{\sqrt{N}}\right) \right)$$

(A.6)

For example ,

$$\bar{\sigma}_1^B = C^R \frac{\sqrt{N}}{3} \left(\bar{V}_1 \mathcal{L}^{-1}\left(\frac{\bar{V}_1}{\sqrt{N}}\right) \cdot \frac{2}{3} - \left(\bar{V}_2 \mathcal{L}^{-1}\left(\frac{\bar{V}_2}{N}\right) - \bar{V}_3 \mathcal{L}^{-1}\left(\frac{\bar{V}_3}{N}\right) \right) \cdot \frac{1}{3} \right) \qquad \text{(A.7)}$$

Fig. 1.6 shows a plot of back stress vs. plastic stretch (ie., Eq. A.7) for two values of N , taking

$$\bar{V}_1 = \frac{1}{\bar{V}_2^2} = \frac{1}{\bar{V}_3^2}$$

This clearly demonstrates " locking " behaviour as the stretch approaches $\sqrt{N}$.

Having obtained the principal back stresses ie., the diagonal values ,

$$\underset{\sim}{\bar{\sigma}}^B$$

we can get the actual back stresses by the orthogonal transformation

$$\underset{\sim}{\sigma}^B = \underset{\sim}{\bar{R}}^p \cdot \underset{\sim}{\bar{\sigma}}^B \cdot \underset{\sim}{\bar{R}}^{pT} \qquad \text{(A.7)}$$

The pre-multiplier

$$C^R$$

has the units of stress and can be obtained either from the molecular data on the polymer, or preferably from a simple-tension test conducted at a temperature T, a little above Tg . For small stretches the Equation A.6 can be written

$$\sigma_1^B = C^R\left(\bar{V}_1^2 - \frac{1}{\bar{V}_1} \right) \quad . \qquad (A.8)$$

Thus the tangent at zero strain (= ln(stretch)) would have the slope

$$3\,C^R$$

Uniaxial tension tests were conducted on polystyrene samples at about 114 C . These were done in several load-unload cycles . Later, each load-curve was plotted as if the length of the specimen when each reloading began had a stretch = 1 and its final stretch calculated accordingly . The slopes of the initial tangents (at zero strain) nearly coincided for all the load-curves. The value of about 1.0 MPa at 378 K for the pre-multiplier thus obtained was considerably higher than the magnitude arrived at ie., about 0.2 MPa based on molecular considerations . equal to nkT as in Eq.A.4. Figures A.1 and A.2 illustrate the test results and the procedure described above . A value ,

$$C^R = 0.75 \text{ MPa}$$

after linearly scaling down the value to room temperature of 293 K , was finally chosen for polystyrene . The gradual reduction in the value of with numbers of cycles is most

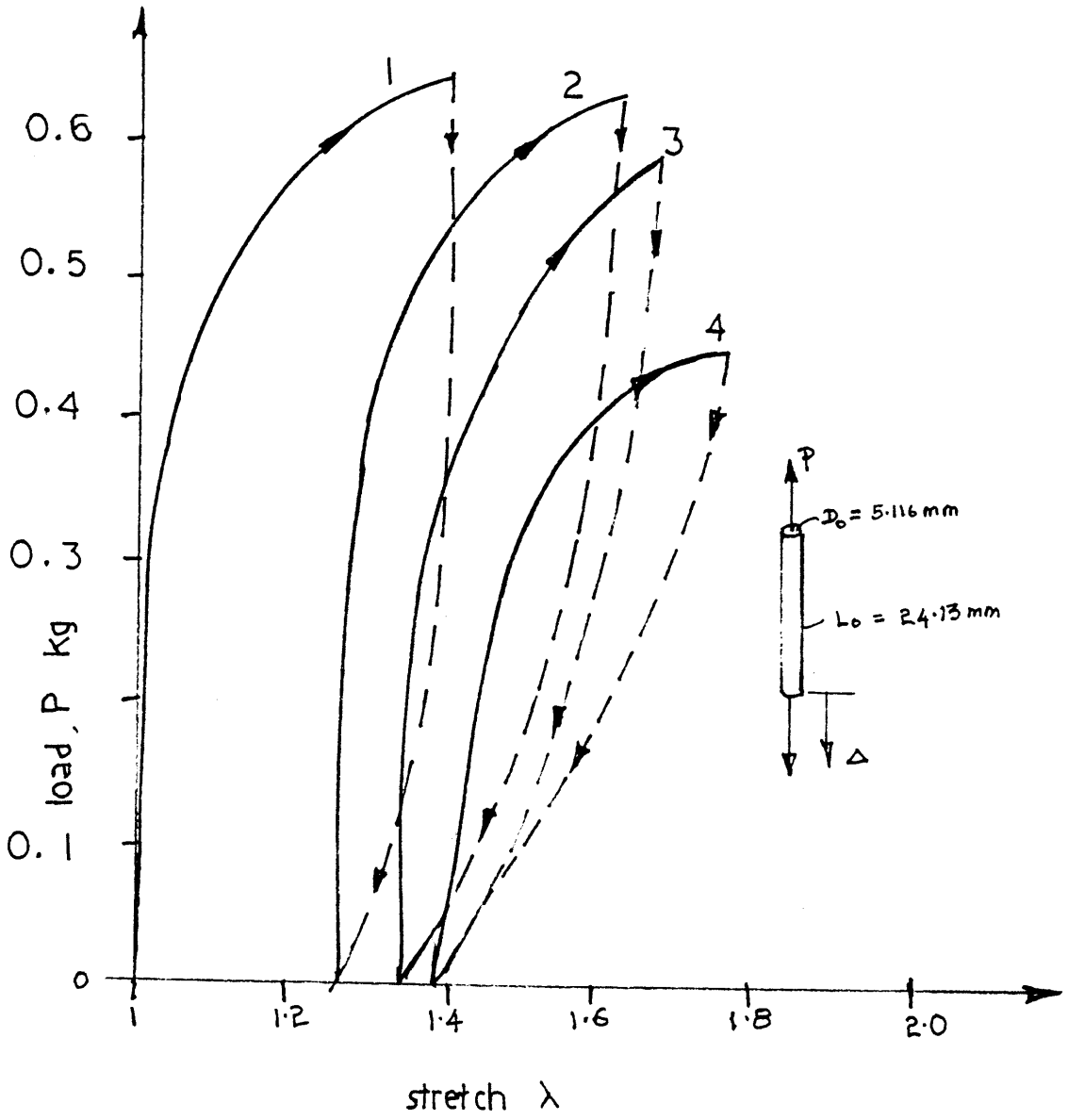

Figure A.1 : Load-unload test curves from a tension test on polystyrene at 114 C -in the " rubbery region ".

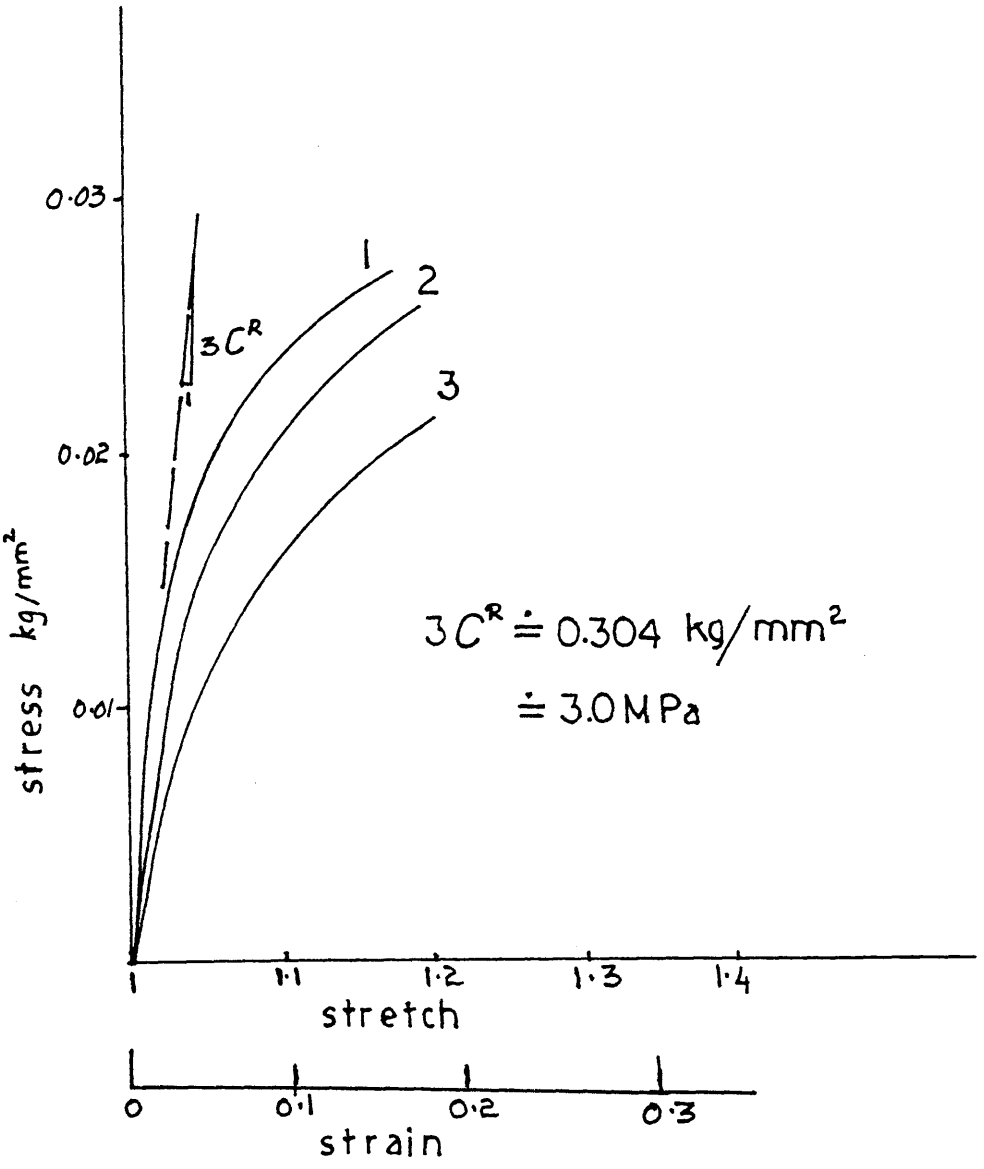

Figure A.2 : Stress vs. strain curves , from test curves in Figure A.1 , showing the initial slopes nearly coinciding .

likely due to the accumulating entanglement drift at the test temperature .

The value , N = 25 , chosen for polystyrene is based on observations of the " network stretch " (of about 5) in typical polystyrene craze-tufts (Kramer, 1983). Similar such observations can be made in uniaxial tension tests of polymers that do not craze . The ratio of the original area to the necked area would give a close estimate of the network stretch in such cases . From chapter 1 we note that the number of links , N , would then be the (integer closest to the) square of the network stretch that was observed . Tension tests done on polystyrene in the rubbery state (ie., T > Tg) showed a much larger network stretch than , 5 , predicted above because of the hysterisis effects that were preseent (see Fig. 1.9) .

APPENDIX : B

Cauchy Stresses in terms of the Elastic Deformation Gradient

For a given elastic deformation gradient ,

$$\underset{\approx}{F}^{e}$$

at any time , we have

$$\underset{\approx}{F}^{e} = \underset{\approx}{F}^{e^{T}}$$

$$= \underset{\approx}{U} \qquad (B.1)$$

and

$$\underset{\approx}{U} = \underset{\approx}{\bar{R}}^{e^{T}} \cdot \underset{\approx}{\bar{U}} \cdot \underset{\approx}{\bar{R}}^{e} \qquad (B.2)$$

is the elastic stretch matrix and has the (diagonal) matrix of eigen values ,

$$\underset{\approx}{\bar{U}} \quad ,$$

whose diagonal entries are the principal elastic stretches

$$(\bar{U}_1 , \bar{U}_2 , \bar{U}_3)$$

and the (orthogonal) matrix of eigen vectors

$$\underset{\approx}{\bar{R}}^{e}$$

With the principal (logarithmic) elastic strains ,

$$\underset{\approx}{\bar{E}}^{e} = \mathrm{Ln}(\underset{\approx}{\bar{U}}) \quad , \qquad (B.3)$$

we have , for a linear isotropic elastic material , for the

Cauchy stresses

$$\underset{\approx}{\sigma} = \frac{1}{\det(U)} \times \underset{\approx}{\tau} \qquad (B.4)$$

where ,

$$\underset{\approx}{\tau} = \underset{\approx}{\bar{R}}^{e^T} \cdot \left(Ln(\underset{\approx}{\bar{U}}) : \underset{\approx\approx}{\mathcal{L}}^{e} \right) \cdot \underset{\approx}{\bar{R}}^{e} \qquad (B.5)$$

are the Kirchhoff stresses , and " det " stands for the determinant . In Eq. B.5 the elastic modulii (in tensor notation) are given by

$$\mathcal{L}^{e}_{ijkl} = \frac{E}{(1+\nu)} \cdot \delta_{ik}\delta_{jl} + \frac{\nu E}{(1+\nu)(1-2\nu)} \cdot \delta_{ij}\delta_{kl} \qquad (B.6)$$

Where ,

δ_{ij} = the Kronecker Delta

E = the Youngs Modulus
(eg., 3250 MPa for polystyrene;
ref: Argon and Bessonov, 1976)

ν = the Poisson Ratio
(eg., 0.3 for polystyrene)

The above development , relating Kirchhoff stresses to logarithmic strains for moderate stretches of up to about 1.4 , using the usual small scale elastic moduli was suggested by Anand (1979) , based on experimental evidence . In Eq. B.5 , note the orthogonal transformation using the eigen vector matrix described above , to transform stresses from local principal coordinates to global coordinates .

APPENDIX : C

The Rate of Plastic Deformation

For a hyperelastic material we have the following

Let ψ denote the stored elastic energy per unit mass (Fardshisheh and Onat , 1972). This energy is a function of the Cauchy-Green tensor, $\underset{\sim}{B}^e$ given by

$$\begin{aligned} \underset{\sim}{B}^e &= \underset{\sim}{F}^e \cdot \underset{\sim}{F}^e \\ &= \underset{\sim}{F}^{e^2} \end{aligned} \tag{C.1}$$

That is ,

$$\psi = \psi(\underset{\sim}{B}^e) \tag{C.2}$$

From Eq. C.1 we have

$$\dot{\underset{\sim}{B}}^e = \dot{\underset{\sim}{F}}^e \cdot \underset{\sim}{F}^e + \underset{\sim}{F}^e \dot{\underset{\sim}{F}}^{e^T} \tag{C.3}$$

Thus , from Eq. 3.2.9 in Chapter 3 we get,

$$\begin{aligned} \dot{\underset{\sim}{B}}^e &= (\underset{\sim}{L} \cdot \underset{\sim}{F}^e - \underset{\sim}{F}^e \cdot (\underset{\sim}{D}^p + \underset{\sim}{W}^p)) \cdot \underset{\sim}{F}^e + \underset{\sim}{F}^e \cdot (\underset{\sim}{F}^{e^T} \cdot \underset{\sim}{L}^T - (\underset{\sim}{D}^p + \underset{\sim}{W}^p) \cdot \underset{\sim}{F}^{e^T}) \\ &= \underset{\sim}{L} \cdot \underset{\sim}{B}^e + \underset{\sim}{B}^e \cdot \underset{\sim}{L}^T - 2 \underset{\sim}{F}^e \cdot \underset{\sim}{D}^p \cdot \underset{\sim}{F}^e \end{aligned} \tag{C.4}$$

Using Eq. 3.2.13 , we have

$$\dot{\underset{\sim}{B}}^e = \underset{\sim}{L} \cdot \underset{\sim}{B}^e + \underset{\sim}{B}^e \cdot \underset{\sim}{L}^T - (\hat{\underset{\sim}{D}}^p \cdot \underset{\sim}{B}^e + \underset{\sim}{B}^e \cdot \hat{\underset{\sim}{D}}^p)$$

ie

$$\dot{\underset{\sim}{\underset{\sim}{B}}}^e = (\underset{\sim}{\underset{\sim}{W}}\cdot\underset{\sim}{\underset{\sim}{B}}^e - \underset{\sim}{\underset{\sim}{B}}^e\cdot\underset{\sim}{\underset{\sim}{W}}) + (\underset{\sim}{\underset{\sim}{D}} - \hat{\underset{\sim}{\underset{\sim}{D}}}^p)\cdot\underset{\sim}{\underset{\sim}{B}}^e + \underset{\sim}{\underset{\sim}{B}}^e\cdot(\underset{\sim}{\underset{\sim}{D}} - \hat{\underset{\sim}{\underset{\sim}{D}}}^p) \tag{C.5}$$

The applied stresses , from Eq. C.2 ,are

$$\underset{\sim}{\underset{\sim}{\sigma}} = \rho\left(\frac{\partial \psi}{\partial \underset{\sim}{\underset{\sim}{B}}^e}\cdot\underset{\sim}{\underset{\sim}{B}}^e + \underset{\sim}{\underset{\sim}{B}}^e\cdot\frac{\partial \psi}{\partial \underset{\sim}{\underset{\sim}{B}}^e}\right), \tag{C.6}$$

ρ = mass density per unit volume

Power

Let us evaluate the quantity

$$P = \rho\dot{\psi} + \underset{\sim}{\underset{\sim}{\sigma}} : \hat{\underset{\sim}{\underset{\sim}{D}}}^p \tag{C.7}$$

We have , using Eqs. C.5 and C.6 ,

$$P = \rho\frac{\partial \psi}{\partial \underset{\sim}{\underset{\sim}{B}}^e} : \dot{\underset{\sim}{\underset{\sim}{B}}}^e + \underset{\sim}{\underset{\sim}{\sigma}} : \hat{\underset{\sim}{\underset{\sim}{D}}}^p \tag{C.8}$$

ie.,

$$P = \rho\frac{\partial \psi}{\partial \underset{\sim}{\underset{\sim}{B}}^e} : \left((\underset{\sim}{\underset{\sim}{W}}\cdot\underset{\sim}{\underset{\sim}{B}}^e - \underset{\sim}{\underset{\sim}{B}}^e\cdot\underset{\sim}{\underset{\sim}{W}}) + (\underset{\sim}{\underset{\sim}{D}} - \hat{\underset{\sim}{\underset{\sim}{D}}}^p)\cdot\underset{\sim}{\underset{\sim}{B}}^e + \underset{\sim}{\underset{\sim}{B}}^e\cdot(\underset{\sim}{\underset{\sim}{D}} - \hat{\underset{\sim}{\underset{\sim}{D}}}^p)\right)$$
$$+ \rho\left(\frac{\partial \psi}{\partial \underset{\sim}{\underset{\sim}{B}}^e}\cdot\underset{\sim}{\underset{\sim}{B}}^e + \underset{\sim}{\underset{\sim}{B}}^e\cdot\frac{\partial \psi}{\partial \underset{\sim}{\underset{\sim}{B}}^e}\right) : \hat{\underset{\sim}{\underset{\sim}{D}}}^p \tag{C.9}$$

On simplifying , we have

$$P = \rho\left(\frac{\partial \psi}{\partial \underset{\sim}{\underset{\sim}{B}}^e}\cdot\underset{\sim}{\underset{\sim}{B}}^e + \underset{\sim}{\underset{\sim}{B}}^e\cdot\frac{\partial \psi}{\partial \underset{\sim}{\underset{\sim}{B}}^e}\right) : \underset{\sim}{\underset{\sim}{D}}$$

ie., from Eq. C.7 ,

$$\rho\dot{\psi} + \underset{\approx}{\sigma} : \underset{\approx}{\hat{D}}^{p} = \underset{\approx}{\sigma} : \underset{\approx}{D} \qquad \text{(C.10)}$$

The right hand side of Eq. C.10 is the " power " or, the " rate of work " of the applied stresses working through the (total) rate of deformation . We can interpret this as the sum of two quantities :

1) $\rho\dot{\psi}$ = the stored (recoverable) elastic work rate

2) $\underset{\approx}{\sigma} : \underset{\approx}{\hat{D}}^{p}$ = the dissipated part of the power

(C.11)

We could now interpret

$$\underset{\approx}{\hat{D}}^{p}$$

as the rate of plastic deformation referred to the <u>loaded</u> configuration .

<u>Notes</u> :

In Eq. C.10 , the stored elastic work rate,

$$\rho\dot{\psi} \ ,$$

has contributions entirely from the elastic strain energy of the material. If however , as in the case of polymers , there are other forms of " recoverable " free energy , we could add (and subtract) these contributions as well. We could thus say , for glassy polymers

$$\underset{\approx}{\sigma} : \underset{\approx}{D} = \rho\dot{\psi} + \underset{\approx}{\sigma} : \underset{\approx}{\hat{D}}^{p} \pm \underset{\approx}{\sigma}^{a} : D^{p} \qquad \text{(C.12)}$$

Here , the quantity

$$\underset{\approx}{\sigma}^{B}:\underset{\approx}{D}^{P}$$

is the rate of work of the back stresses working through the rate of plastic deformation in the unloaded configuration .

Thus in the case of polymers ,

$$\rho\dot{\psi}+\underset{\approx}{\sigma}^{B}:\underset{\approx}{D}^{P}$$

is interpreted as the stored work rate which is recoverable , and

$$\underset{\approx}{\sigma}:\underset{\approx}{\hat{D}}^{P}-\underset{\approx}{\sigma}^{B}:\underset{\approx}{D}^{P}$$

is interpreted as the " lossy " part or , the dissipated part of the power .

APPENDIX : D

The spin of the unloaded state

From Ch. 3 , Eq. 3.2.19 , we have (in index notation)

$$(F^{e}_{ip}\delta_{jk} + \delta_{ip}F^{e}_{jk})(W^{p}_{ij} - W_{ij}) = -(\delta_{ip}F^{e}_{jk} - F^{e}_{ip}\delta_{jk})(D_{ij} + D^{p}_{ij}) \tag{D.1}$$

By writing

$$\underline{\underline{\mathcal{L}}} = \underline{\underline{\mathcal{L}}}^{T} = \underline{\underline{D}} + \underline{\underline{D}}^{p} \tag{D.2}$$

and

$$\underline{\underline{\mathcal{W}}} = -\underline{\underline{\mathcal{W}}}^{T} = \underline{\underline{W}}^{p} - \underline{\underline{W}} \quad , \tag{D.3}$$

we can write Eq. D.1 as

$$\mathcal{A}_{ipjk}\mathcal{W}_{ij} = -\mathcal{B}_{ipjk}\mathcal{L}_{ij} \tag{D.4}$$

In Table D.1 we have represented Eq. D.4 . We can hence easily get

$$\underline{\underline{W}}^{p} - \underline{\underline{W}} = -\underline{\underline{\underline{\mathcal{A}}}}^{-1} : \underline{\underline{\underline{\mathcal{B}}}} : \underline{\underline{\mathcal{L}}} \quad , \tag{D.5}$$

by suitably inverting

$$\underline{\underline{\underline{\mathcal{A}}}} \quad ,$$

as represented in table D.1 .

As an example , for the 2D axisymmetric / plane-strain case , we have

$$W^{p}_{12} - W_{12} = \frac{(D_{12}+D^{p}_{12})(F^{e}_{11}-F^{e}_{22}) - (D_{11}+D^{p}_{11}-D_{22}-D^{p}_{22})F^{e}_{12}}{(F^{e}_{11}+F^{e}_{22})} \quad . \tag{D.6}$$

TABLE D.1: matrix representation of Eq. D.4

$2F_{11}^e$						$\mathcal{W}_{11}$							$\mathcal{D}_{11}$
	$2F_{22}^e$					$\mathcal{W}_{22}$							$\mathcal{D}_{22}$
		$2F_{33}^e$				$\mathcal{W}_{33}$							$\mathcal{D}_{33}$
	F_{23}^e	F_{32}^e	$F_{33}^e+F_{22}^e$	$-F_{12}^e$	$-F_{13}^e$	$\mathcal{W}_{32}$	$=-$		$-F_{23}^e$	F_{32}^e	$F_{22}^e-F_{33}^e$	F_{12}^e	$-F_{13}^e$	$\mathcal{D}_{32}$
F_{13}^e		F_{31}^e	$-F_{21}^e$	$F_{11}^e+F_{33}^e$	$-F_{23}^e$	$\mathcal{W}_{13}$		F_{13}^e		$-F_{31}^e$	$-F_{21}^e$	$F_{33}^e-F_{11}^e$	F_{23}^e	$\mathcal{D}_{13}$
F_{12}^e	F_{21}^e		$-F_{31}^e$	$-F_{32}^e$	$F_{22}^e+F_{11}^e$	$\mathcal{W}_{21}$		$-F_{12}^e$	F_{21}^e		F_{31}^e	$-F_{32}^e$	$F_{11}^e-F_{22}^e$	$\mathcal{D}_{21}$

(zeros in unfilled boxes)

APPENDIX : E

The rate of change of yield status

From Chapter 2 , Eq. 2.2.5 we have , for the yield status ,

$$Y = \underset{\sim}{\sigma}^{*\prime} : \underset{\sim}{\sigma}^{*\prime} - 2\tau_o^2 \leqslant 0 \qquad \text{(E.1)}$$

We shall work with Kirchhoff stresses (see Appendix B , Eq. B.6) and back stresses (see Appendix A) since they are easier to work with . From Eq. B.5 we have

$$\underset{\sim}{\tau} = J\,\underset{\sim}{\sigma}$$

with

$$J = \det(\underset{\sim}{F}^{e}) \qquad \text{(E.2)}$$

We thus have , for the rate of change of yield status ,

$$\dot{Y} = \frac{\partial Y}{\partial \underset{\approx}{\tau}} : \dot{\underset{\approx}{\tau}} + \frac{\partial Y}{\partial \underset{\sim}{\sigma}^{B}} : \dot{\underset{\sim}{\sigma}}^{B} \qquad \text{(E.3)}$$

From Eq. E.1 we have

$$\frac{\partial Y}{\partial \underset{\approx}{\tau}} = \frac{\partial \underset{\sim}{\sigma}^{*\prime}}{\partial \underset{\approx}{\tau}} : \underset{\sim}{\sigma}^{*\prime} + \underset{\sim}{\sigma}^{*\prime} : \frac{\partial \underset{\sim}{\sigma}^{*\prime}}{\partial \underset{\approx}{\tau}} \qquad \text{(E.4)}$$

ie., in index notation (using symmetry conditions) we have

$$\frac{\partial Y}{\partial \tau_{pq}} = 2\,\sigma_{ij}^{*\prime}\frac{\partial \sigma_{ij}^{*\prime}}{\partial \tau_{pq}} \qquad \text{(E.5)}$$

Now ,

$$\frac{\partial \sigma_{ij}^{*\prime}}{\partial \tau_{pq}} = \frac{\partial \sigma_{ij}^{*}}{\partial \tau_{pq}} - \frac{\partial}{\partial \tau_{pq}}\left(\frac{\sigma_{kk}^{*}}{3}\right)\delta_{ij} \qquad \text{(E.6)}$$

Thus , using Eqs. 2.2.2 and 2.2.3 , we get

$$\frac{\partial \sigma_{ij}^{*}}{\partial \tau_{pq}} = \frac{\partial}{\partial \tau_{pq}}\left(\frac{\tau_{ij}}{J} - \frac{1}{J} F_{iL}^{e}\, \sigma_{lm}^{B}\, F_{mj}^{e}\right) \qquad \text{(E.7)}$$

ie.,

$$\begin{aligned}\frac{\partial \sigma_{ij}^{*}}{\partial \tau_{pq}} &= \frac{1}{J}\delta_{ip}\delta_{jq} - \frac{1}{J^2}\left(\frac{\partial J}{\partial \tau_{pq}}\right)\tau_{ij} \\ &+ \frac{1}{J^2}\left(\frac{\partial J}{\partial \tau_{pq}}\right)F_{iL}^{e}\, \sigma_{lm}^{B}\, F_{mj}^{e} \\ &- \frac{1}{J}\left(\frac{\partial F_{iL}^{e}}{\partial \tau_{pq}}\right)\sigma_{lm}^{B}\, F_{mj}^{e} \\ &- \frac{1}{J} F_{iL}^{e}\, \sigma_{lm}^{B}\left(\frac{\partial F_{mj}^{e}}{\partial \tau_{pq}}\right) \qquad \text{(E.8)}\end{aligned}$$

The rates ,

$$\frac{\partial J}{\partial \underset{\sim}{\underset{\sim}{\tau}}} \quad \text{and} \quad \frac{\partial \underset{\sim}{F}^{e}}{\partial \underset{\sim}{\underset{\sim}{\tau}}}$$

are evaluated in Sub-Appendices E1 and E2 respectively , included at the end of this appendix . Substituting in Eq. E.8 , we get

$$\begin{aligned}\frac{\partial \sigma_{ij}^{*}}{\partial \tau_{pq}} &= \frac{1}{J}\delta_{ip}\delta_{jq} - \frac{1}{J^2}\left(\frac{J(1-2\nu)}{E}\delta_{pq}\right)\tau_{ij} \\ &+ \frac{1}{J^2}\left(\frac{J(1-2\nu)}{E}\delta_{pq}\right)F_{iL}^{e}\, \sigma_{lm}^{B}\, F_{mj}^{e}\end{aligned}$$

(contd...)

$$-\frac{1}{J}\left\{\frac{1}{2}\left(F^e_{ir}C_{rlpq}+F^e_{lr}C_{ripq}\right)\sigma^B_{lm}F^e_{mj}\right\}$$

$$-\frac{1}{J}\left\{\frac{1}{2}\left(F^e_{mr}C_{rjpq}+F^e_{jr}C_{rmpq}\right)\sigma^B_{lm}F^e_{il}\right\} .$$

(E.9)

Hence , using Eq. E2.7 in Eq. E.9 , and on simplifying , substituting into Eq. E.5 , we get

$$\frac{\partial \sigma^{*'}_{ij}}{\partial \tau_{pq}}\sigma^{*'}_{ij} = \frac{1}{J}\Bigg[\sigma^{*'}_{pq} - \frac{(1-2\nu)}{E}\left(\delta_{pq}\tau_{ij}\sigma^{*'}_{ij}+\delta_{pq}F^e_{il}\sigma^B_{lm}F^e_{mj}\sigma^{*'}_{ij}\right)$$

$$-\frac{(1+\nu)}{2E}\left(\sigma^{*'}_{ij}F^e_{mj}F^e_{ip}\sigma^B_{qm}+\sigma^{*'}_{qj}F^e_{mj}F^e_{lp}\sigma^B_{lm}\right.$$

$$\left.+\sigma^{*'}_{iq}F^e_{il}F^e_{mp}\sigma^B_{lm}+\sigma^{*'}_{ij}F^e_{il}F^e_{jp}\sigma^B_{lq}\right)$$

$$+\frac{\nu}{2E}\left(\sigma^{*'}_{ij}F^e_{mj}F^e_{il}\sigma^B_{lm}\delta_{pq}+\sigma^{*'}_{ij}F^e_{mj}F^e_{li}\sigma^B_{lm}\delta_{pq}\right.$$

$$\left.+\sigma^{*'}_{ij}F^e_{il}F^e_{mj}\sigma^B_{ml}\delta_{pq}+\sigma^{*'}_{ij}F^e_{il}F^e_{mj}\sigma^B_{lm}\delta_{pq}\right)\Bigg]$$

(E.10)

In Eq. E.3 , using Eqs. 2.2.2 and 2.2.3 , we have the quantity

$$\frac{\partial Y}{\partial \underset{\approx}{\sigma}^B} = \underset{\approx}{\sigma}^{*'}:\frac{\partial \underset{\approx}{\sigma}^{*'}}{\partial \underset{\approx}{\sigma}^B}+\frac{\partial \underset{\approx}{\sigma}^{*'}}{\partial \underset{\approx}{\sigma}^B}:\underset{\approx}{\sigma}^{*'}$$

$$= 2\underset{\approx}{\sigma}^{*'}:\frac{\partial \underset{\approx}{\sigma}^{*'}}{\partial \underset{\approx}{\sigma}^B}$$

(contd . . .)

ie,

$$\frac{\partial Y}{\partial \underset{\sim}{\sigma}^{B}} = -\frac{2}{J}\underset{\sim}{F}^{e}\cdot\underset{\sim}{\sigma}^{*\prime}\cdot\underset{\sim}{F}^{e} \qquad \text{(E.11)}$$

Hence , using Eqs. E.4 , E.10 and E.11 in Eq. E.3 we have

$$\dot{Y} = \frac{2}{J}\underset{\sim}{\alpha} : \overset{\nabla}{\underset{\sim}{\tau}} - \frac{2}{J}\underset{\sim}{\beta} : \dot{\underset{\sim}{\sigma}}^{B} \qquad \text{(E.12)}$$

where

$$\underset{\sim}{\alpha} = \underset{\sim}{\sigma}^{*\prime} - \frac{J(1-2\nu)}{E}\left[\operatorname{tr}(\underset{\sim}{\sigma}\cdot\underset{\sim}{\sigma}^{*\prime})\underset{\sim}{I}\right]$$

$$-\frac{(1+\nu)}{E}(\underset{\sim}{A}+\underset{\sim}{A}^{T}) + \frac{1}{E}\left[\operatorname{tr}(\underset{\sim}{A})\underset{\sim}{I}\right] \qquad \text{(E.13)}$$

with

$$\underset{\sim}{A} = \underset{\sim}{\sigma}^{*\prime}\cdot\underset{\sim}{F}^{e}\cdot\underset{\sim}{\sigma}^{B}\cdot\underset{\sim}{F}^{e} \qquad \text{(E.14)}$$

,

and

$$\underset{\sim}{\beta} = \underset{\sim}{F}^{e}\cdot\underset{\sim}{\sigma}^{*\prime}\cdot\underset{\sim}{F}^{e} \qquad \text{(E.15)}$$

In Eq. E.12 we also have

$$\overset{\nabla}{\underset{\sim}{\tau}} = \overset{\nabla}{\underset{\sim}{\tau}} + \underset{\sim}{W}\cdot\underset{\sim}{\tau} - \underset{\sim}{\tau}\cdot\underset{\sim}{W} \qquad \text{(E.16)}$$

with

$$\left.\begin{aligned}\overset{\nabla}{\underset{\sim}{\tau}} &= \underset{\approx}{\mathcal{L}}^{e} : (\underset{\sim}{D} - \underset{\sim}{D}^{p}) \\ &= \underset{\approx}{\mathcal{L}}^{ep} : \underset{\sim}{D}\end{aligned}\right\} \qquad \text{(E.17)}$$

and

$$\dot{\underset{\approx}{\sigma}}^{B} = \overset{\nabla}{\underset{\approx}{\sigma}}^{B} + \underset{\approx}{W}^{p} \cdot \underset{\approx}{\sigma}^{B} - \underset{\approx}{\sigma}^{B} \cdot \underset{\approx}{W}^{p} \qquad \text{(E.18)}$$

with

$$\overset{\nabla}{\underset{\approx}{\sigma}}^{B} = \underset{\approx\approx}{\mathcal{L}}^{R} : \underset{\approx}{D}^{p} \qquad \text{(E.19)}$$

Eqs. E.17 and E.19 are the co-rotational (Jaumann) rates based on spin of the Kirchhoff and the back stresses respectively ; these are denoted by the symbol (∇). In these equations the moduli are as follows :

The isotropic elastic moduli are

$$\mathcal{L}^{e}_{ijkl} = \frac{E}{(1+\nu)} \delta_{ik} \delta_{jl} + \frac{E\nu}{(1+\nu)(1-2\nu)} \delta_{ij} \delta_{kl} \qquad \text{(E.20)}$$

Hence the active tangent (elastic-plastic) modulii are

$$\mathcal{L}^{ep}_{ijkl}$$

and are determined in Sub-Appendix E4 included at the end of this appendix . The " rubbery rate mudulii " are

$$\mathcal{L}^{R}_{ijkl}$$

and are determined in Sub-Appendix E3 included at the end of this appendix . The various rates of deformation and spin tensors referred to in Eqs. E.16 to E.19 are defined in Eqs. 3.2.3 , 3.2.4 , 3.2.20 and 3.2.23 .

Invariance under spin

Since we have no change in yield status with spin alone , we have for

$$\underset{\approx}{D} = \underset{\approx}{0} = \underset{\approx}{D}^{p} ,$$

$$\dot{Y}\Big|_{\underset{\sim}{D},\,\underset{\sim}{D}^{p}=\underset{\sim}{0}} = 0$$

ie.,

$$\underset{\sim}{\mathcal{L}} : (\underset{\sim}{W}\cdot\underset{\sim}{\sigma} - \underset{\sim}{\sigma}\cdot\underset{\sim}{W}) - \underset{\sim}{\beta} : (\underset{\sim}{W}^{p}\cdot\underset{\sim}{\sigma}^{B} - \underset{\sim}{\sigma}^{B}\cdot\underset{\sim}{W}^{p}) = 0 \qquad \text{(E.21)}$$

Hence in Eq. E.12 , using Eqs. E.16 and E.18 we have

$$\dot{Y} = \frac{2}{J}\Big\{\Big[\underset{\sim}{\mathcal{L}} : \underset{\sim\sim}{\mathcal{L}}^{e} : (\underset{\sim}{D} - \underset{\sim}{D}^{p}) - \underset{\sim}{\beta} : (\underset{\sim\sim}{\mathcal{L}}^{R} : \underset{\sim}{D}^{p} - (\underset{\sim\sim}{W} : (\underset{\sim}{D} + \underset{\sim}{D}^{p}))\cdot\underset{\sim}{\sigma}^{B} + \underset{\sim}{\sigma}^{B} : (\underset{\sim\sim}{W} : (\underset{\sim}{D} + \underset{\sim}{D}^{p}))\Big]\Big\} \qquad \text{(E.22)}$$

or in index notation ,

$$\dot{Y} = \frac{2}{J}\Big\{\Big[\mathcal{L}_{ij}\mathcal{L}^{e}_{ijkl}(D_{kl} - D^{p}_{kl}) - \beta_{ij}(\mathcal{L}^{R}_{ijkl}D^{p}_{kl} - \sigma^{B}_{pj}W_{ipkl}(D_{kl} + D^{p}_{kl}) + \sigma^{B}_{ip}W_{pjkl}(D_{kl} + D^{p}_{kl}))\Big]\Big\} \qquad \text{(E.23)}$$

Elastic increments

For elastic increments the yield status is evaluated assuming no plastic increments ie.. with

$$\underset{\sim}{D}^p = \underset{\sim}{0} \ ,$$

$$\dot{Y}\Big|_{\text{elastic increments}} = \dot{Y}_e$$

Hence from Eq. E.22 we get

$$\dot{Y}_e = \frac{2}{J}\Big[\underset{\sim}{\alpha} : \underset{\sim\sim}{\mathcal{L}}^{e} : \underset{\sim}{D} - \underset{\sim}{\beta} : (\underset{\sim}{\sigma}^{B} \cdot (\underset{\sim\sim}{W} : \underset{\sim}{D}) - (\underset{\sim\sim}{W} : \underset{\sim}{D}) \cdot \underset{\sim}{\sigma}^{B})\Big] \qquad \text{(E.24)}$$

This can easily be written in index notation as in Eq. E.23 . Eq. E.24 can be written as

$$\dot{Y}_e = \underset{\sim}{Z} : \underset{\sim}{D} \qquad \text{(E.25)}$$

We have evaluated $\underset{\sim}{Z}$ in Sub-Appendix E4 for the axi-symmetric/ plane strain case (see Eq. E4.5).

Elastic-plastic increments

Using the flow rule , we have from Eq. 3.2.23

$$\underset{\sim}{D}^p = \Lambda \, \underset{\sim}{\sigma}^{*\prime} \qquad \text{(E.26)}$$

Hence , for elastic-plastic increments we have , from Eq. E.22

$$\dot{Y}_{ep} = \frac{2}{J}\Big[\underset{\sim}{\alpha} : (\underset{\sim\sim}{\mathcal{L}}^{e} : (\underset{\sim}{D} - \Lambda \underset{\sim}{\sigma}^{*\prime})$$

(contd...)

(contd...)

$$-\underset{\sim}{\beta}:(\underline{\underline{\mathcal{L}}}^{eR}:(\Lambda\,\underset{\sim}{\sigma}^{*\prime})$$

$$-(\underline{\underline{w}}:(\underset{\sim}{D}+\Lambda\,\underset{\sim}{\sigma}^{*\prime}))\cdot\underset{\sim}{\sigma}^{B}$$

$$+\ \underset{\sim}{\sigma}^{B}\cdot(\underline{\underline{w}}:(\underset{\sim}{D}+\Lambda\,\underset{\sim}{\sigma}^{*\prime}))\ )\ \Big\}\ \Big] \qquad \text{(E.27)}$$

In order not to violate the yield status , Eq. E.1 during elastic-plastic deformation , we have

$$\dot{Y}_{ep} = 0 \qquad \text{(E.28)}$$

Hence , from Eqs. E.27 and E.28 , we get the scalar

$$\Lambda = \frac{\dot{Y}_e}{\mathcal{J}} \qquad \text{(E.29)}$$

where the scalar denominator of Eq. E.29 is given by

$$\mathcal{J} = \frac{2}{J}\Big\{\Big[\underset{\sim}{\alpha}:(\underline{\underline{\mathcal{L}}}^{e}:\underset{\sim}{\sigma}^{*\prime})-\underset{\sim}{\beta}:(\underline{\underline{\mathcal{L}}}^{eR}:\underset{\sim}{\sigma}^{*\prime}$$

$$-(\underline{\underline{w}}:\underset{\sim}{\sigma}^{*\prime})\cdot\underset{\sim}{\sigma}^{B}$$

$$+\underset{\sim}{\sigma}^{B}\cdot(\underline{\underline{w}}:\underset{\sim}{\sigma}^{*\prime})\ )\ \Big\}\ \Big] \qquad \text{(E.30)}$$

SUB-APPENDIX : E1

Determination of $\partial J / \partial \underset{\approx}{\tau}$

From Appendix B (Eq. B.4) , the principal elastic strains are

$$\varepsilon^e_{ii} = \mathrm{Ln}(\bar{U}_{ii}) \qquad \text{(no sum)} \quad \text{(E1.1)}$$

Hence with

$$\begin{aligned} J &= \det(\underset{\approx}{F}^e) \\ &= \det(\underset{\approx}{\bar{U}}) \\ &= \bar{U}_{11} \bar{U}_{22} \bar{U}_{33} \quad , \end{aligned} \qquad \text{(E1.2)}$$

from Eq. E1.1 ,we have

$$\begin{aligned} J &= \exp(\varepsilon^e_{11} + \varepsilon^e_{22} + \varepsilon^e_{33}) \\ &= \exp(\mathrm{tr}(\underset{\approx}{\varepsilon}^e)) \end{aligned} \qquad \text{(E1.3)}$$

From Eqs. 1.6.2 and B.5 we have

$$J = \exp(\mathrm{tr}(\underset{\approx}{\tau} \tfrac{1-2\nu}{E})) \qquad \text{(E1.4)}$$

Therefore taking partial derivatives ,

$$\frac{\partial J}{\partial \underset{\approx}{\tau}} = \exp\left[\mathrm{tr}\left(\underset{\approx}{\tau} \frac{1-2\nu}{E} \right) \right] \left(\underset{\approx}{I} \frac{1-2\nu}{E} \right)$$

$$\frac{\partial J}{\partial \underset{\approx}{\tau}} = J\left(\underset{\approx}{I}\frac{1-2\nu}{E}\right) \qquad \text{(E1.5)}$$

In index notation we have

$$\frac{\partial J}{\partial \tau_{ij}} = J\frac{(1-2\nu)}{E}\delta_{ij} \qquad \text{(E1.6)}$$

SUB-APPENDIX : E2

Determination of $\partial \underset{\approx}{F}^e / \partial \underset{\approx}{\tau}$

From Appendix B, Eq. B.6 , we have for the principle Kirchoff stresses ,

$$\underset{\approx}{\bar{\tau}} = \mathrm{Ln}(\underset{\approx}{\bar{U}}) : \underset{=}{\mathcal{L}}^e \qquad \text{(E2.1)}$$

where

$$\underset{\approx}{\bar{\tau}} = \underset{\approx}{\bar{R}}^e \cdot \underset{\approx}{\tau} \cdot \underset{\approx}{\bar{R}}^{e^T} \qquad \text{(E2.2)}$$

Therefore

$$\mathrm{Ln}(\underset{\approx}{\bar{U}}) = \underset{\approx}{\bar{\tau}} : \underset{=}{C} \qquad \text{(E2.3)}$$

where the elastic compliance tensor is

$$C_{ijkl} = \frac{(1+\nu)}{E} \delta_{ik}\delta_{jl} - \frac{\nu}{E}\delta_{ij}\delta_{kl} \qquad \text{(E2.4)}$$

Hence differentiating Eq. E2.3 we have

$$C_{ijkl} = \bar{U}^{-1}_{ip} \frac{\partial \bar{U}_{pj}}{\partial \bar{\tau}_{kl}} \qquad \text{(E2.5)}$$

Since the compliance in Eq. E2.3 is isotropic (hence invariant under orthogonal transformations) we get

$$C_{ijkl} = U^{-1}_{ip} \frac{\partial U_{pj}}{\partial \tau_{kl}} \qquad \text{(E2.6)}$$

This is the most complete text of the thesis available. The following page(s) were not included in the copy of the thesis deposited in the Institute Archives by the author:

138

SUB-APPENDIX : E3

The Rubbery Rate Moduli $-\underline{\underline{\mathcal{L}}}^R$

In this section we employ Hill's principal axis technique (R Hill , 1970). Having known the expressions for the principal back stresses ,

$$(\bar{\sigma}_1^B, \bar{\sigma}_2^B, \bar{\sigma}_3^B),$$

(Eq. A.5 in Appendix A) in terms of the principal plastic stretches ,

$$(\bar{V}_1, \bar{V}_2, \bar{V}_3),$$

we can obtain the entries for the rate modulus in Eq. E.19 as follows :

The isotropic part of Eq. E.19 is written as

$$\overset{\nabla}{\bar{\sigma}}_{ii}^B = \bar{V}_1 \frac{\partial \bar{\sigma}_i^B}{\partial \bar{V}_1} D_{11}^p + \bar{V}_2 \frac{\partial \bar{\sigma}_i^B}{\partial \bar{V}_2} D_{22}^p + \bar{V}_3 \frac{\partial \bar{\sigma}_i^B}{\partial \bar{V}_3} D_{33}^p \qquad \text{(E3.1)}$$

The off-diagonal terms are

$$\overset{\nabla}{\bar{\sigma}}_{ij}^B = \frac{(\bar{V}_i^2 + \bar{V}_j^2)}{(\bar{V}_i - \bar{V}_j)} (\bar{\sigma}_i^B - \bar{\sigma}_j^B) D_{ij}^p$$

$$\text{no sum}, \quad (i \neq j, \ \bar{V}_i \neq \bar{V}_j) \qquad \text{(E3.2)}$$

For the special case (eg., equi-biaxial),

$\bar{V}_i = \bar{V}_j = \bar{V}$, ie.,

$$\bar{\sigma}_i^B = \bar{\sigma}_j^b = \bar{\sigma}^B \ ,$$

we have

$$\overset{g}{\sigma}{}_{ij}^B = \left(\frac{\partial \bar{\sigma}^B}{\partial \bar{V}_i} - \frac{\partial \bar{\sigma}^B}{\partial \bar{V}_j}\right)\frac{\bar{V}}{2} D_{ij}^b \Big|_{\bar{V}_i \to \bar{V}_j} \ . \qquad \text{(E3.3)}$$

Thus Eq. E.19 is schematically shown in Table E3.1 (in the principal plastic stretch coordinates), in which we have the following :

With

$$\beta_1 = \mathcal{L}^{-1}(\bar{V}_1/\sqrt{N})$$

and

$$\beta_3 = \mathcal{L}^{-1}(1/\bar{V}_1\bar{V}_2\sqrt{N})$$

from Eq. A.3 in Appendix A , we get

$$\bar{V}_1 \frac{\partial \bar{\sigma}_1^B}{\partial \bar{V}_1} = C^R\frac{\sqrt{N}}{3}\left\{\bar{V}_1\beta_1 - \frac{1}{\bar{V}_1\bar{V}_2}\beta_3 + \frac{\bar{V}_1^2}{\sqrt{N}}\left(\frac{1}{(1/\beta_1)^2-(1/\sinh\beta_1)^2}\right) + \frac{2}{\bar{V}_1\bar{V}_2}\beta_3 + \frac{1}{(\bar{V}_1\bar{V}_2)^2}\cdot\frac{1}{\sqrt{N}}\left(\frac{1}{(1/\beta_3)^2-(1/\sinh\beta_3)^2}\right)\right\}. \qquad \text{(E3.4)}$$

We can in a similar manner find $\bar{V}_2\frac{\partial \bar{\sigma}_2^B}{\partial \bar{V}_2}$.

TABLE E3.1 The rubbery rate modulii

$\overset{\nabla}{\sigma}{}^{B}_{11}$	$\bar{V}_1\frac{\partial \bar{\sigma}_1^{B}}{\partial \bar{V}_1}$	$\bar{V}_2\frac{\partial \bar{\sigma}_1^{B}}{\partial \bar{V}_2}$	$\bar{V}_3\frac{\partial \bar{\sigma}_1^{B}}{\partial \bar{V}_3}$				D^{b}_{11}
$\overset{\nabla}{\sigma}{}^{B}_{22}$	$\bar{V}_1\frac{\partial \bar{\sigma}_2}{\partial \bar{V}_1}$	$\bar{V}_2\frac{\partial \bar{\sigma}_2}{\partial \bar{V}_2}$	$\bar{V}_3\frac{\partial \bar{\sigma}_2^{B}}{\partial \bar{V}_3}$				D^{b}_{22}
$\overset{\nabla}{\sigma}{}^{B}_{33}$	$\bar{V}_1\frac{\partial \bar{\sigma}_3^{B}}{\partial \bar{V}_1}$	$\bar{V}_2\frac{\partial \bar{\sigma}_3^{B}}{\partial \bar{V}_2}$	$\bar{V}_3\frac{\partial \bar{\sigma}_3^{B}}{\partial \bar{V}_3}$				D^{b}_{33}
$\overset{\nabla}{\sigma}{}^{B}_{12}$				$\left(\frac{\bar{V}_1^2+\bar{V}_2^2}{\bar{V}_1^2-\bar{V}_2^2}\right)(\bar{\sigma}_1^{B}-\bar{\sigma}_2^{B})$			D^{b}_{12}
$\overset{\nabla}{\sigma}{}^{B}_{23}$					$\left(\frac{\bar{V}_2^2+\bar{V}_3^2}{\bar{V}_2^2-\bar{V}_3^2}\right)(\bar{\sigma}_2^{B}-\bar{\sigma}_3^{B})$		D^{b}_{23}
$\overset{\nabla}{\sigma}{}^{B}_{31}$						$\left(\frac{\bar{V}_3^2+\bar{V}_1^2}{\bar{V}_3^2-\bar{V}_1^2}\right)(\bar{\sigma}_3^{B}-\bar{\sigma}_1^{B})$	D^{b}_{31}

We also have

$$\bar{V}_1 \frac{\partial \bar{\sigma}_2^B}{\partial \bar{V}_1} = \bar{V}_2 \frac{\partial \bar{\sigma}_1^B}{\partial \bar{V}_2} = C^R \frac{\sqrt{N}}{3} \left\{ \frac{1}{\bar{V}_1 \bar{V}_2} \beta_3 + \frac{1}{(\bar{V}_1 \bar{V}_2)^2} \cdot \frac{1}{\sqrt{N}} \left(\frac{1}{(1/\beta_3)^2 - (1/\sinh \beta_3)^2} \right) \right\} \quad \text{(E3.5)}$$

Using Eq. A.3 we have

$$\bar{V}_3 \frac{\partial \bar{\sigma}_1^B}{\partial \bar{V}_3} = -\left(\bar{V}_1 \frac{\partial \bar{\sigma}_1^B}{\partial \bar{V}_1} + \bar{V}_2 \frac{\partial \bar{\sigma}_1^B}{\partial \bar{V}_2} \right) \quad \text{(E3.6)}$$

In a similar manner we can find

$$\bar{V}_3 \frac{\partial \bar{\sigma}_2^B}{\partial \bar{V}_3} .$$

Also ,

$$\bar{V}_3 \frac{\partial \bar{\sigma}_3^B}{\partial \bar{V}_3} = \bar{V}_1 \frac{\partial \bar{\sigma}_1^B}{\partial \bar{V}_1} + \bar{V}_2 \frac{\partial \bar{\sigma}_2^B}{\partial \bar{V}_2} + \bar{V}_2 \frac{\partial \bar{\sigma}_1^B}{\partial \bar{V}_2} + \bar{V}_1 \frac{\partial \bar{\sigma}_2^B}{\partial \bar{V}_1} . \quad \text{(E3.7)}$$

For the special case in Eq. E3.3 we have

$$\bar{\sigma}_{12}^B = C^R \frac{N}{\sqrt{3}} \left\{ \frac{\bar{V}}{2} \beta_1 - \left(\frac{1}{\bar{V}^4} - \frac{3}{2\bar{V}^2} \right) \beta_3 + \frac{\bar{V}^2}{2\sqrt{N}} \left(\frac{1}{(1/\beta_1)^2 - (1/\sinh \beta_1)} \right) + \left(\frac{1}{\bar{V}^6} + \frac{1}{\bar{V}^4} \right) \cdot \frac{1}{\sqrt{N}} \left(\frac{1}{(1/\beta_3)^2 - (1/\sinh \beta_3)^2} \right) \right\} D_{12}^b \quad \text{(E3.8)}$$

where

$$\bar{\beta}_1 = \bar{\mathcal{L}}^{-1}(\bar{V}/\sqrt{N}) \; ; \; \bar{\beta}_3 = \bar{\mathcal{L}}^{-1}(1/\bar{V}^2\sqrt{N})$$

The expressions for the entries in Table E3.1 are instantaneous rate moduli referred to the local principal plastic stretch coordinates . We however , have to perform orthogonal transformations on this in order to use it in Eq. E.19 , which deals with quantities referred to a global (Cartesian) frame . We thus have

$$\mathcal{L}^R_{ijkl} = \bar{\mathcal{L}}^{\bar{R}}_{pqrs} \bar{R}^p_{pi} \bar{R}^p_{qj} \bar{R}^p_{rk} \bar{R}^p_{sl} \qquad \text{(E3.9)}$$

where

$$\bar{\mathcal{L}}^{\bar{R}}_{pqrs}$$

are the entries in Table E3.1 , and

$$\bar{\bar{R}}^p$$

is the matrix of eigen vectors found in Appendix A (see Eq. A.2).

SUB-APPENDIX : E4

The Active Tangent Moduli — $\underline{\underline{\underline{\underline{\mathcal{L}}}}}^{ep}$

We can evaluate the entries in the incremental moduli , by rewriting Eq. E.17 as

$$\overset{\nabla}{\tau}_{ij} = \mathcal{L}^{e}_{ijkl}(D_{kL} - D^{p}_{kL}\langle 1\rangle) \tag{E4.1}$$

$$= \left\{\frac{E}{1+\nu}\delta_{ik}\delta_{jl} + \frac{E\nu}{(1+\nu)(1-2\nu)}\delta_{ij}\delta_{kL}\right\}\left(D_{kL} - \frac{\dot{\gamma}_e}{\varphi}\sigma^{*\prime}_{kL}\langle 1\rangle\right) \tag{E4.2}$$

where <1> is a " switch " and is

= 0 , for elastic increments

= 1 , for elastic-plastic increments .

Let

$$\underset{\approx}{P} = \beta \cdot \underset{\approx}{\sigma}^{B} \tag{E4.3}$$

where

$$\underset{\approx}{\sigma}^{B}$$

is the back stress , and

$$\beta$$

is defined in Eq. E.15 . Then from Eqs. E.24 and E.25 we have

$$\dot{Y}_e = Z_{ij} D_{ji} \qquad \text{(E4.4)}$$

where , for the special 2D case of axial symmetry / plane strain , we have

$$Z_{11} = \frac{2}{J}\left(2G\mathcal{L}_{11} + \lambda\mathcal{L}_{ii} - \frac{P_{21} - P_{12}}{F^e_{11} + F^e_{22}} 2F^e_{12}\right)$$

$$Z_{22} = \frac{2}{J}\left(2G\mathcal{L}_{22} + \lambda\mathcal{L}_{ii} + \frac{P_{21} - P_{12}}{F^e_{11} + F^e_{22}} 2F^e_{12}\right)$$

$$Z_{33} = \frac{2}{J}\left(2G\mathcal{L}_{33} + \lambda\mathcal{L}_{ii}\right)$$

$$Z_{12} = Z_{21} = \frac{2}{J}\left(2G\mathcal{L}_{12} + 2\frac{P_{21} - P_{12}}{F^e_{11} + F^e_{22}}\left(F^e_{11} - F^e_{22}\right)\right)$$

(E4.5)

with

$$2G = \frac{E}{1+\nu}$$

$$\lambda = \frac{E}{(1+\nu)(1-2\nu)}$$

Table E4.1 shows the entries in the tangent modulus in Eq. E4.1 for the special 2D case of axi-symmetric / plane strain deformations . These are obtained using Eqs. E.30 , 3.2.21 , E4.4 etc. in Eq. E4.2 and after much simplification .

TABLE E4.1 The active tangent modulii

∇_{11}	$2G\left(1-\frac{\sigma_{11}^{*\prime}Z_{11}}{ef}\langle 1\rangle\right)+\lambda$	$2G\left(-\frac{\sigma_{11}^{*\prime}Z_{22}}{ef}\langle 1\rangle\right)+\lambda$	$2G\left(-\frac{\sigma_{11}^{*\prime}Z_{33}}{ef}\langle 1\rangle\right)+\lambda$	$2G\left(-\frac{\sigma_{11}^{*\prime}Z_{21}}{ef}\langle 1\rangle\right)$	D_{11}
∇_{22}	$2G\left(-\frac{\sigma_{22}^{*\prime}Z_{11}}{ef}\langle 1\rangle\right)+\lambda$	$2G\left(1-\frac{\sigma_{22}^{*\prime}Z_{22}}{ef}\langle 1\rangle\right)+\lambda$	$2G\left(-\frac{\sigma_{22}^{*\prime}Z_{33}}{ef}\langle 1\rangle\right)+\lambda$	$2G\left(-\frac{\sigma_{22}^{*\prime}Z_{21}}{ef}\langle 1\rangle\right)$	D_{22}
∇_{33}	$2G\left(-\frac{\sigma_{33}^{*\prime}Z_{11}}{ef}\langle 1\rangle\right)+\lambda$	$2G\left(-\frac{\sigma_{33}^{*\prime}Z_{22}}{ef}\langle 1\rangle\right)+\lambda$	$2G\left(1-\frac{\sigma_{33}^{*\prime}Z_{33}}{ef}\langle 1\rangle\right)+\lambda$	$2G\left(-\frac{\sigma_{33}^{*\prime}Z_{21}}{ef}\langle 1\rangle\right)$	D_{33}
∇_{12}	$2G\left(-\frac{\sigma_{12}^{*\prime}Z_{11}}{ef}\langle 1\rangle\right)$	$2G\left(-\frac{\sigma_{12}^{*\prime}Z_{22}}{ef}\langle 1\rangle\right)$	$2G\left(-\frac{\sigma_{12}^{*\prime}Z_{33}}{ef}\langle 1\rangle\right)$	$G\left(1-\frac{\sigma_{12}^{*\prime}Z_{21}}{ef}\langle 1\rangle\right)$	$2D_{12}$

REFERENCES

ANAND, L
J. Appl. Mech., 46, pp. 78-82. (1979).

ANAND, L
J. Appl. Mech., 47, pp.349-441 (1980).

ANAND, l and SPITZIG, W A
J. Mech. Phys. Solids; 31, pp.105-122 (1980).

ANDREWS, R D and KIMMEL, R M
J. Polymer Sci. (B) , 3,p.167 (1965).

ARGON, A S Phil. Mag. 28. p. 839 (1973).

ARGON, A S and BESSONOV, M I
Third International Conference on " Deformation, Yield and Fracture of Polymers " in Cambrigde, England, (March 26, 1976) .

BATHE, K J
Finite Element Procedures in Engineering Analysis, Prentice Hall,(1982)

BAUWENS, J C
J. Mater. Sci., 7,p. 577 (1972)

BAUWENS-CROWET,C , BAUWENS, J-C and HOMES, G
J. Mater. Sci. , 176-183 (1972) .

FERRY, J
Viscoelastic Properties of Polymers, Wiley, 1970.

FARDSHISHEH, F and ONAT, E T
Problems in plasticity, A. Sawczuk ,ed., Noordhoff International : Leyden , pp. 89-115 (1972).

HAWARD, R N
Physics of Glassy Polymers , edited by RN Haward, Halsted Press : New York, Chapt. 6 , p.340 (1973).

HILL, R
Proc. Roy. Soc. Lond. A 314,457-472 (1970).

HUGHES, T J R and WINGET, J
Int. J. Num. Meth. Eng., 15, p1862, (1980)

HUTCHINSON, J W and NEALE, K W
Harvard University Report , MECH-37, March (1983).

JAMES, H M and GUTH, E
J. Chem. Phys.,11, p455, (1943)

KRAMER, E J
in Advances in Polymer Science : Crazing in Polymers , ed. H H Kausch, Springer, Berlin Ch.1 (1983).

LEE, E H , MALLETT, R L and McMEEKING, R M
"Numerical Modelling of Manufacturing Processes" Eds. R F Jones Jr., H Armen , J T Fong ASME New York, (1977).

ONAT, E T
Private communication with Prof. D M Parks of MIT (1981).

PARKS, D M
Unpublished private communication , (1983).

ROLPH, W D and BATHE, K J
Mechanical Engineering Report , MIT #82448-11, July(1983).

SPITZIG, W A and RICHMOND, O
Polym. Eng. & Sci. Vol.19, No.16, (1979).

TRELOAR, L R G
Rubber Elasticity ,(Oxford University Press , 1975).